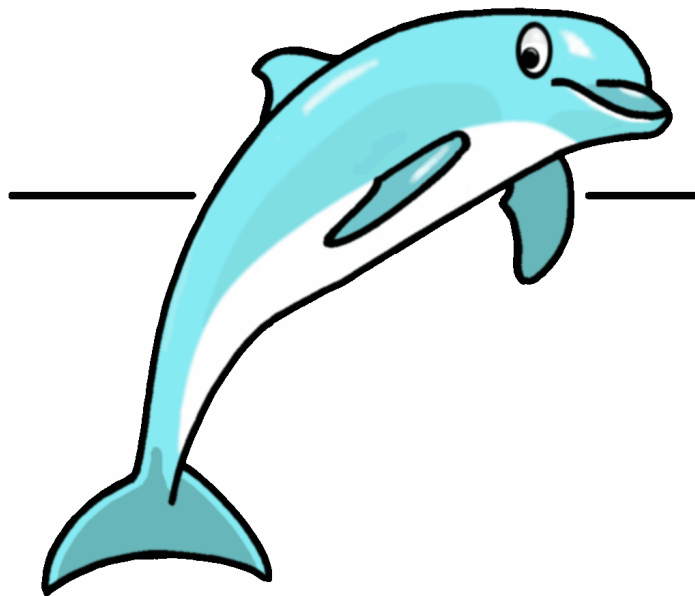


Dolfyn Test Results

DRAFT



CFD-11xxxx
21st January 2011

 Cyclone Fluid Dynamics B.V.

Sweelincklaan 4

Tel.: +31-40-22 30 491

Web: www.cyclone.nl

NL-5583 XM Waalre

Fax.: +31-40-22 30 490

email: info@cyclone.nl

Dolfyn Test Results

DRAFT

Cyclone Fluid Dynamics BV

Author:
H.W. Krüs

CFD-11xxxx
Cyclone Fluid Dynamics B.V.
21st January 2011

Copyright © Cyclone Fluid Dynamics B.V., 2011. All rights reserved.

Cyclone Fluid Dynamics B.V.

Sweelincklaan 4 Tel.: +31-40-22 30 491 Web: www.cyclone.nl
NL-5583 XM Waalre Fax.: +31-40-22 30 490 email: info@cyclone.nl



Contents

Contents	iii
List of Figures	v
1 Verification with equidistant Lid Driven Cavity tests	1
2 C1 Unstructured	17
3 C3 Leonard tests	23
3.1 Step cases	24
3.2 Sin2 cases	27
3.3 Semi ellipse cases	30
4 C4 Wild test	33
5 C6 Wedges	37
6 C7 Mesh jump	41
7 C8 Embedded refinement	45
8 M6 Stagnation flow with embedded refinement	49
9 CAV Lid driven cavities	53
9.1 Hexahedra at 45 degrees	54
9.2 Hexahedra at 20 degrees	57
10 W1/W2 Wedge cell tests	61
10.1 Step cases	61
10.2 Sin2 cases	65
10.3 Semi ellipse cases	69
10.4 Lid driven cavity	73
11 M3/M5 Tetrahedral cell tests	79
11.1 Lid driven cavity m3	79
11.2 Plain flow from left to right	82
11.3 Stagnation flow from top	85
11.4 Lid driven cavity m5	88
11.5 Plain flow from left to right	91
11.6 Stagnation flow from top	94



List of Figures

1.1	Streamlines at Reynolds 25, 100, 400, 1,000, 3,200, 5,000, 7,500 and 10,000 with 128x128 and LUX	4
1.2	Velocity magnitude at Reynolds 25, 100, 400, 1,000, 3,200, 5,000, 7,500 and 10,000 with 128x128 and LUX	5
1.3	Results from Ghia et.al	6
1.4	Reynolds 25	7
1.5	Reynolds 100	8
1.6	Reynolds 400	9
1.7	Reynolds 1,000	10
1.8	Reynolds 3,200	11
1.9	Reynolds 5,000	12
1.10	Reynolds 7,500	13
1.11	Reynolds 10,000	14
1.12	Reynolds 10,000 at 256x256 and influence of differencing scheme (UD, CD, CD1, LUD, Gamma, MinMod, LUX)	15
2.1	Mesh model c1	17
2.2	Standard case, all Gauss, no limiter	18
2.3	Standard case, left Gauss/right Least Squares, no limiter	19
2.4	Standard case, Gauss, left no limiter/right VNF	20
2.5	Standard case, profiles at x=1	21
3.1	Mesh model c3	23
3.2	Standard Leonard step cases with Gauss, no limiter	24
3.3	Standard Leonard step cases with Gauss (GS) and Least Squares (LS), no limiters used	25
3.4	Leonard step cases with Gauss and face based limiters	26
3.5	Standard Leonard sin2 cases with Gauss, no limiter	27
3.6	Standard Leonard sin2 cases with Gauss (GS) and Least Squares (LS), no limiters used	28
3.7	Leonard sin2 cases with Gauss and face based limiters	29
3.8	Standard Leonard semi cases with Gauss, no limiter	30
3.9	Standard Leonard semi cases with Gauss (GS) and Least Squares (LS), no limiters used	31
3.10	Leonard semi cases with Gauss and face based limiters	32
4.1	Wild case, all Gauss, no limiter	33
4.2	Mesh model c4	33
4.3	Wild case, left Gauss/right Least Squares, no limiters	34
4.4	Wild case, Gauss, left no limiter/right VNF	35
5.1	c6 standard wedge cases with Gauss, no limiter	37

5.2	c6 standard wedge cases with Gauss (GS) and Least Squares (LS), no limiters used	38
5.3	c6 wedge cases with Gauss and face based limiters	39
5.4	Mesh model c6	40
6.1	c7 mesh jump cases with Gauss, no limiter	41
6.2	c7 mesh jump cases with Gauss (GS) and Least Squares (LS), no limiters used	42
6.3	c7 mesh jump cases with Gauss and face based limiters	43
6.4	Mesh model c7	44
7.1	c8 refinement cases with Gauss, no limiter	45
7.2	c8 refinement cases with Gauss (GS) and Least Squares (LS), no limiters used	46
7.3	c8 refinement cases with Gauss and face based limiters	47
7.4	Mesh model c8	48
8.1	m6 refinement cases with Gauss, no limiter	49
8.2	m6 refinement cases with Gauss (GS) and Least Squares (LS), no limiters used	50
8.3	m6 refinement cases with Gauss and face based limiters	51
8.4	Mesh model m6	52
9.1	Mesh model cav45	53
9.2	Mesh model cav20	53
9.3	cav45 LDC at 45 degrees with Gauss, no limiter	54
9.4	cav45 LDC 45 cases with Gauss and Least Squares, no limiters used	55
9.5	cav45 LDC 45 cases with Gauss and face based limiters	56
9.6	cav20 LDC at 20 degrees with Gauss, no limiter	57
9.7	cav20 LDC 20 cases with Gauss and Least Squares, no limiters used	58
9.8	cav20 LDC 20 cases with Gauss and face based limiters	59
10.1	Standard Leonard step cases with Gauss, no limiter	61
10.2	Standard Leonard step cases with Least Squares, no limiter	62
10.3	Standard Leonard step cases with Gauss (GS) and Least Squares (LS), no limiters used	63
10.4	Leonard step cases with Gauss and face based limiters	64
10.5	Standard Leonard sin2 cases with Gauss, no limiter	65
10.6	Standard Leonard sin2 cases with Least Squares, no limiter	66
10.7	Standard Leonard sin2 cases with Gauss (GS) and Least Squares (LS), no limiters used	67
10.8	Leonard sin2 cases with Gauss and face based limiters	68
10.9	Standard Leonard semi cases with Gauss, no limiter	69
10.10	Standard Leonard semi cases with Least Squares, no limiter	70
10.11	Standard Leonard semi cases with Gauss (GS) and Least Squares (LS), no limiters used	71
10.12	Leonard semi cases with Gauss and face based limiters	72
10.13	W2 LDC wedge cases with Gauss, no limiter	73
10.14	W2 LDC wedge cases with Least Squares, no limiter	74

10.15W2 LDC wedge cases with Gauss and Least Squares, no limiters used	75
10.16W2 LDC wedge cases with Gauss and face based limiters	76
10.17Mesh model w1	77
10.18Mesh model w2	77
11.1 m3a LDC tet cases with Gauss, no limiter	79
11.2 m3a LDC tet cases with Gauss and Least Squares, no limiters used	80
11.3 m3a LDC tet cases with Gauss and face based limiters	81
11.4 m3b plain flow tet cases with Gauss, no limiter	82
11.5 m3b plain flow tet cases with Gauss and Least Squares, no limiters used	83
11.6 m3b plain flow cases with Gauss and face based limiters	84
11.7 m3c stagnation flow tet cases with Gauss, no limiter	85
11.8 m3c stagnation flow tet cases with Gauss and Least Squares, no limiters used	86
11.9 m3c stagnation flow cases with Gauss and face based limiters	87
11.10m5a LDC tet cases with Gauss, no limiter	88
11.11m5a LDC tet cases with Gauss and Least Squares, no limiters used	89
11.12m5a LDC tet cases with Gauss and face based limiters	90
11.13m5b plain flow tet cases with Gauss, no limiter	91
11.14m5b plain flow tet cases with Gauss and Least Squares, no limiters used	92
11.15m5b plain flow cases with Gauss and face based limiters	93
11.16m5c stagnation flow tet cases with Gauss, no limiter	94
11.17m5c stagnation flow tet cases with Gauss and Least Squares, no limiters used	95
11.18m5c stagnation flow cases with Gauss and face based limiters	96
11.19Mesh model m5	97
11.20Mesh model m3	97



1 Verification with equidistant Lid Driven Cavity tests

Following Roache¹, an error analysis has been performed using ‘Richardson Extrapolation’ on various meshes and convective differencing schemes. All the meshes are simple orthogonal and equidistant. Although dolfyn contains non-orthogonal corrections etcetera, still this is a valuable test because all additions should not break the basic fundament of the code. The reference data is by Ghia, Ghia, and Shin².

The cavity has dimensions of one by one and the lid has a velocity of one, leaving the (laminar) viscosity of the fluid with density one to determine the Reynolds number ($Re = \rho V_{lid} L_{lid} / \mu$). The calculations were done with Gauss for the gradients and various convective differencing schemes:

UD Classic standard first order Upwind Differencing.

CD 0.8 Blend of 80% second order Central Differencing and 20% first order upwind differencing.

CD1 Pure second order Central Differencing.

LUD Second order Linear Upwind Differencing with a Convection Bounded Criterion (UD outside the Normalised Variable range of $0 \leq \tilde{\Phi}_C \leq 1$).

Gamma The Gamma CBC differencing scheme (blending with CD).

MinMod The MinMod CBC differencing scheme (based on LUD and CD).

LUX Pure LUD not based on NVD..

Shown are the u component velocity profiles half way the cavity ($x = 0.5$, $0 \leq y \leq 1$) for all the schemes at the finest mesh (128x128) and UD and LUX only as a function of the mesh (8x8, 16x16, 32x32, 64x64, 128x128). And the development of the interpolated u component at $x = 0.5$, $y = 0.5$. The latter value has been linearly interpolated (which might have some effects on the final results) and is shown as a function of mesh size h (linear) and h^2 (quadratic). A second order method will have to show up as a straight line at the smallest meshes.

¹P.J. Roache, *Verification and Validation in Computational Science and Engineering*, Hermosa Publishers, Albuquerque NM, 1998

²U. Ghia, K.N. Ghia, C.T. Shin, *High-Re solutions for incompressible flow using the Navier-Stokes equations and a multigrid method*, Journal of Computational Physics, 1982

Also shown are streamlines based on the LUX data like in Figure 1.1. They were made with OpenDX after the cell-centered velocities have been interpolated to the nodes and creating streamlines (the ‘post’ and ‘streamline’ modules of OpenDX). Because of this procedure the streamlines will lose some of their accuracy near the walls. However nice closed streamlines do show up in the center of the main vortex.

In all this study is the result of at least 432 runs.

Brief discussion of the results:

Re 25 A very very viscous flow. The flow is dominated by the (second order) viscous forces. All convective schemes coincide on the largest mesh (128x128). The first order behaviour of UD is clearly visible as well as the second order nature of CD1 and LUX (note that CD 0.8 lays nicely in between of CD1 and UD).

Re 100 The first case where data is available from Ghia et.al. As can be seen LUX on at a mesh of 32x32, or even 16x16, already produces the final result. The Richardson Extrapolation curves clearly supports this. Note the start of the two lower corner vortices.

Re 400 A 16 times lower viscosity compared to *Re 25* starts to show some differences especially with UD; a good result is only possible at the finest 128x128 mesh. The second order schemes CD1 and LUX reproduce the reference data exactly, closely followed by CD 0.8. The LUX results are already there on the 64x64 mesh (but the 32x32 are not bad either). The lower right corner vortex increases.

Re 1,000 Basically the same results as for *Re 400*. In the top left the vortex is about to appear.

Re 3,200 Now the differences between the schemes get very clear. Note that the NVD blended schemes follow the UD scheme whereas the two unbounded second order schemes provide the best result (again followed by the CD/UD blend). The LUX scheme is the best and the Richardson Extrapolation curve of h^2 shows a ‘tail’ for the CD1 scheme. The latter is now starting to deteriorate.

Re 5,000 Now only LUX is the only one which follows the data, and only on the finest 128x128 mesh. The ‘tail’ of CD1 in the h^2 Richardson Extrapolation curve is more pronounced. In the paper by Ghia et.al the results are show on a 257x257 mesh and a second vortex starts to appear in the lower left corner (see Figure 1.3).

Re 7,500 At Reynolds 7,500 and on a mesh of 128x128 even LUX is not able to reproduce the reference data. Also instabilities start to occur; see Figure 1.10.

Re 10,000 The results of Reynolds 10,000 resemble the Reynolds 7,500 results. The results in Figure 1.11 are based on a 256x256 mesh and Figure 1.12 shows the corresponding streamlines. It is clearly visible that the upwind

and CBC upwinded schemes are the most stable. The (unbounded) second order schemes CD1 and LUX show unsteady effects; the latter is also visible in the residual drop which do not reach machine accuracy levels anymore. The results in the reference paper are based on a high order upwind scheme with a larger stencil (with a face based unstructured solver one has to restrict to a small stencil). Nevertheless at some point instabilities as can be seen in Figure 1.12 will have to pop up at some point.

General conclusion is that dolfyn is a second order accurate code which provides for this particular case and mesh topology very accurate and correct results. Also for testing purposes the lid driven cavity can be used at medium Reynolds numbers; for example only at Re 400 or the combination Re 100 and Re 1,000.

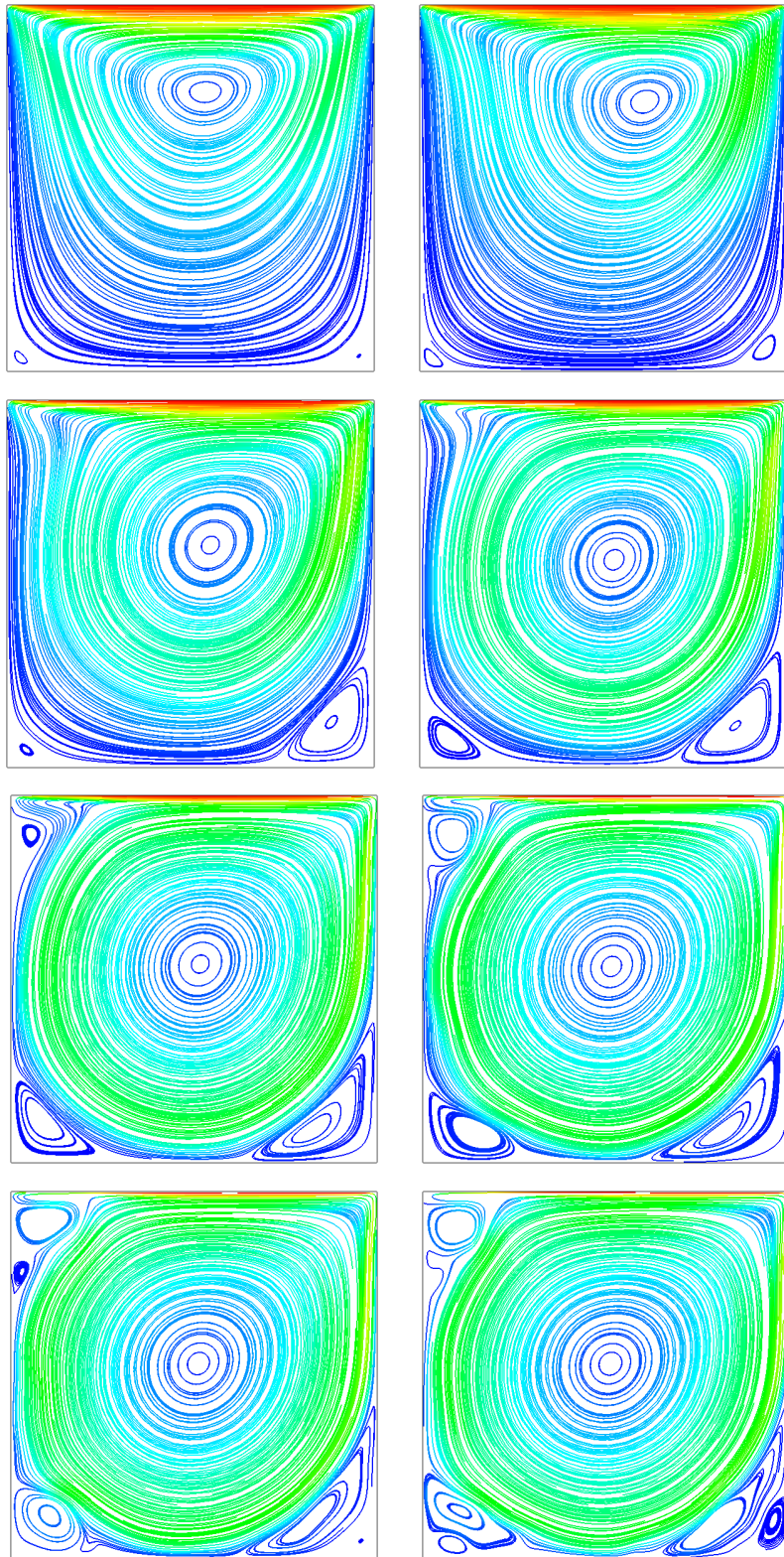


Figure 1.1: Streamlines at Reynolds 25, 100, 400, 1,000, 3,200, 5,000, 7,500 and 10,000 with 128x128 and LUX

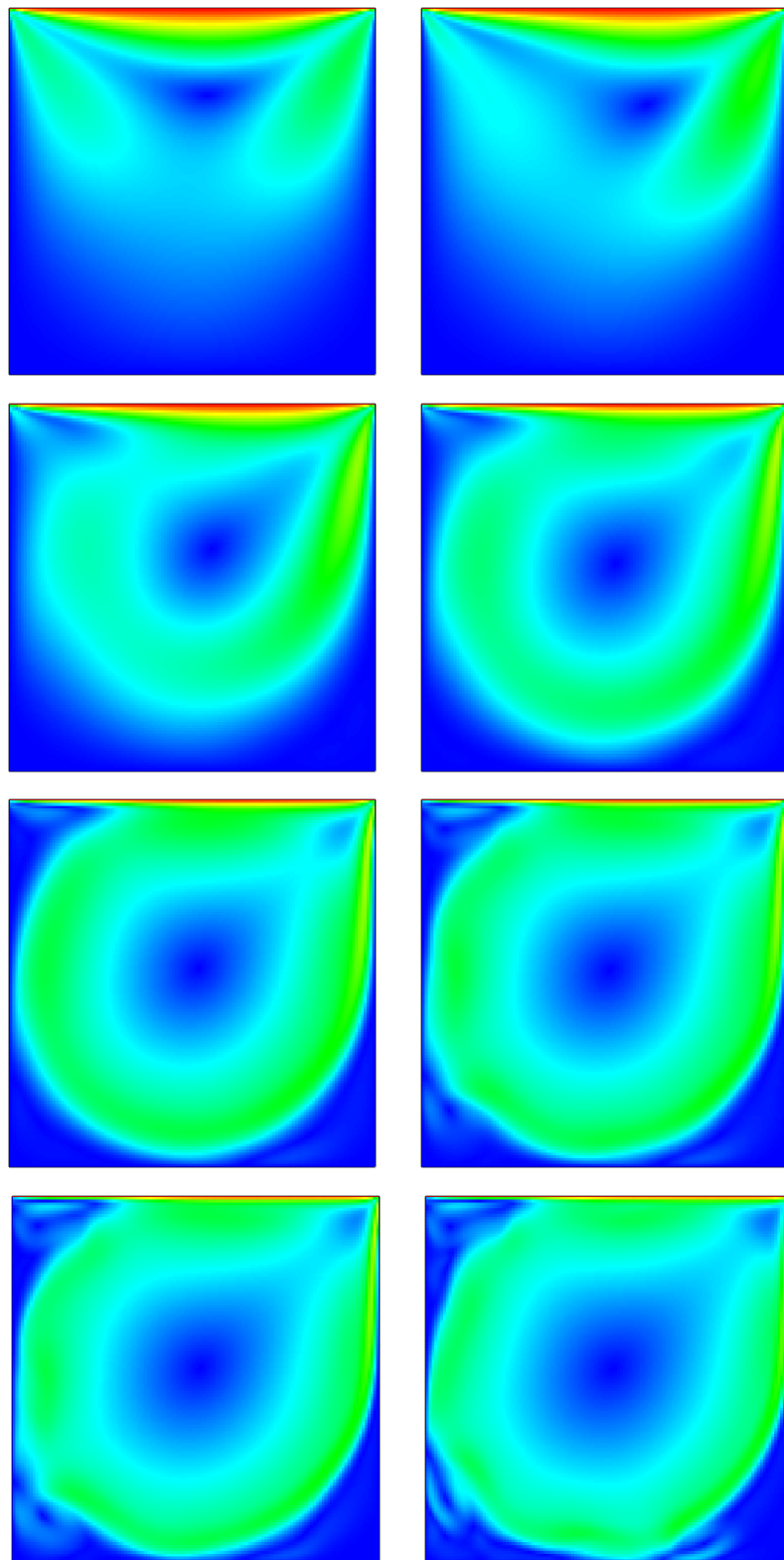


Figure 1.2: Velocity magnitude at Reynolds 25, 100, 400, 1,000, 3,200, 5,000, 7,500 and 10,000 with 128x128 and LUX

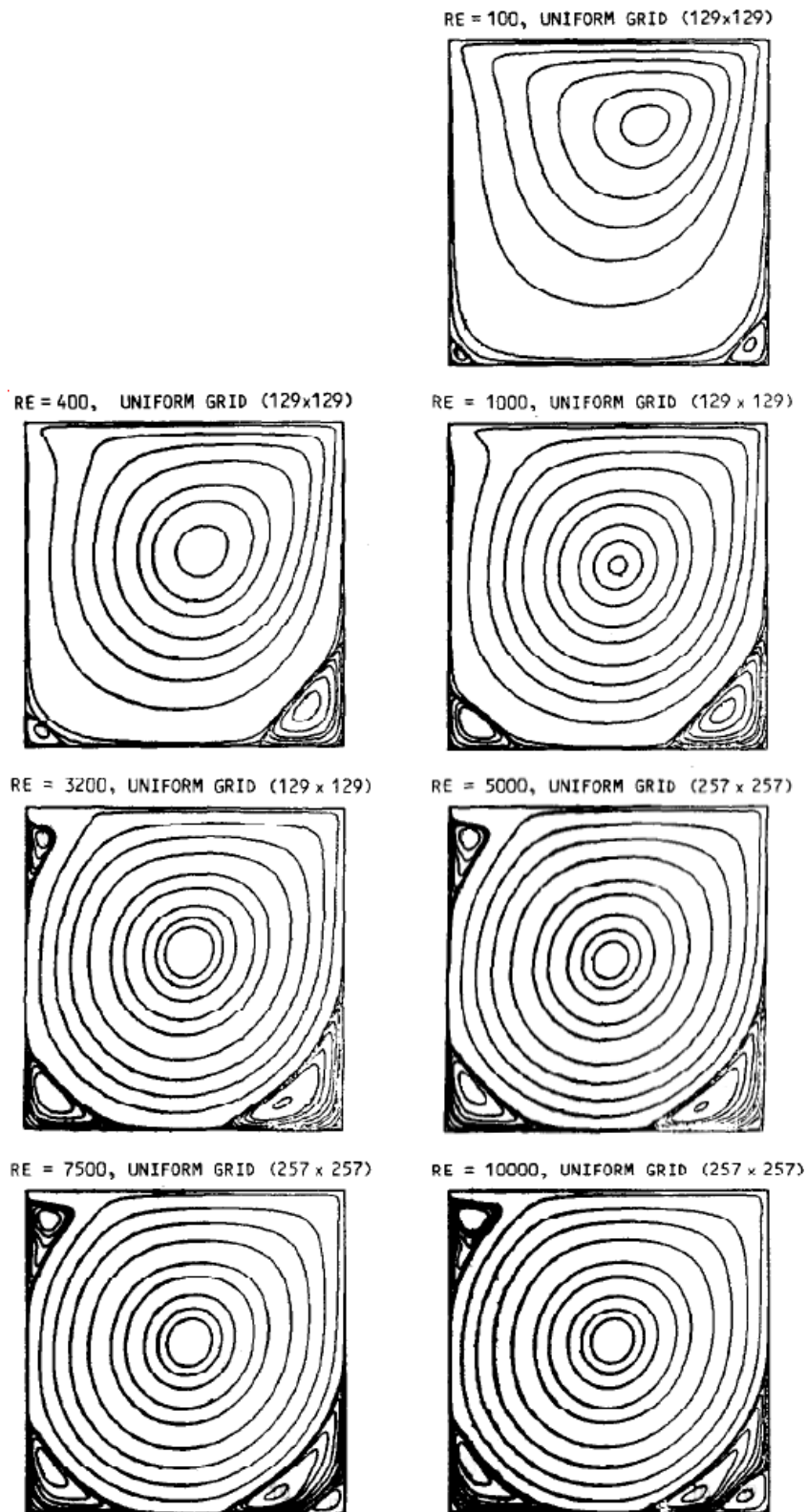
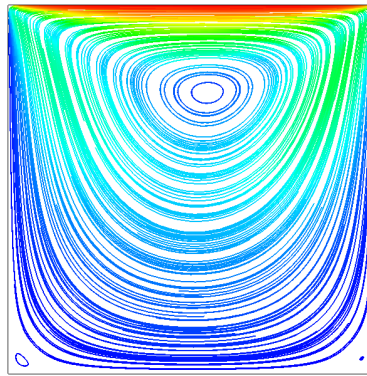


Figure 1.3: Results from Ghia et.al



Lid Driven Cavity, Re=25, U(x=0.5), GS off

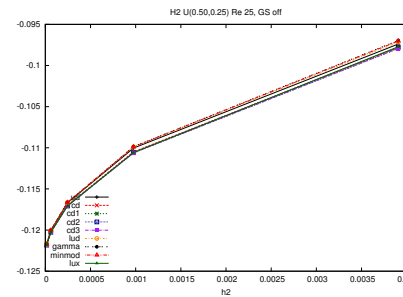
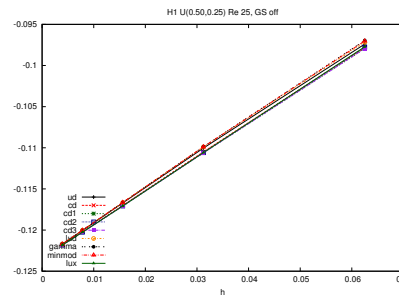
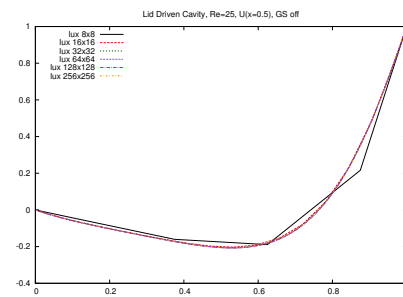
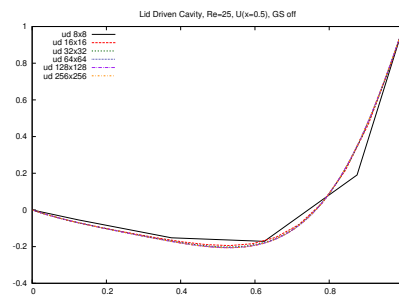
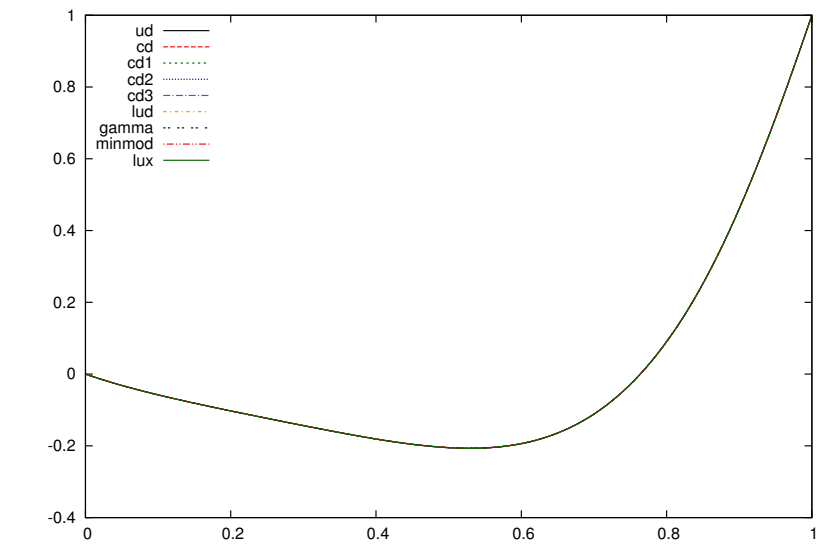


Figure 1.4: Reynolds 25

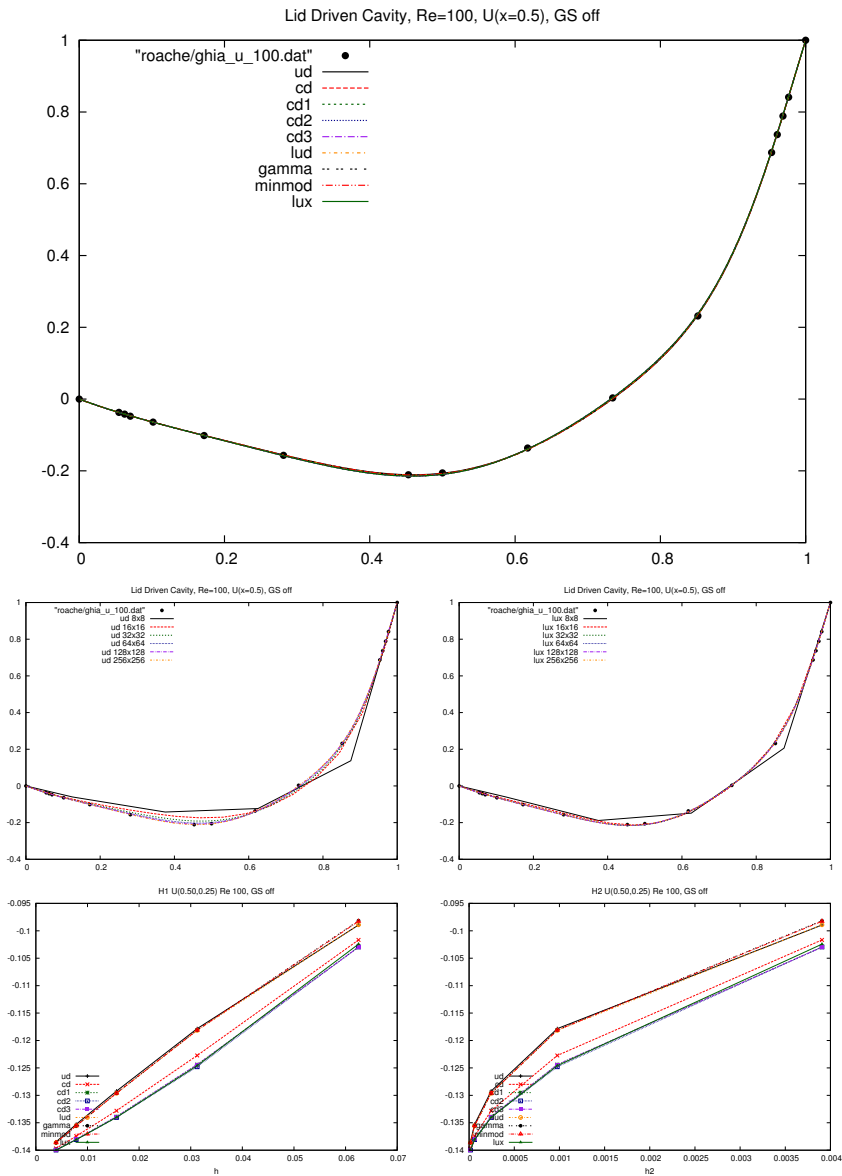
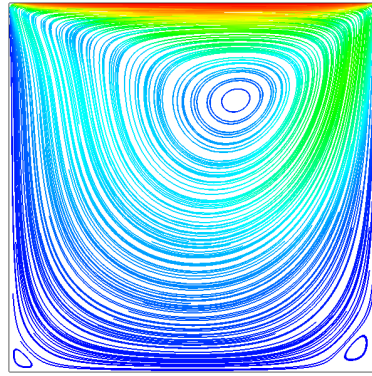


Figure 1.5: Reynolds 100

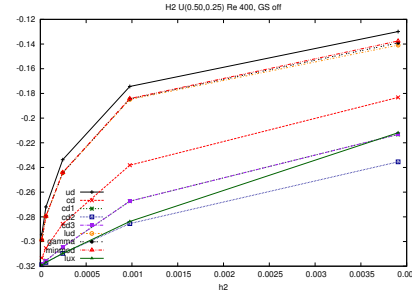
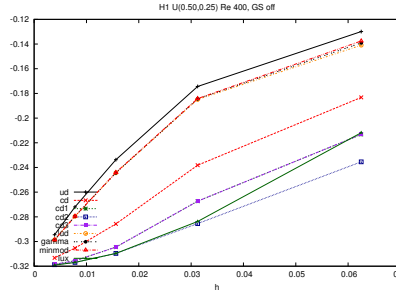
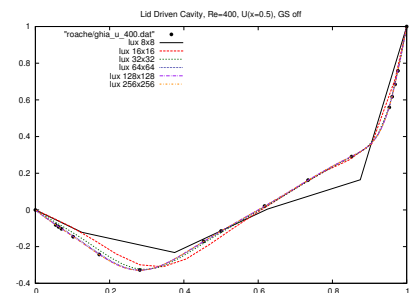
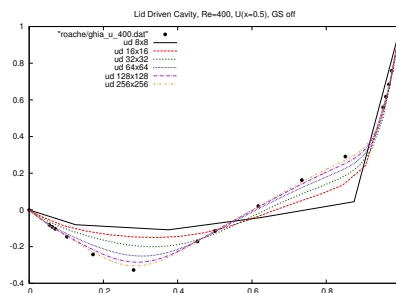
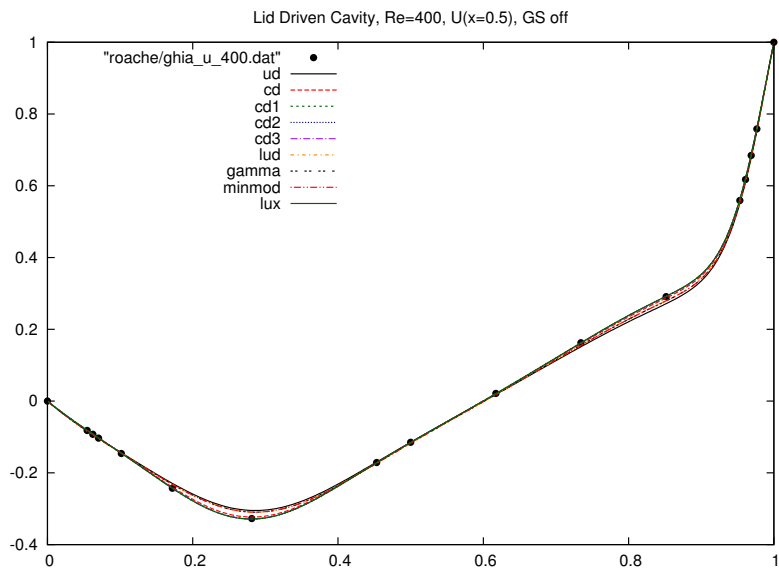
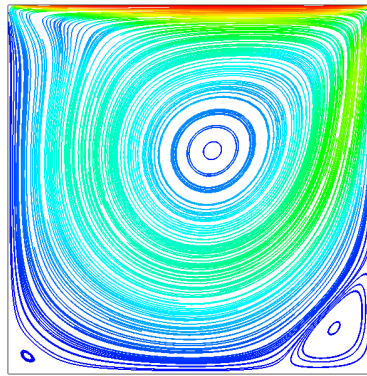


Figure 1.6: Reynolds 400

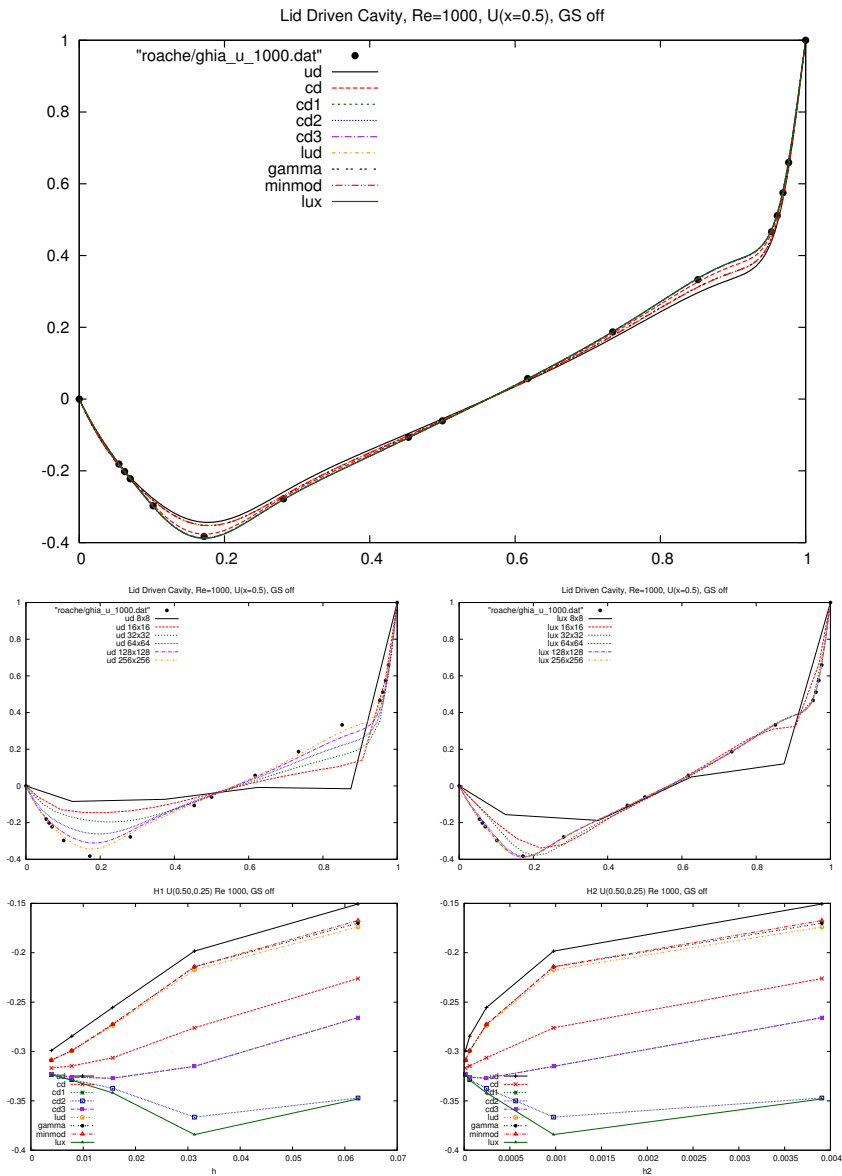
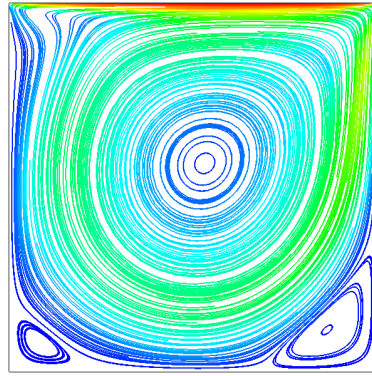


Figure 1.7: Reynolds 1,000

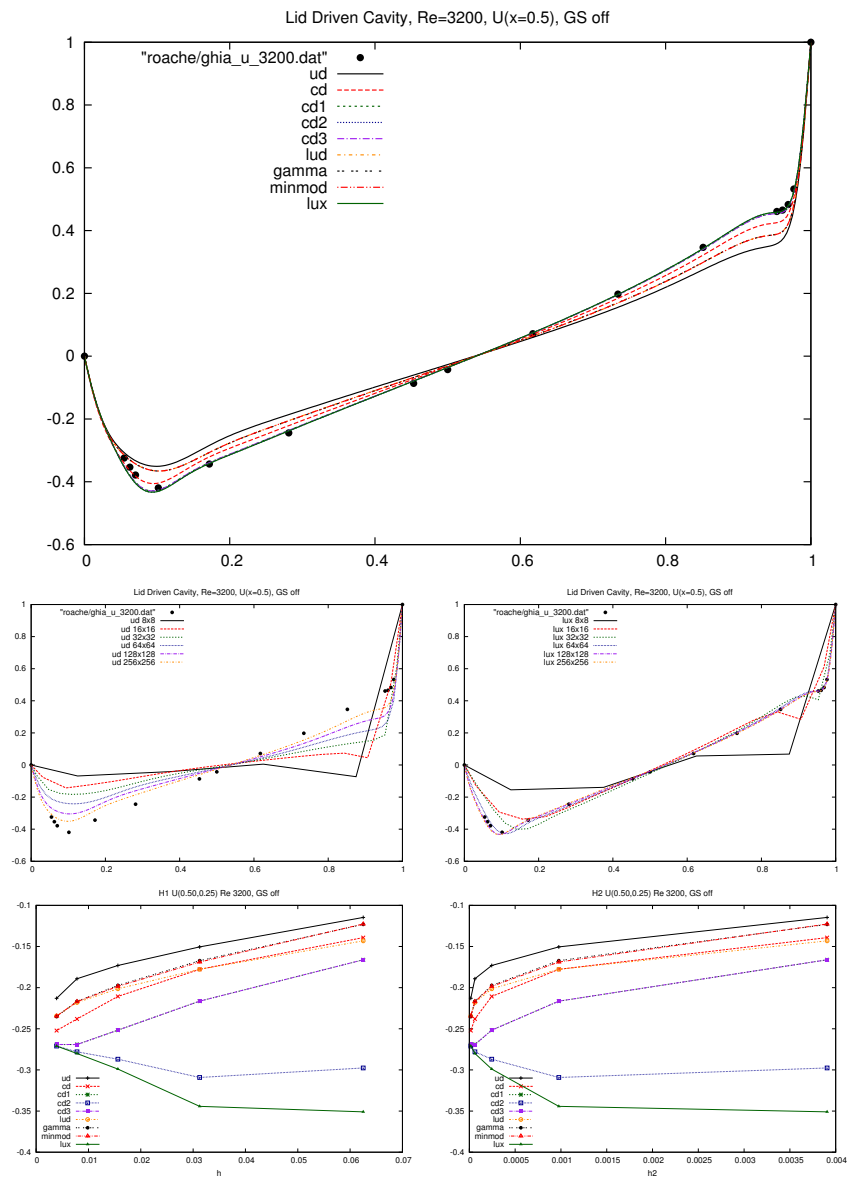
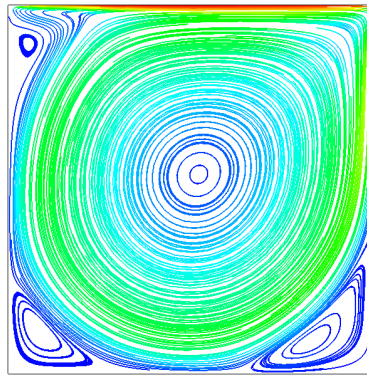


Figure 1.8: Reynolds 3,200

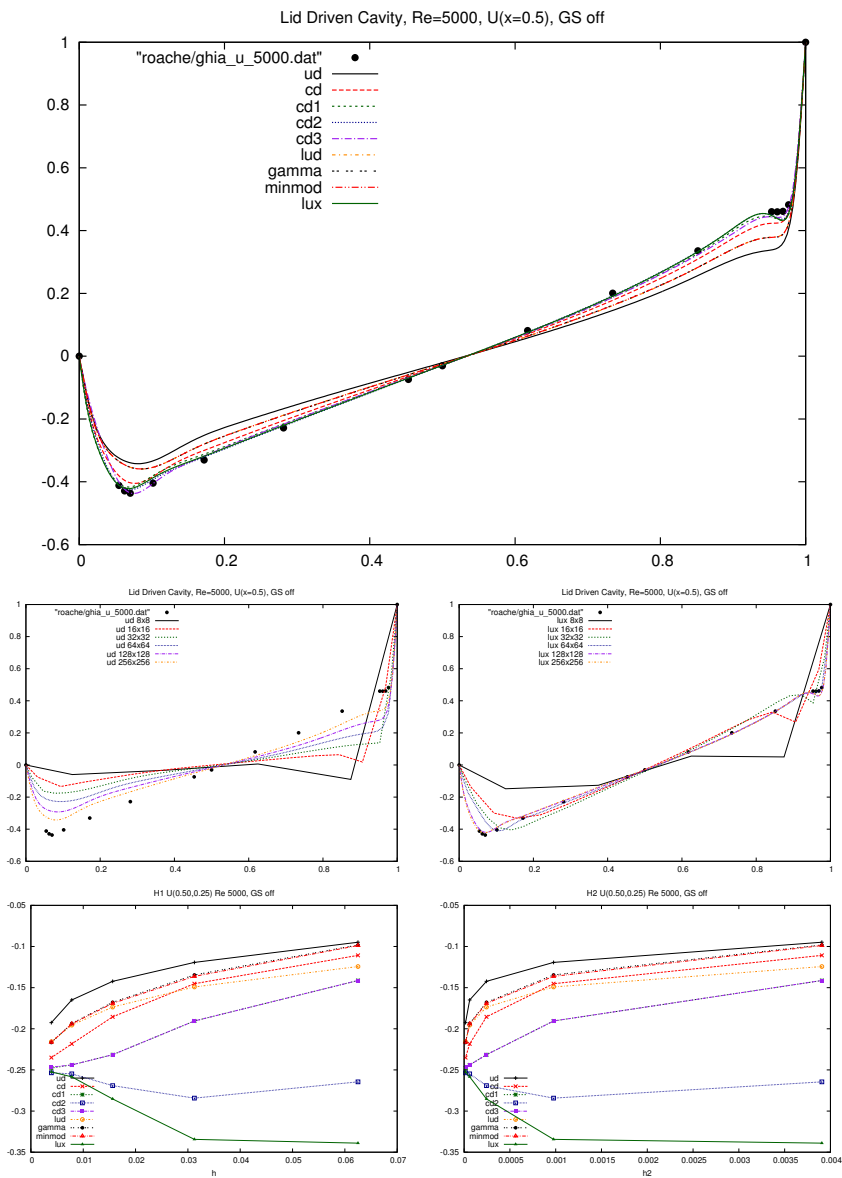
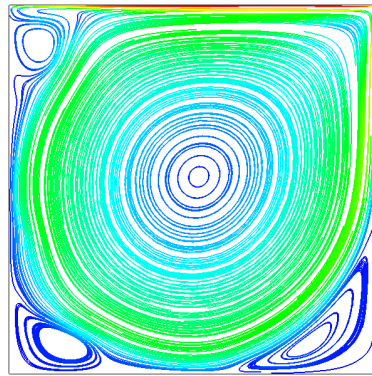


Figure 1.9: Reynolds 5,000

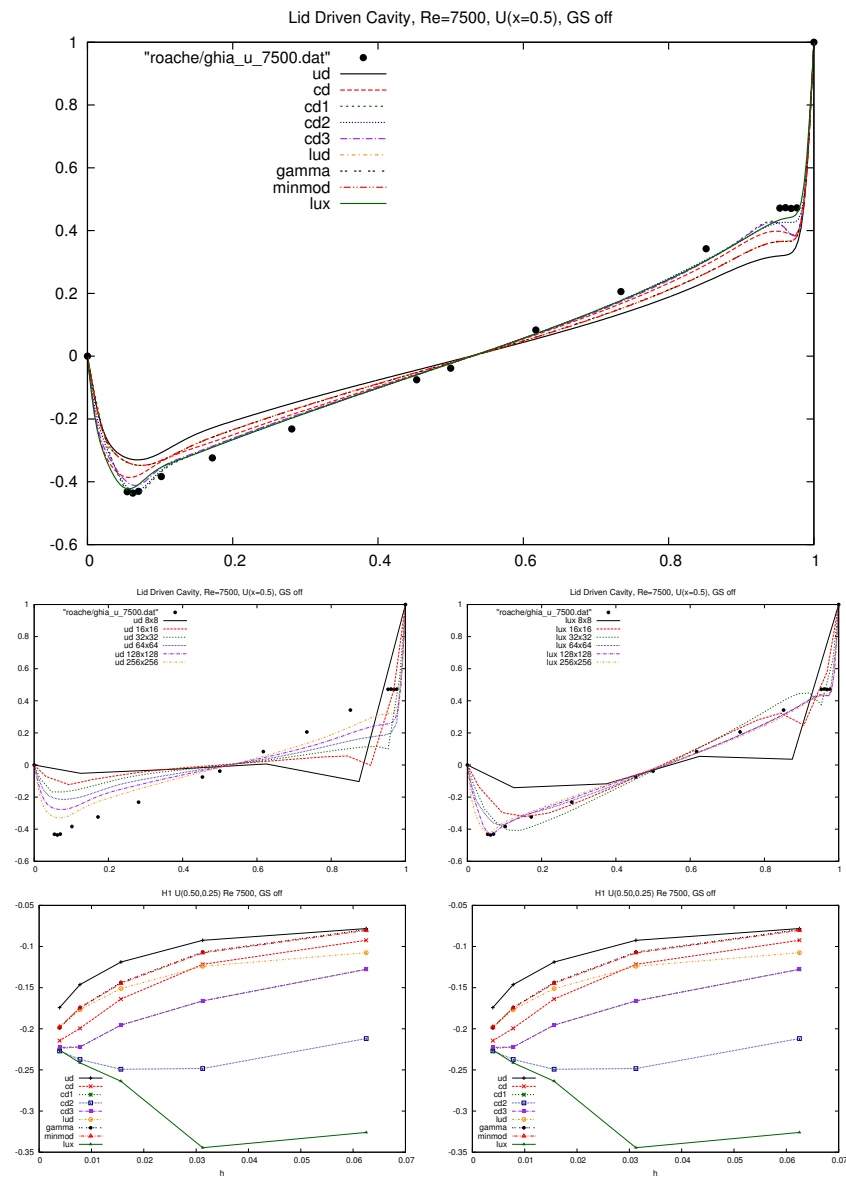
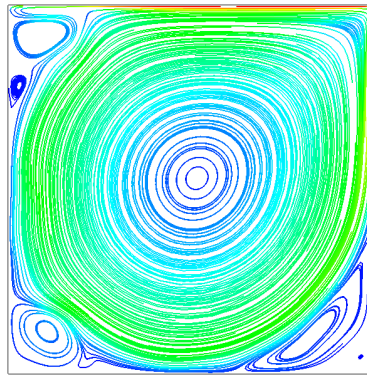


Figure 1.10: Reynolds 7,500

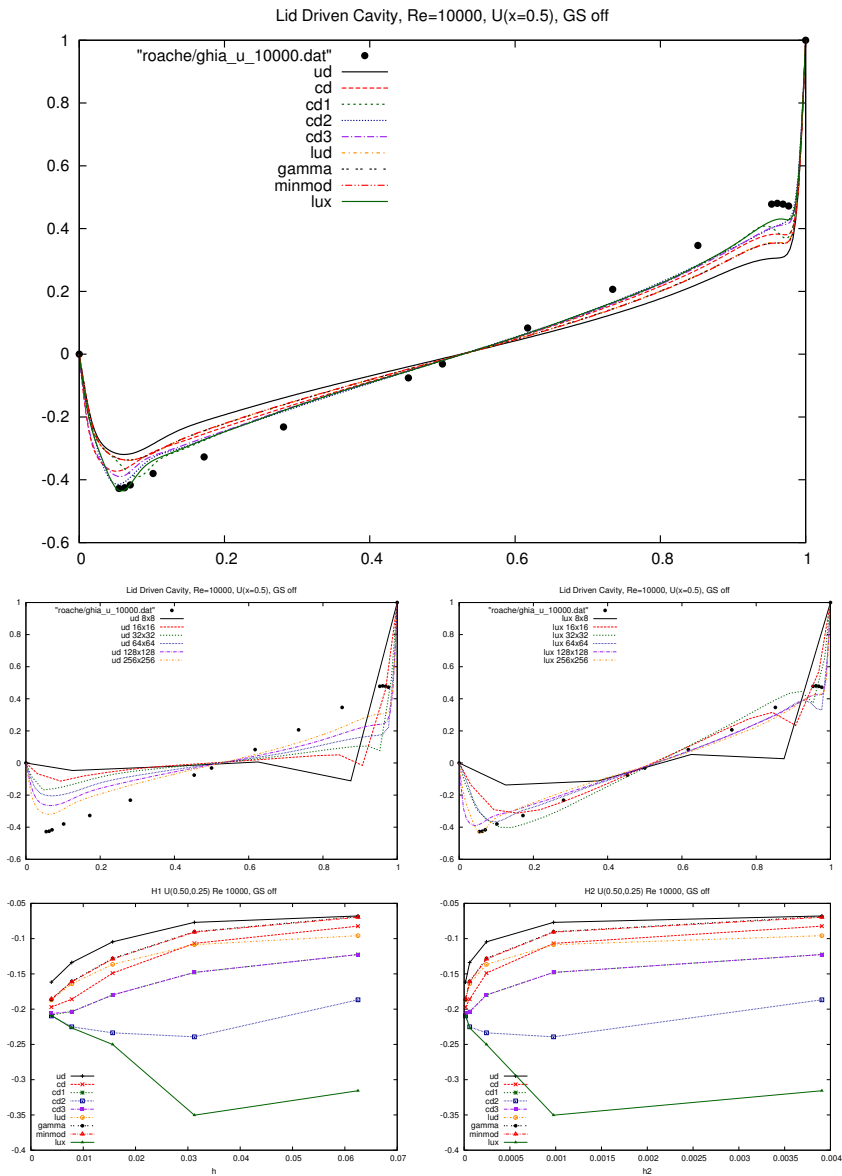
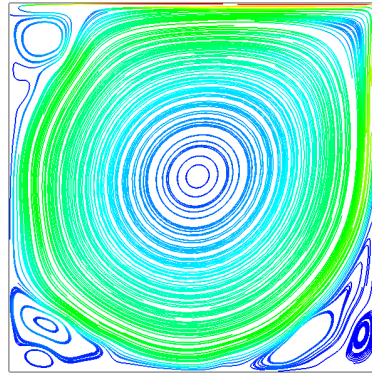


Figure 1.11: Reynolds 10,000

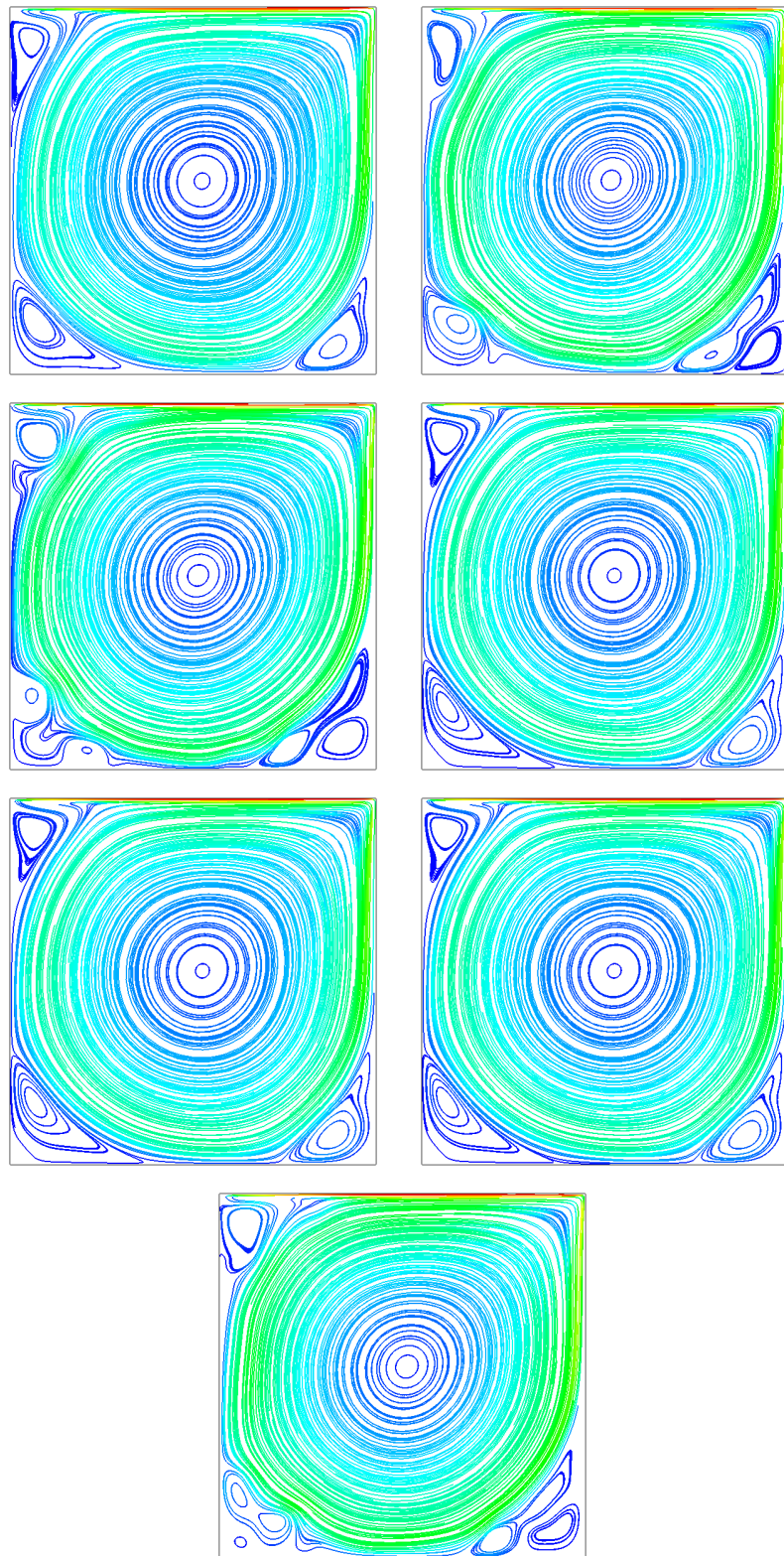


Figure 1.12: Reynolds 10,000 at 256x256 and influence of differencing scheme (UD, CD, CD1, LUD, Gamma, MinMod, LUX)

2 C1 Unstructured

Flow from left to right with scalar temperature convection top 21 C and bottom half 20 C. Uniform unity velocity. In the middle the mesh is tilted by 45 degrees, beginning just after the splitter plate at distance 1. Old test which shows the peculiar upstream influence of CD type and based schemes.

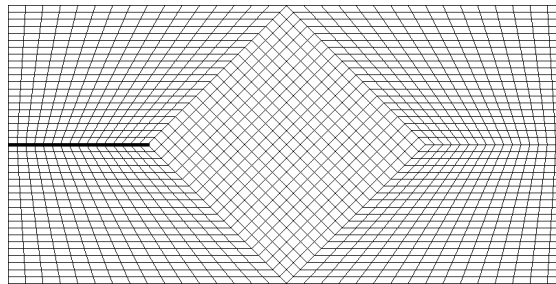


Figure 2.1: Mesh model c1

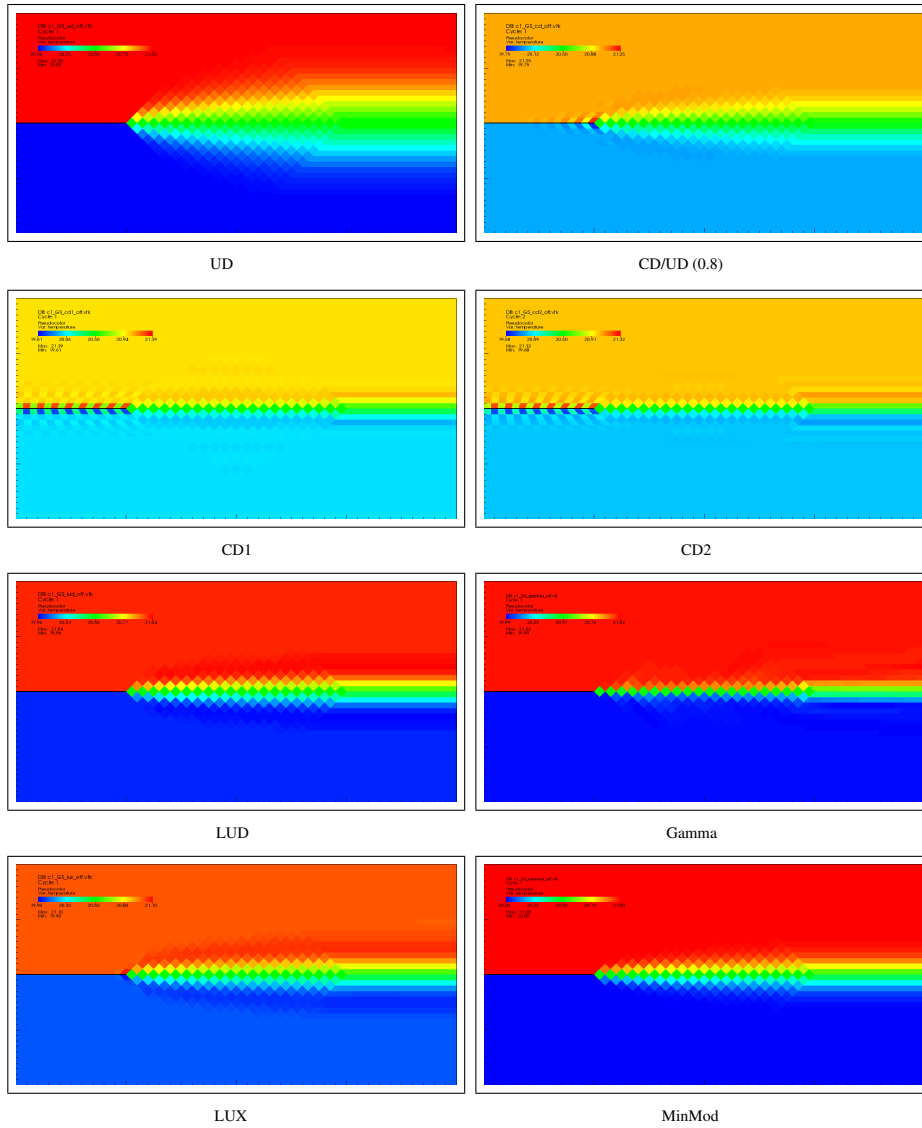


Figure 2.2: Standard case, all Gauss, no limiter

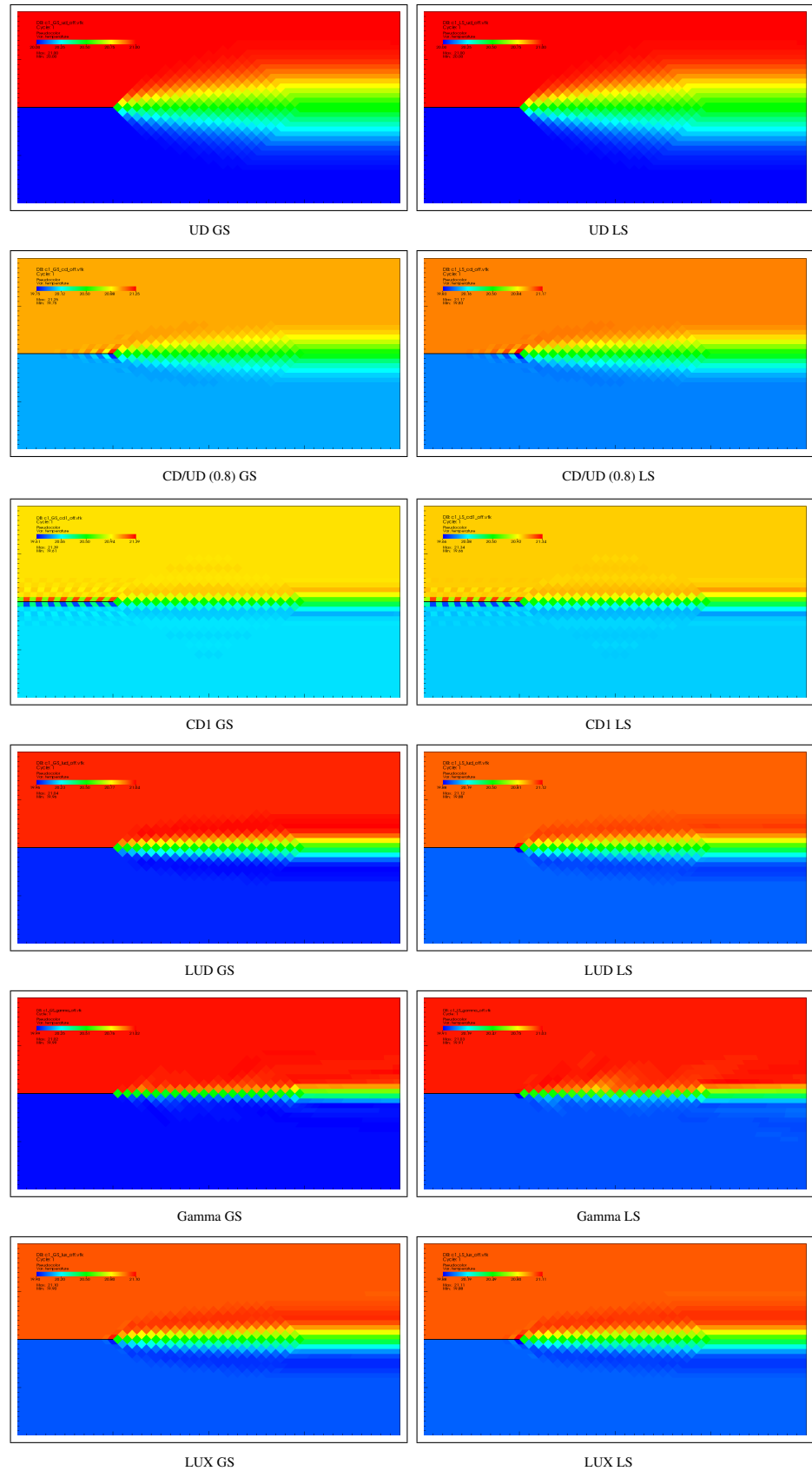


Figure 2.3: Standard case, left Gauss/right Least Squares, no limiter

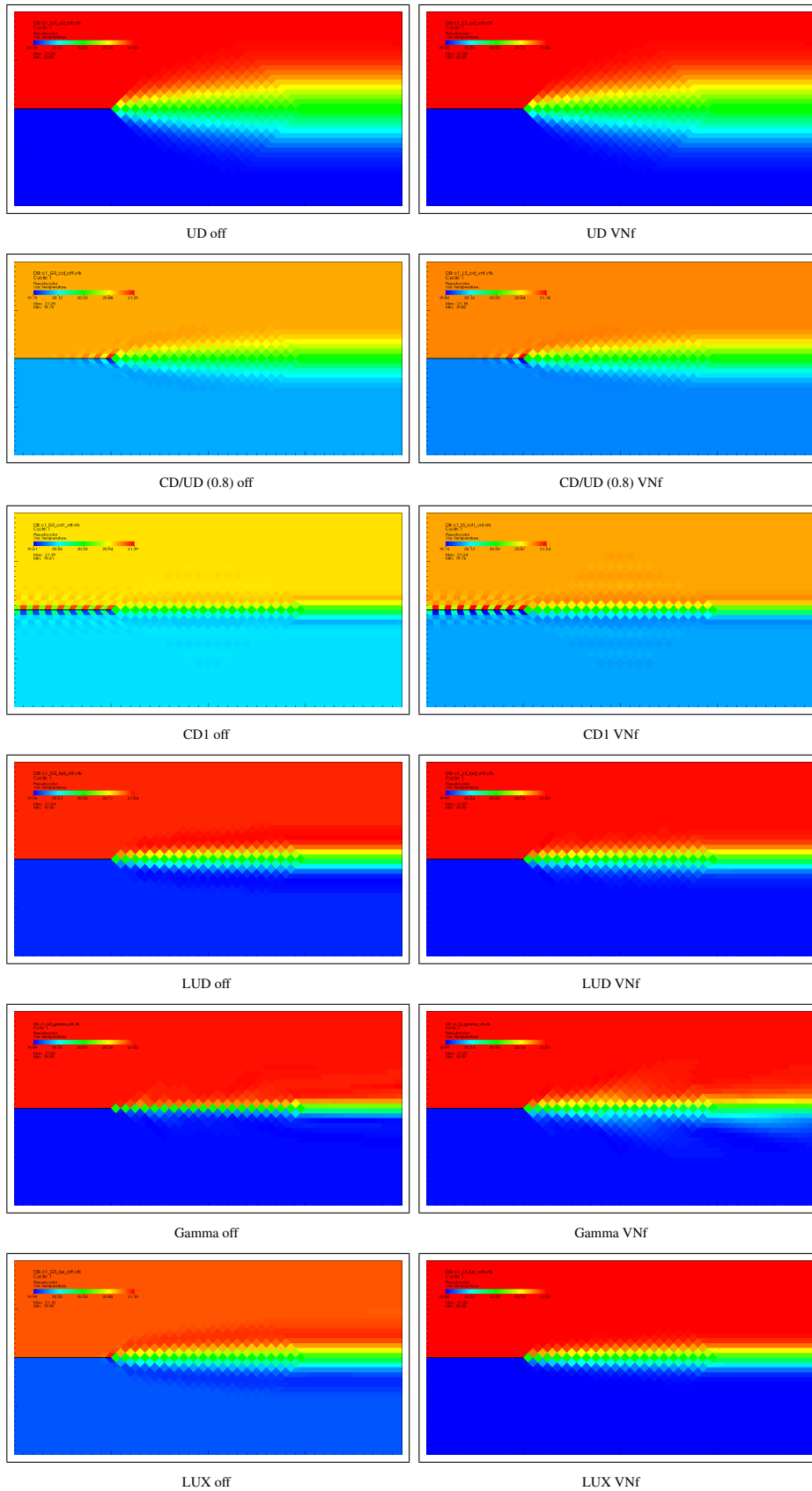


Figure 2.4: Standard case, Gauss, left no limiter/right VNF

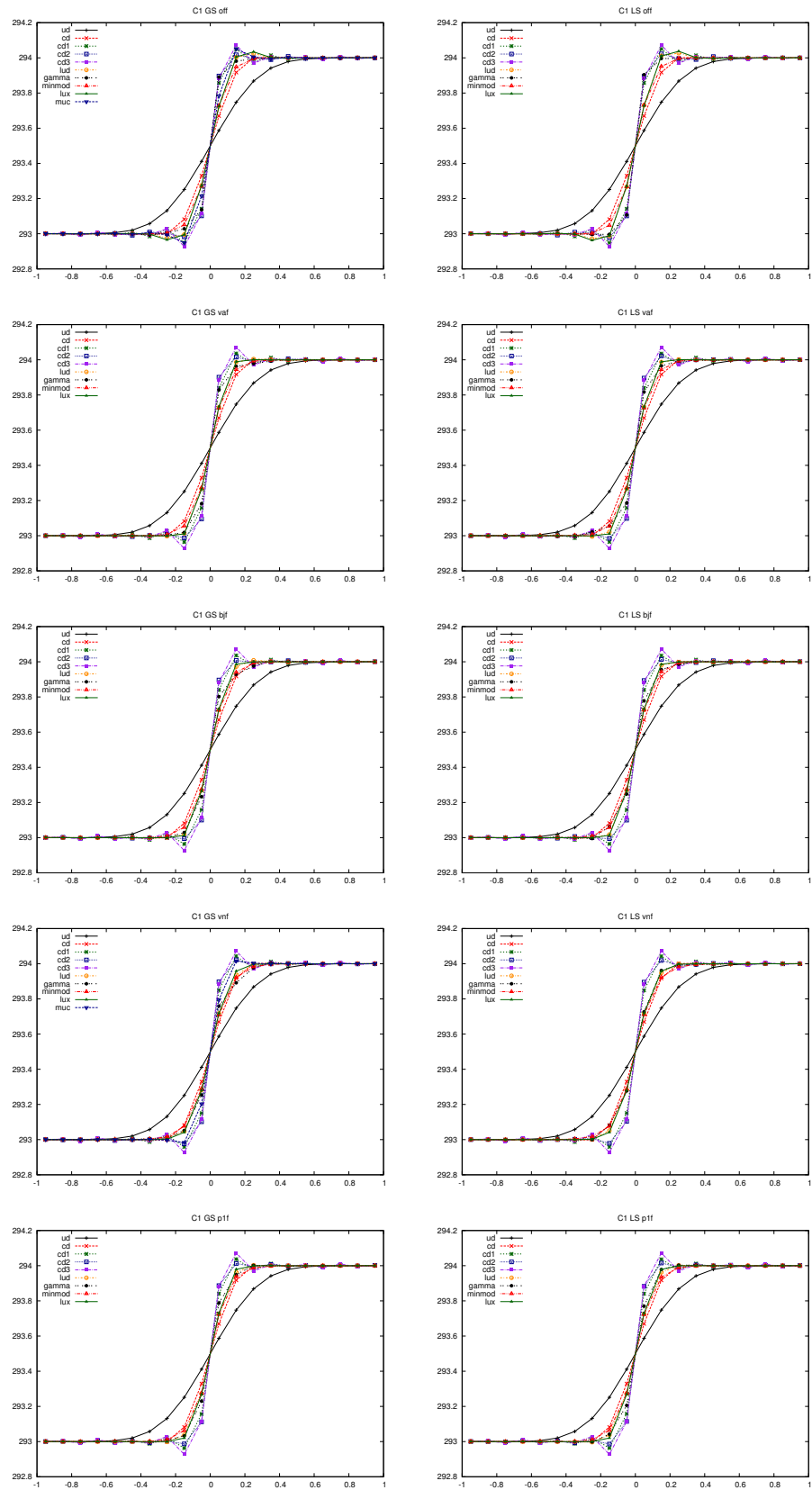


Figure 2.5: Standard case, profiles at $x=1$

3 C3 Leonard tests

Flow in a simple equidistant domain with 45 degrees which is the worst case for numerical diffusion. Three different profiles are considered:

step Very simple sudden step profile. The interface should remain sharp:

$$\phi(x) = \begin{cases} 20 & \text{for } 0 \leq x \leq \frac{1}{6}, \\ 21 & \text{for } \frac{1}{6} \leq x \leq 1. \end{cases} \quad (3.1)$$

sin2 The smooth varying \sin^2 profile (smooth beginning and end, smooth maximum). The maximum should be preserved and not be clipped to a lower value:

$$\phi(x) = \begin{cases} 21 \sin^2(3\pi(x - \frac{1}{6})) & \text{for } \frac{1}{6} \leq x \leq \frac{1}{2}, \\ 20 & \text{elsewhere.} \end{cases} \quad (3.2)$$

semi The semi ellipse which is basically a combination of the two previous profiles:

$$\phi(x) = \begin{cases} 21 \sqrt{1 - (\frac{x - \frac{1}{3}}{\frac{1}{6}})^2} & \text{for } \frac{1}{6} \leq x \leq \frac{1}{2}, \\ 20 & \text{elsewhere.} \end{cases} \quad (3.3)$$

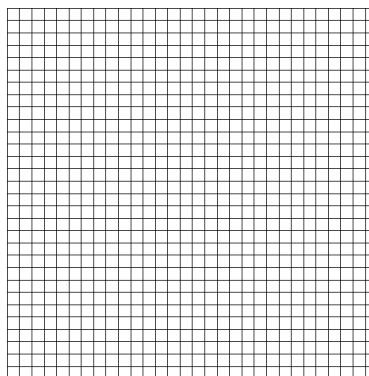


Figure 3.1: Mesh model c3

3.1 Step cases

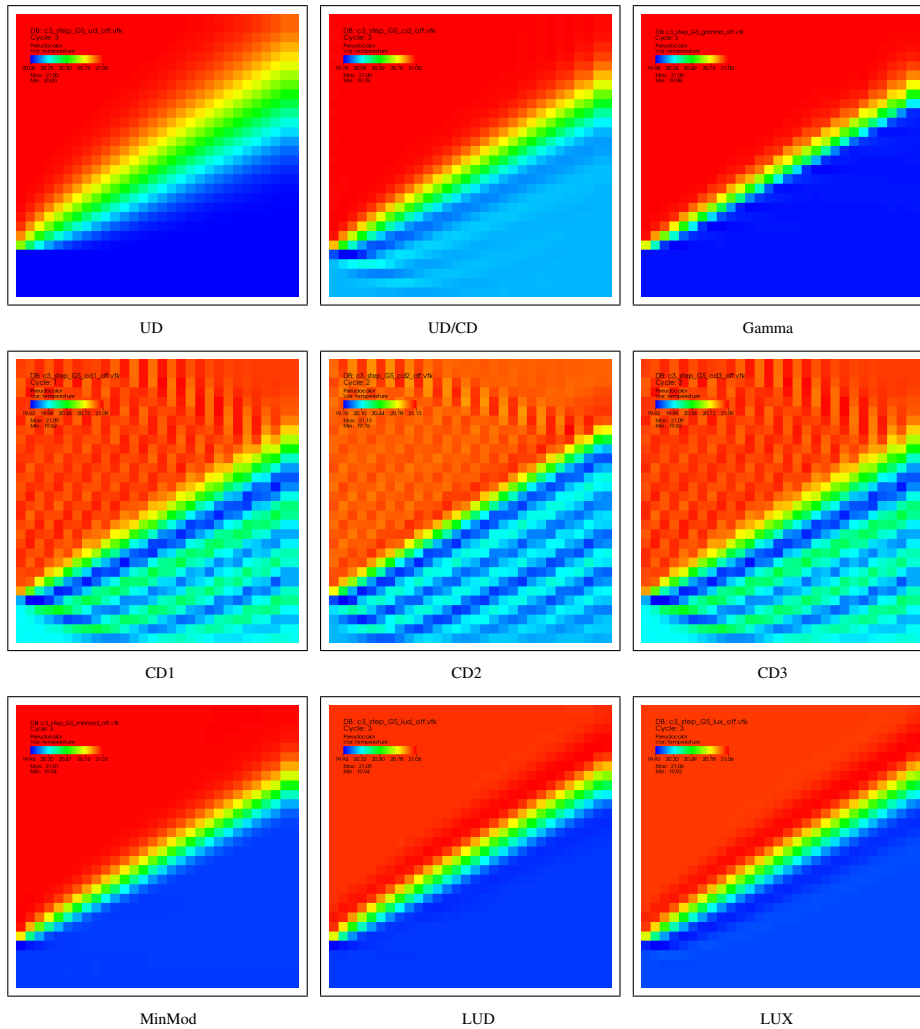


Figure 3.2: Standard Leonard step cases with Gauss, no limiter

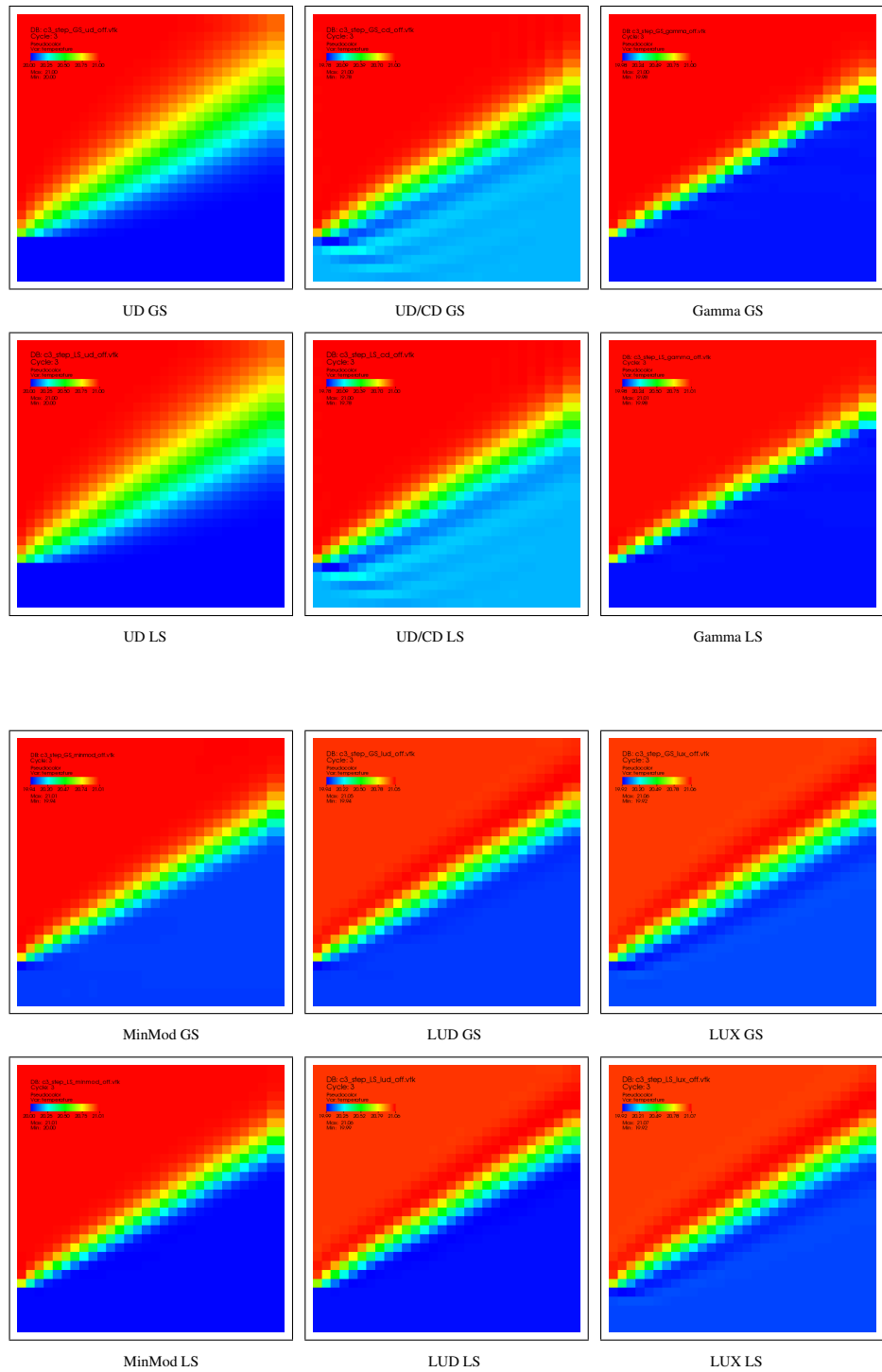


Figure 3.3: Standard Leonard step cases with Gauss (GS) and Least Squares (LS), no limiters used

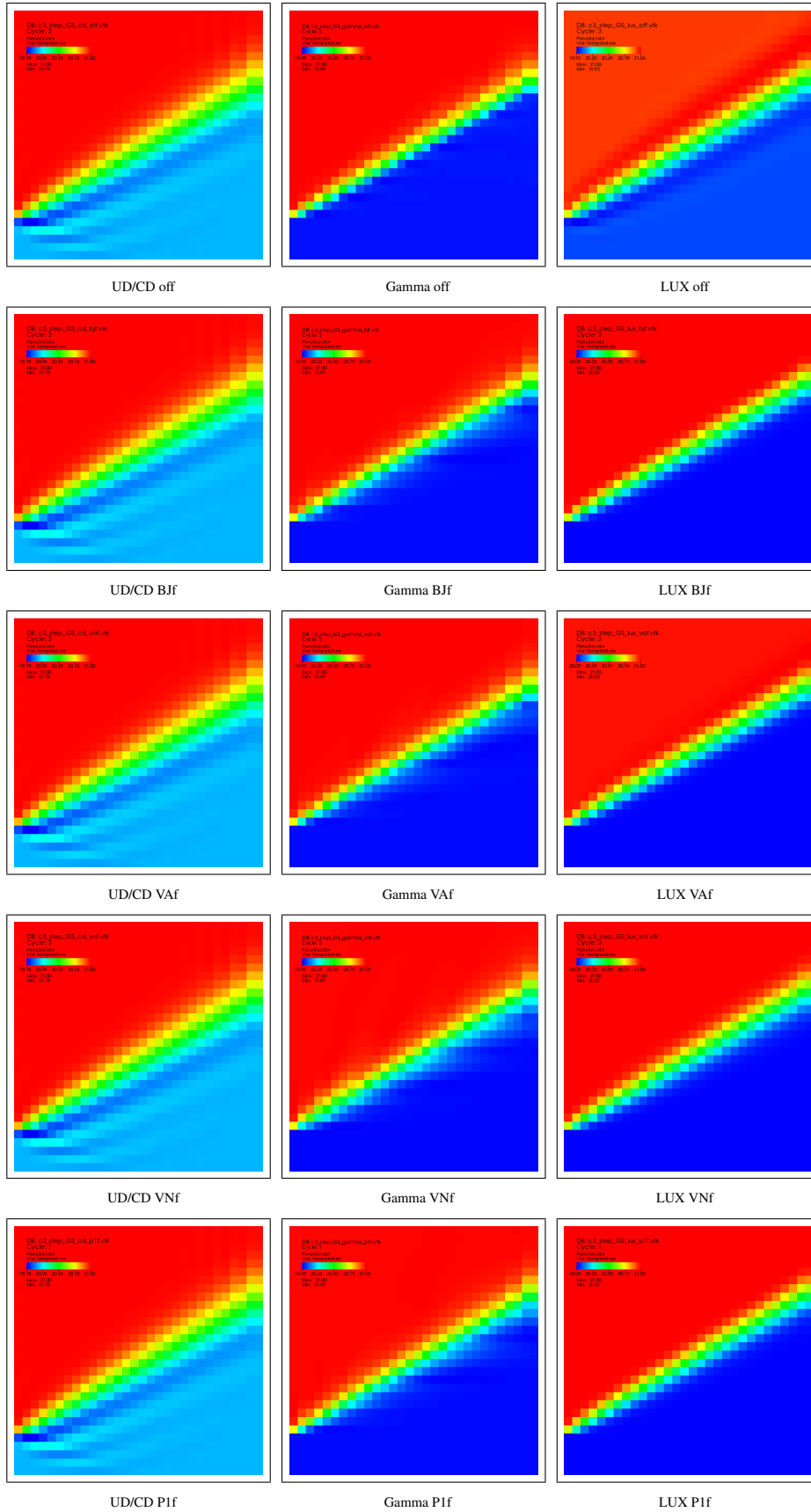


Figure 3.4: Leonard step cases with Gauss and face based limiters

3.2 Sin2 cases

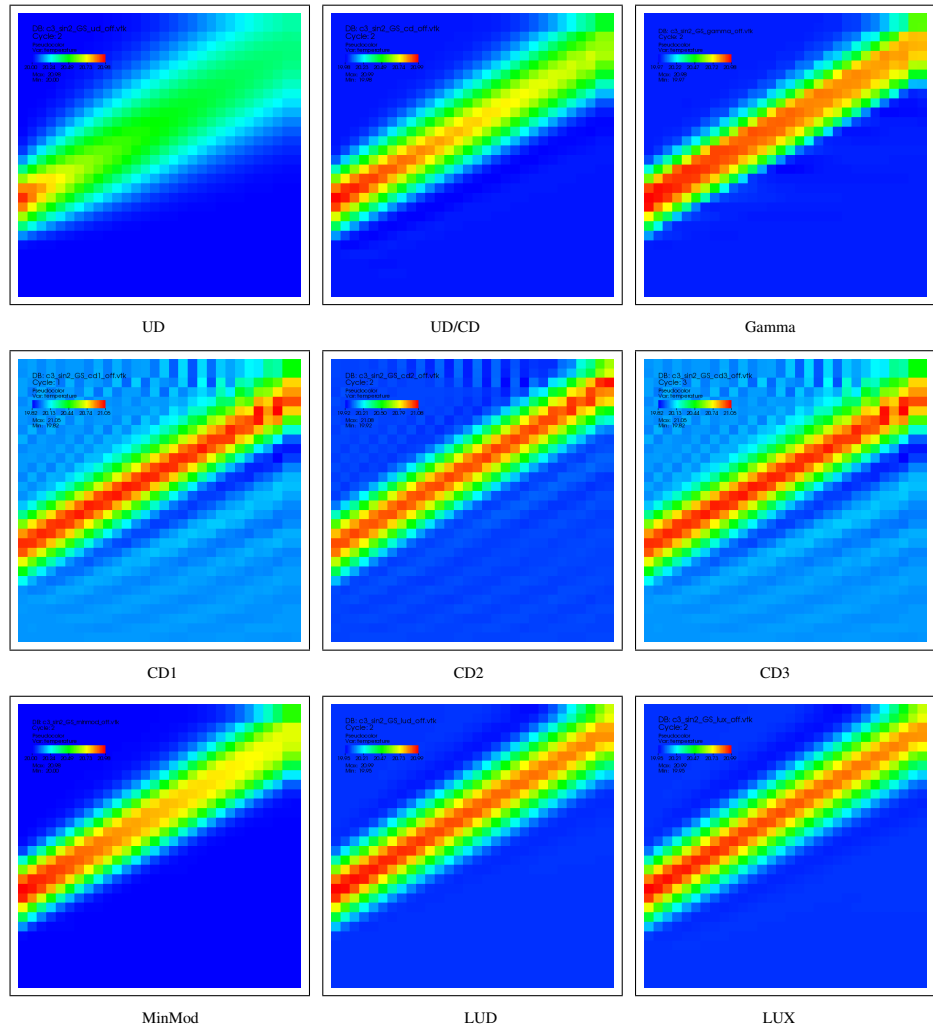


Figure 3.5: Standard Leonard sin2 cases with Gauss, no limiter

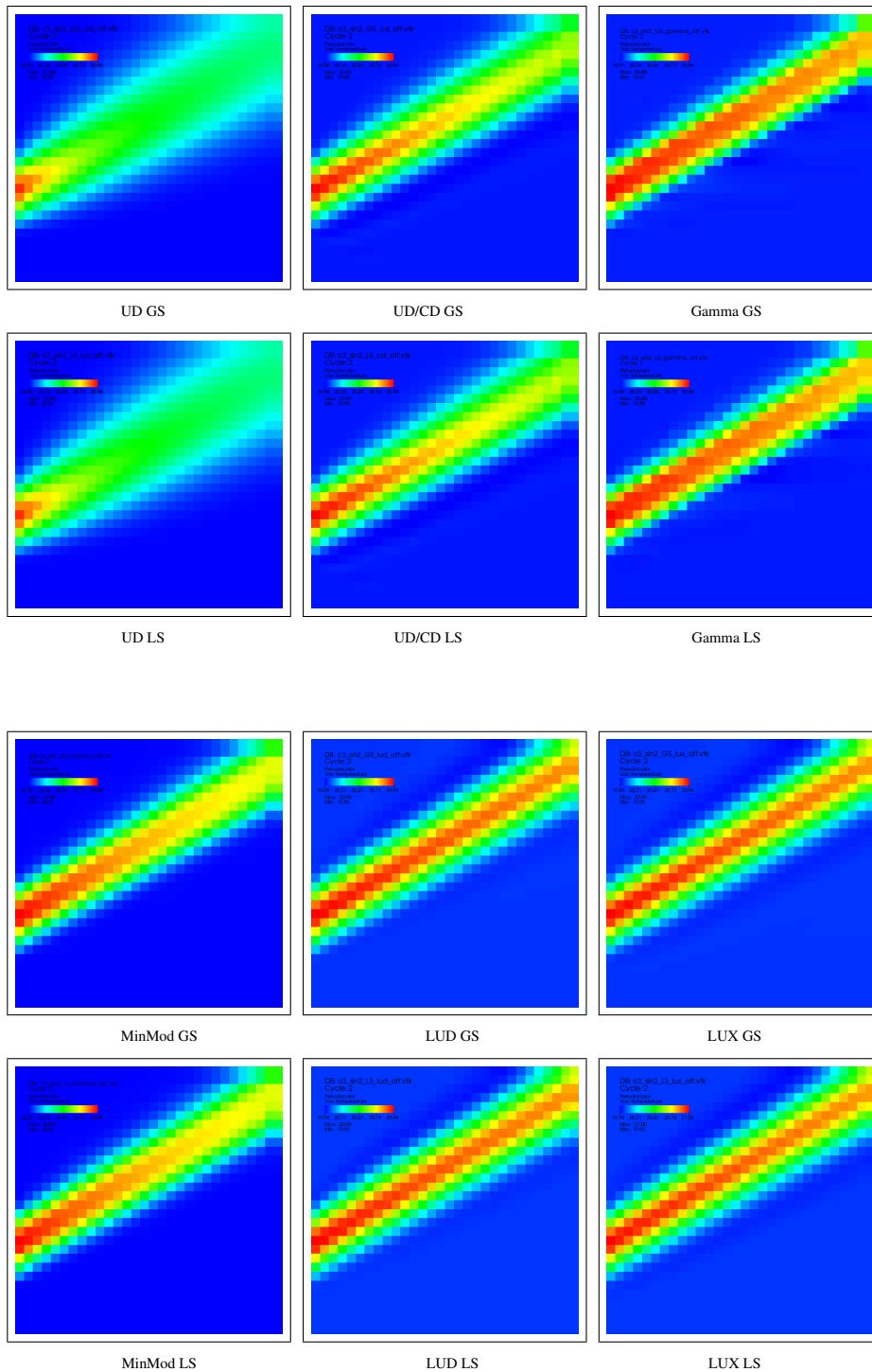


Figure 3.6: Standard Leonard sin2 cases with Gauss (GS) and Least Squares (LS), no limiters used

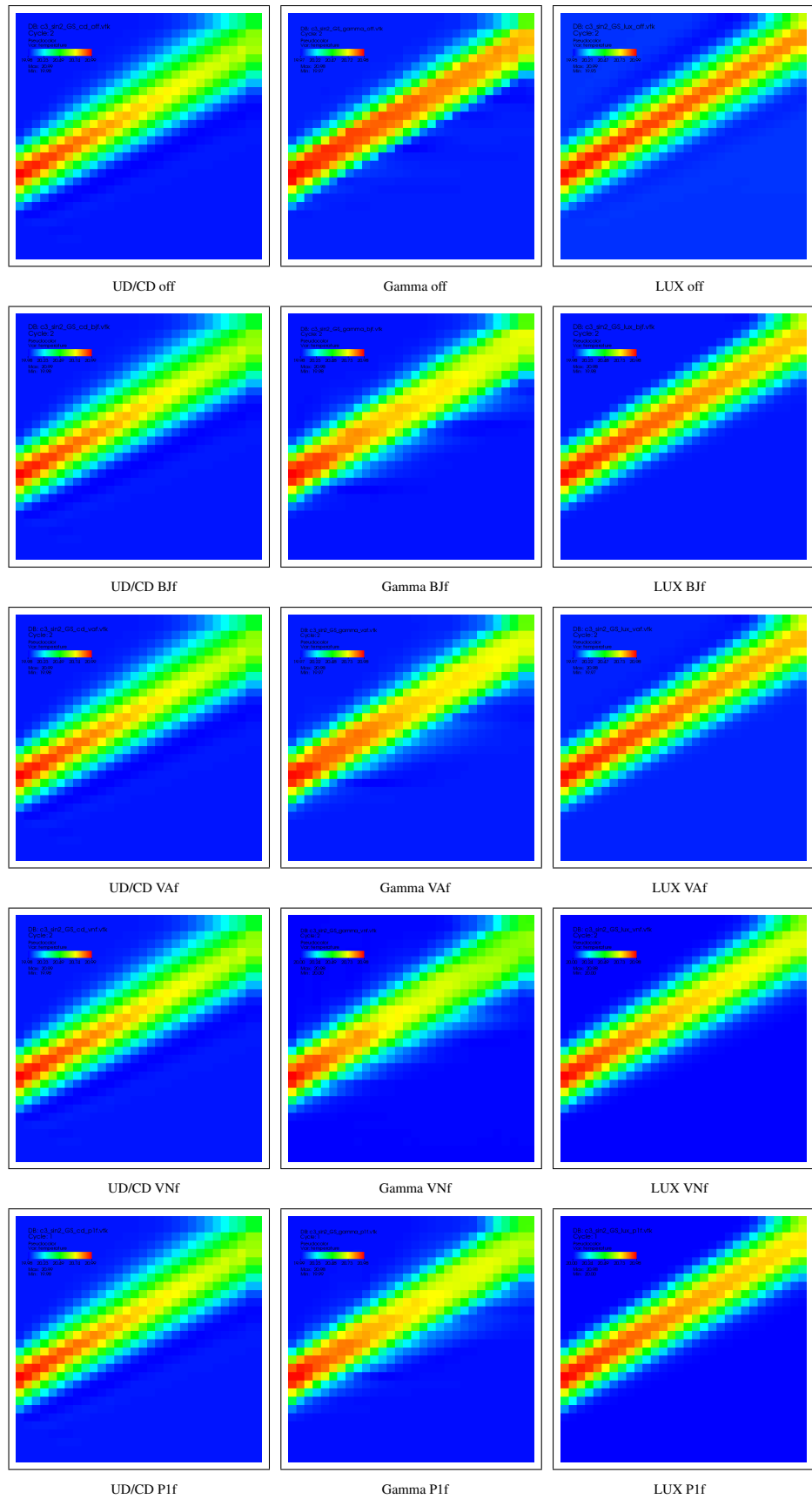


Figure 3.7: Leonard sin2 cases with Gauss and face based limiters

3.3 Semi ellipse cases

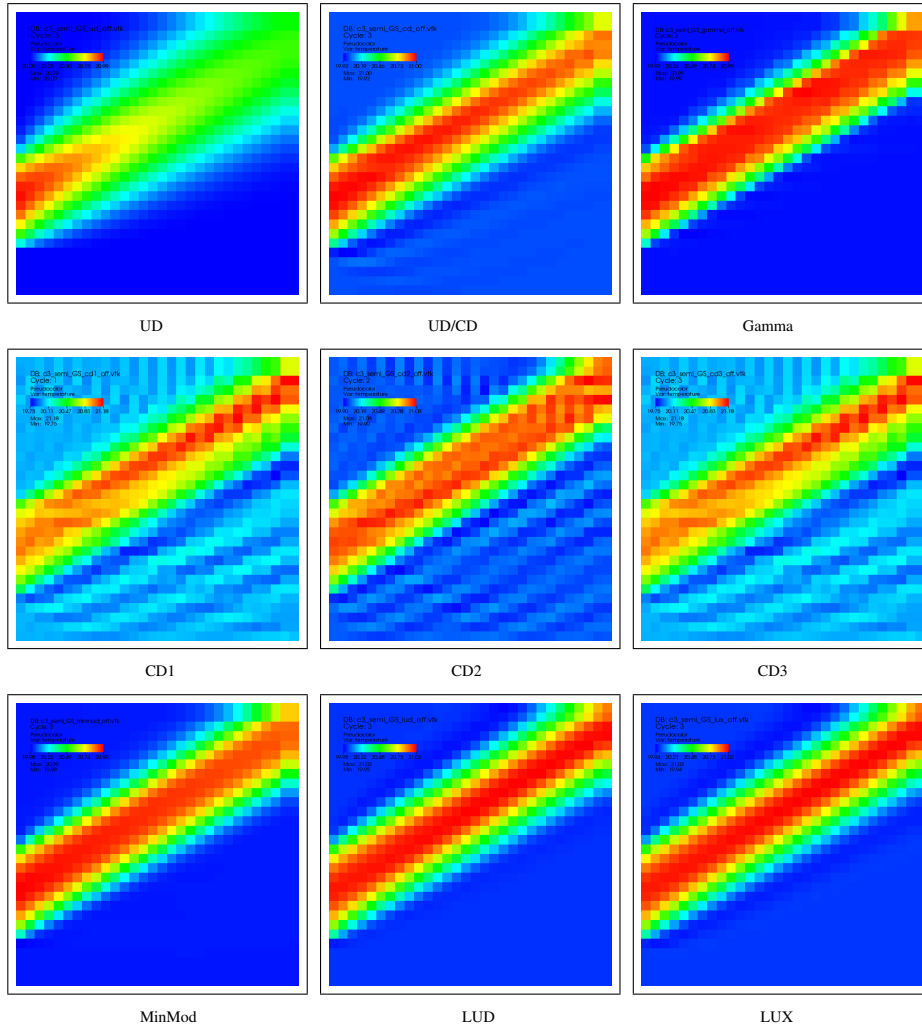


Figure 3.8: Standard Leonard semi cases with Gauss, no limiter

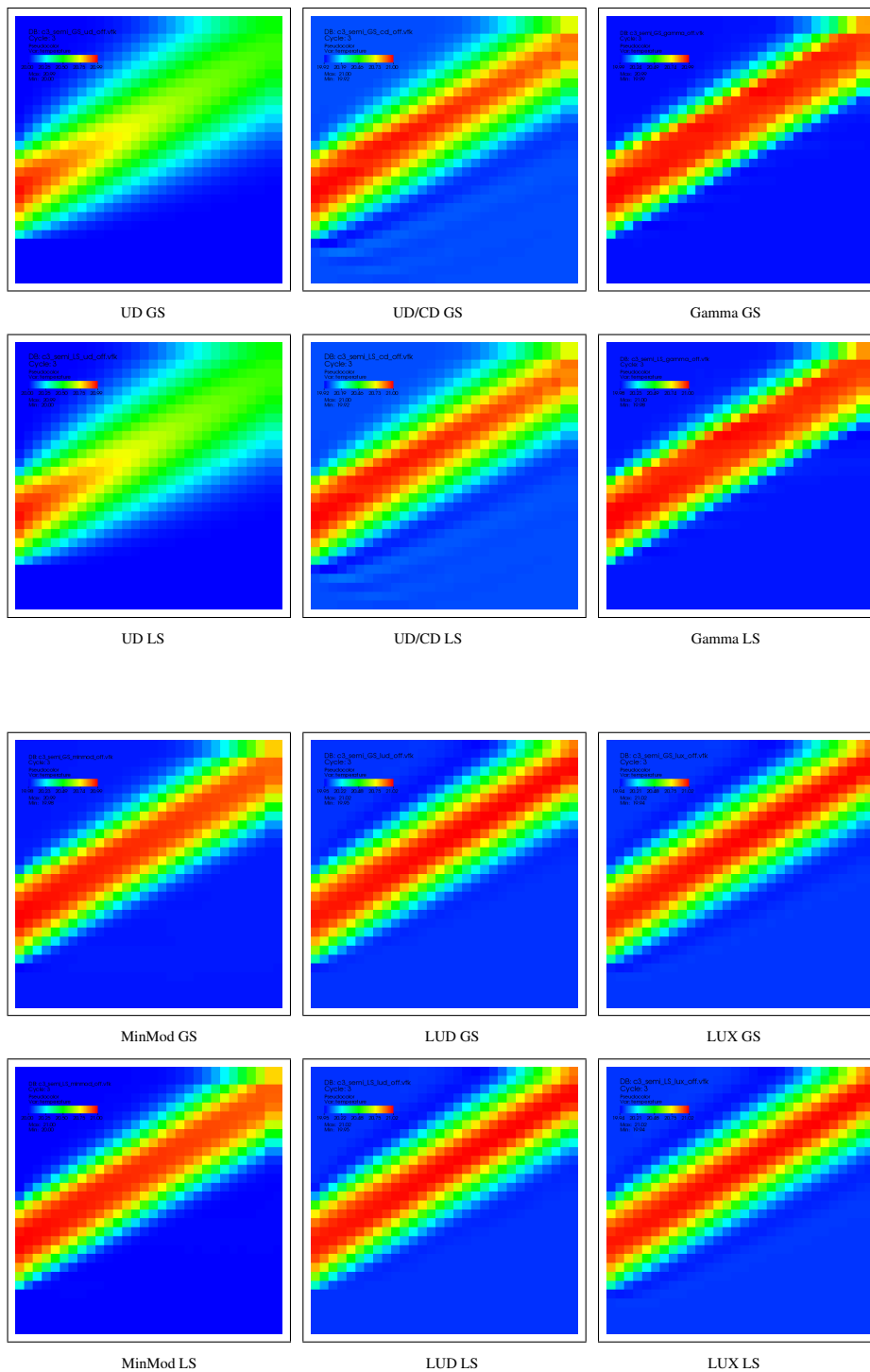


Figure 3.9: Standard Leonard semi cases with Gauss (GS) and Least Squares (LS), no limiters used

4

C4 Wild test

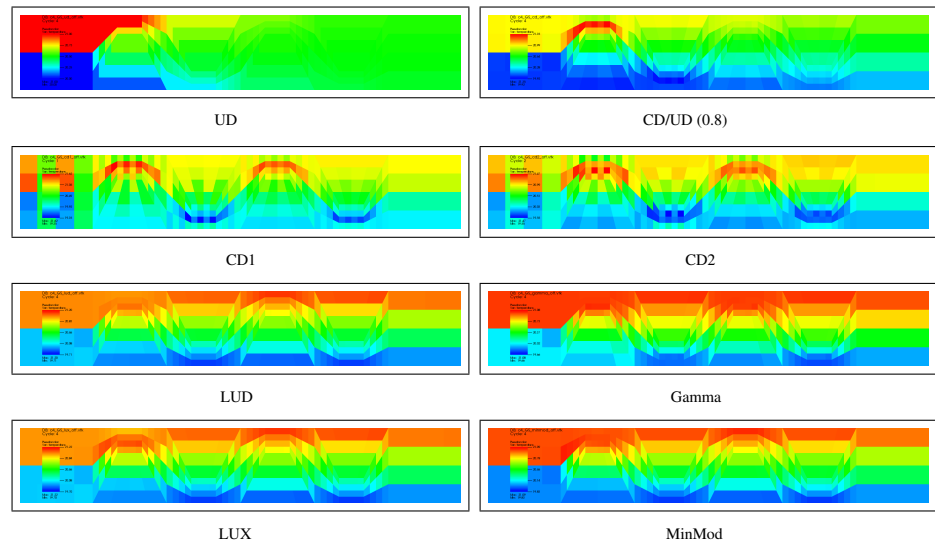


Figure 4.1: Wild case, all Gauss, no limiter

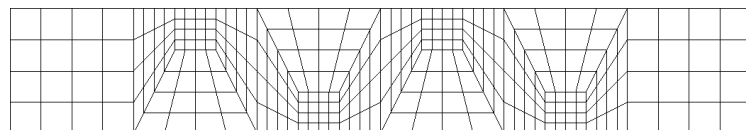


Figure 4.2: Mesh model c4

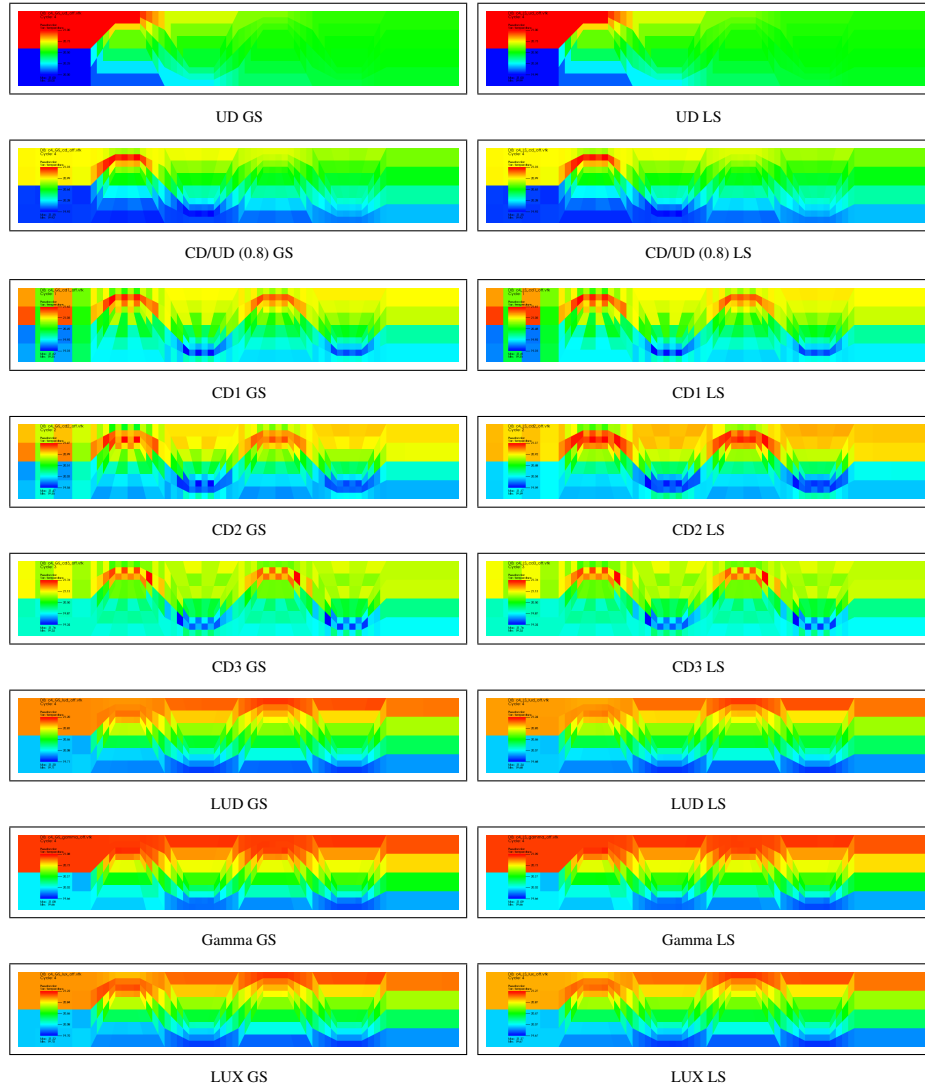


Figure 4.3: Wild case, left Gauss/right Least Squares, no limiters

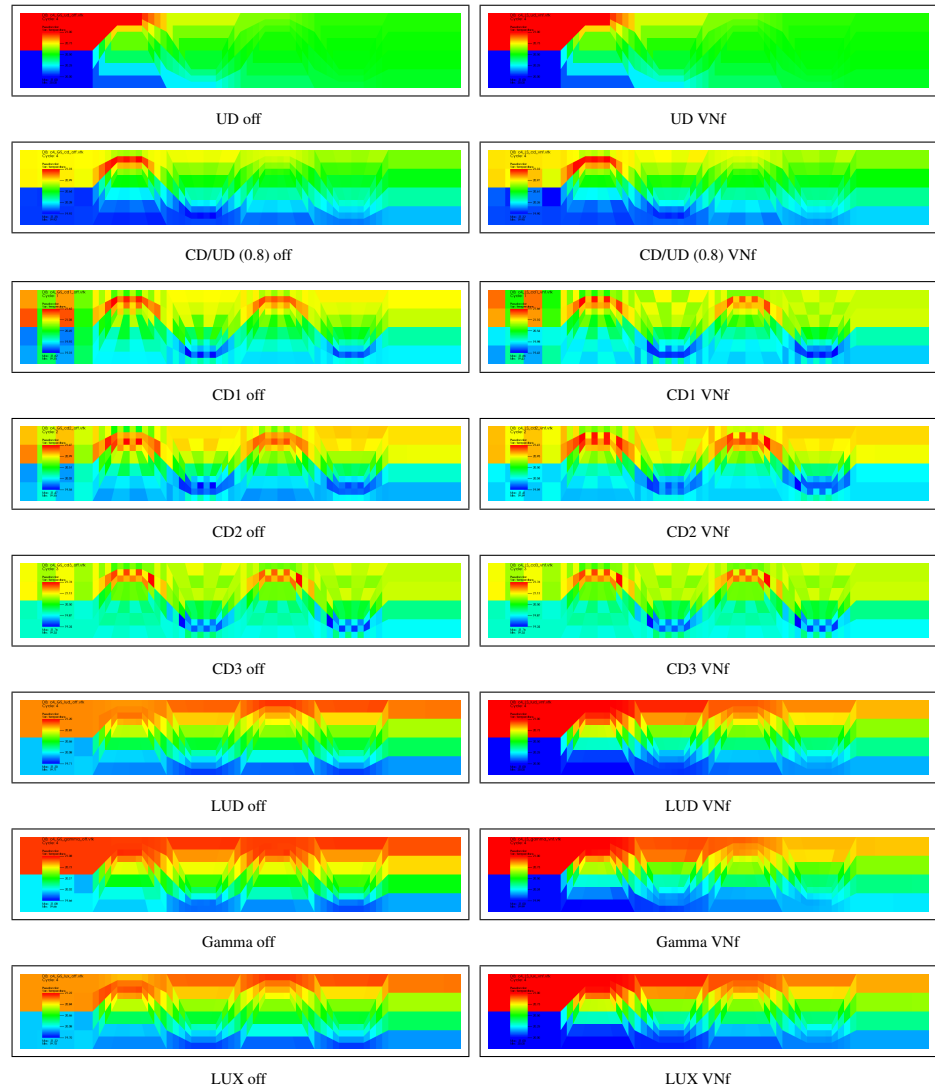


Figure 4.4: Wild case, Gauss, left no limiter/right VNF

5

C6 Wedges

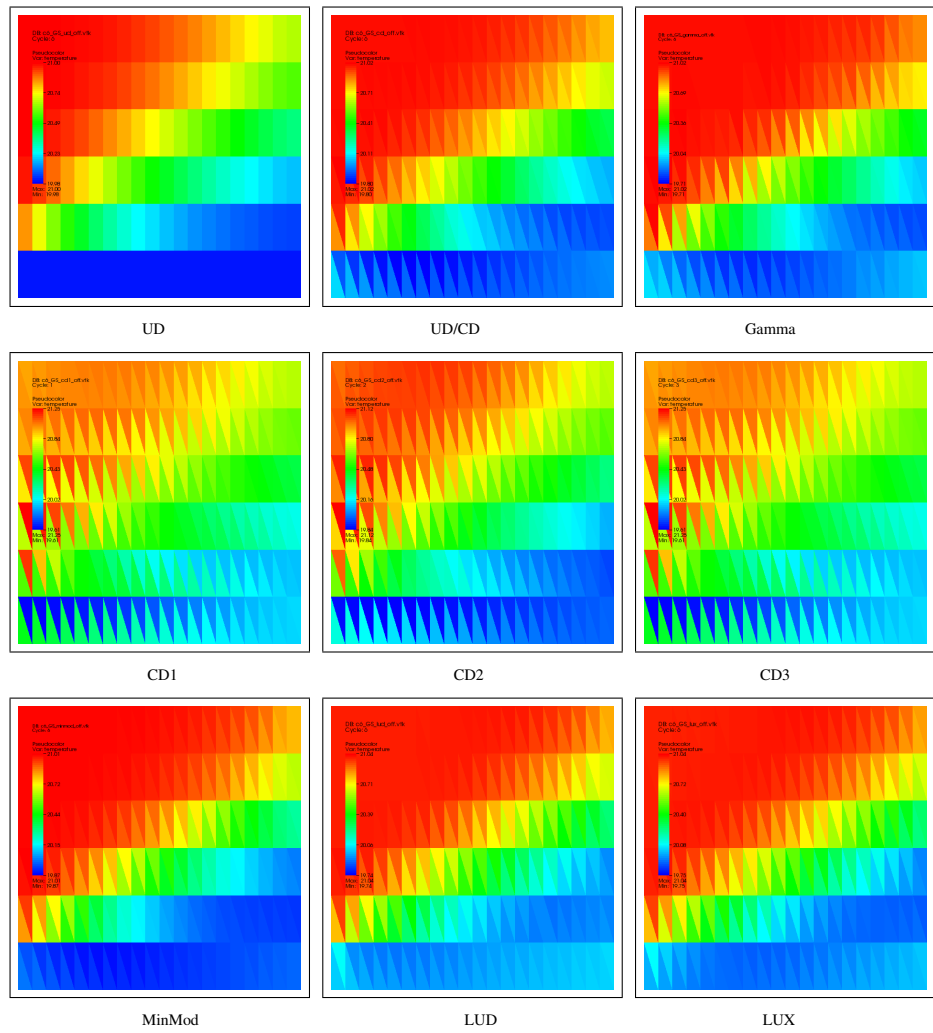


Figure 5.1: c6 standard wedge cases with Gauss, no limiter

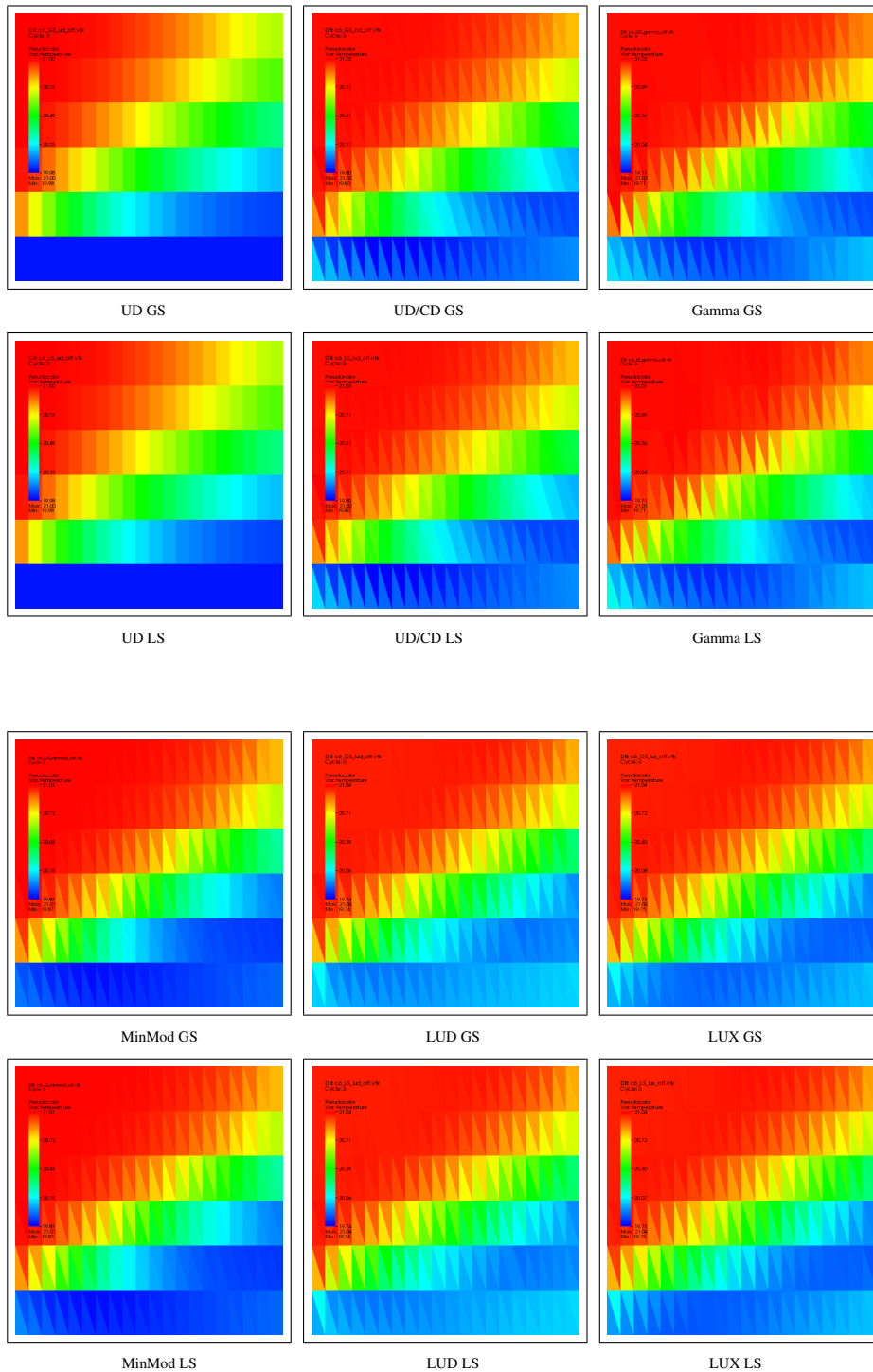


Figure 5.2: c6 standard wedge cases with Gauss (GS) and Least Squares (LS), no limiters used

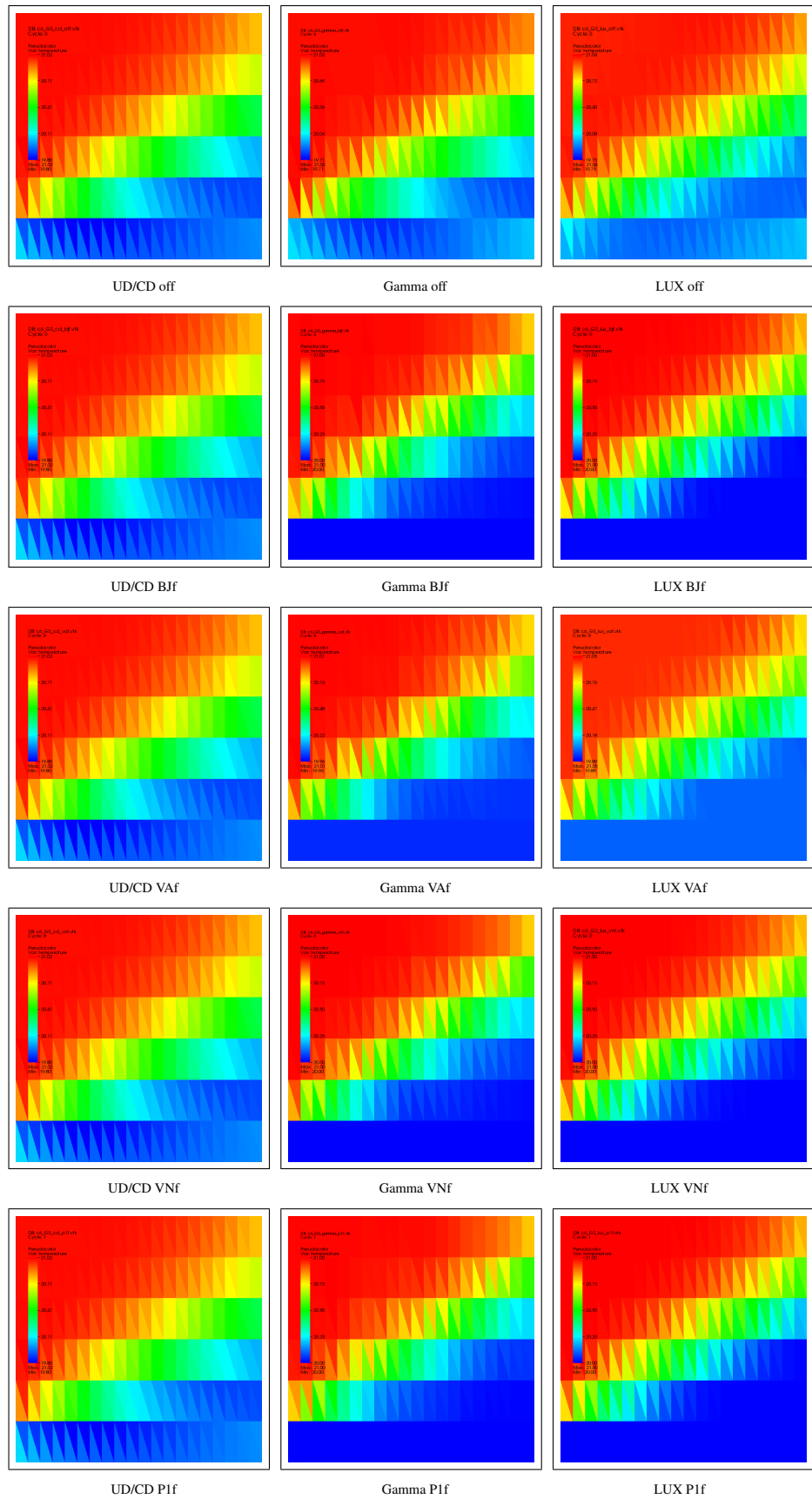


Figure 5.3: c6 wedge cases with Gauss and face based limiters

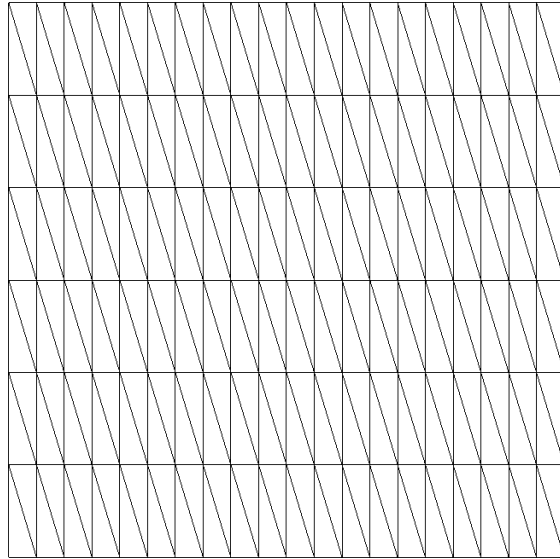


Figure 5.4: Mesh model c6

6

C7 Mesh jump

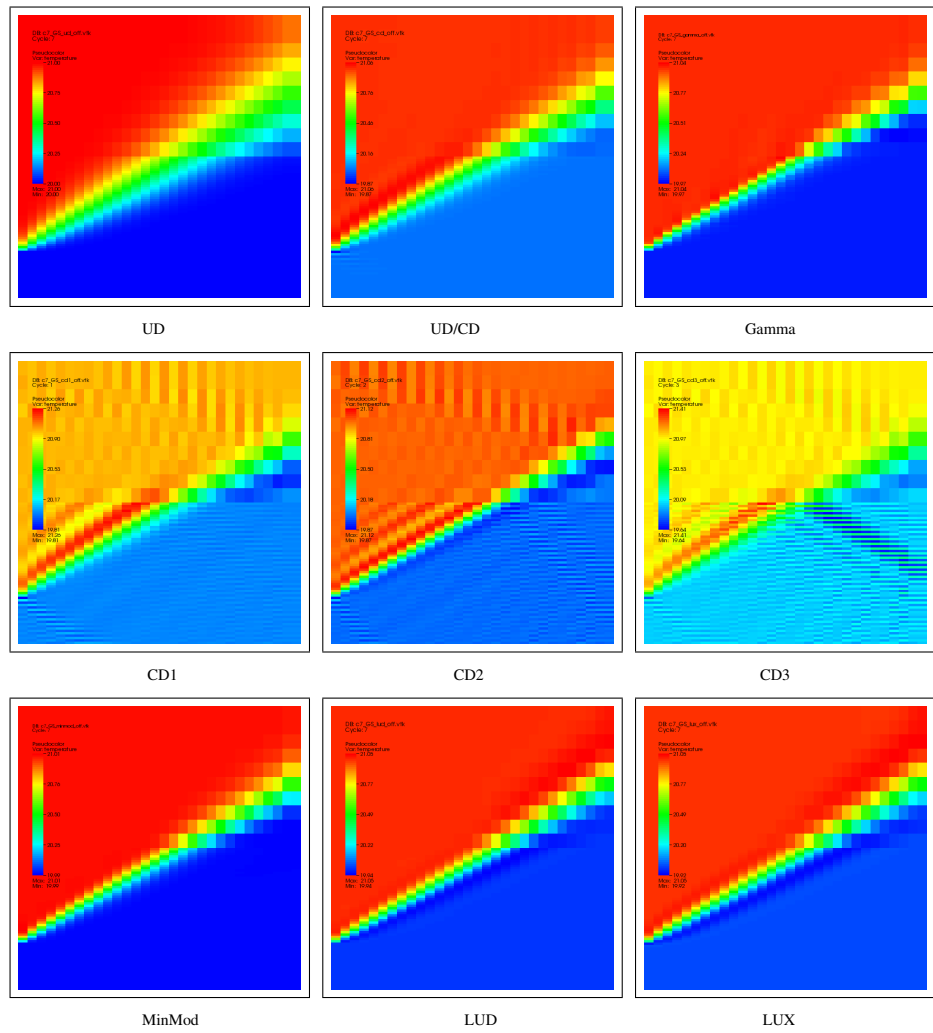


Figure 6.1: c7 mesh jump cases with Gauss, no limiter

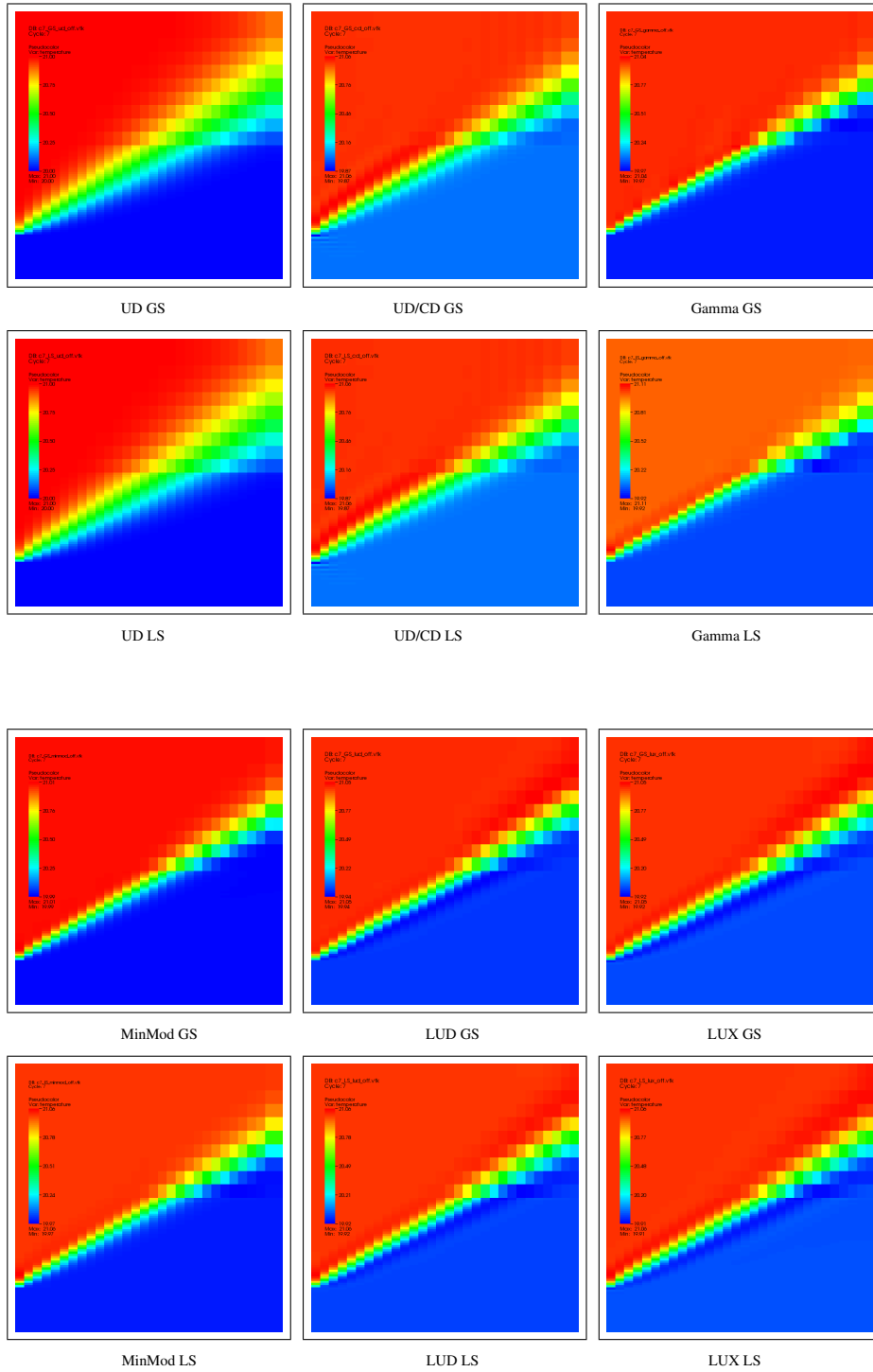


Figure 6.2: c7 mesh jump cases with Gauss (GS) and Least Squares (LS), no limiters used

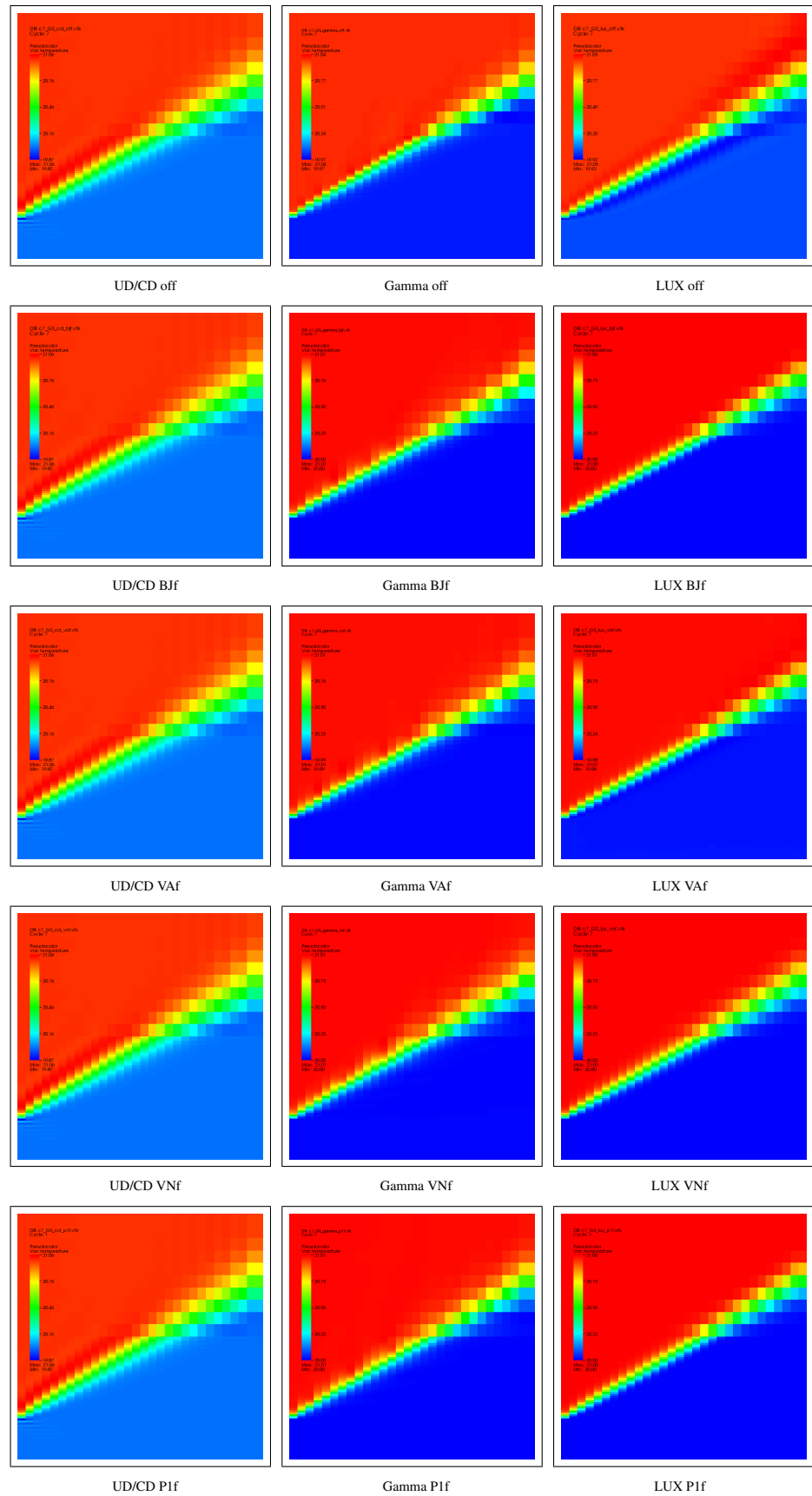


Figure 6.3: c7 mesh jump cases with Gauss and face based limiters

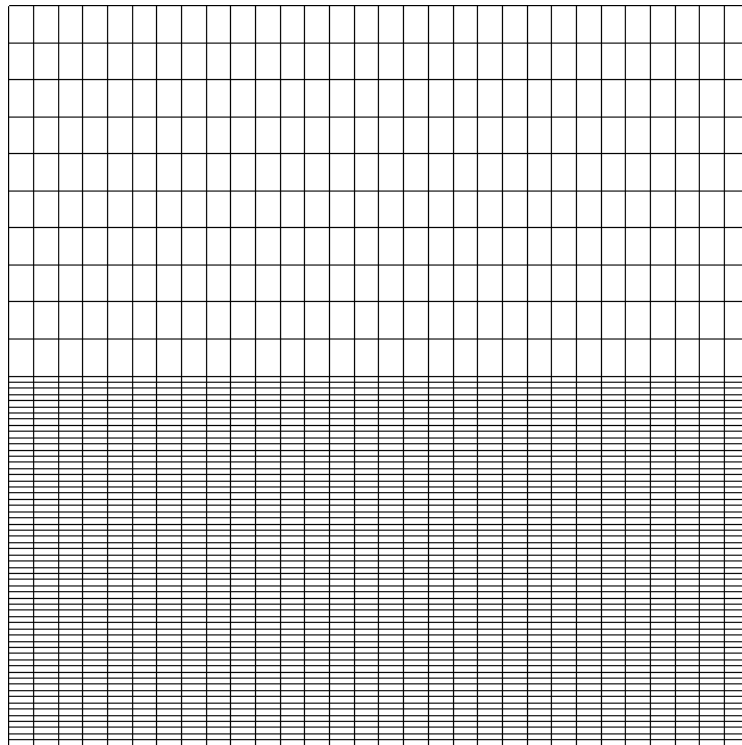


Figure 6.4: Mesh model c7

7

C8 Embedded refinement

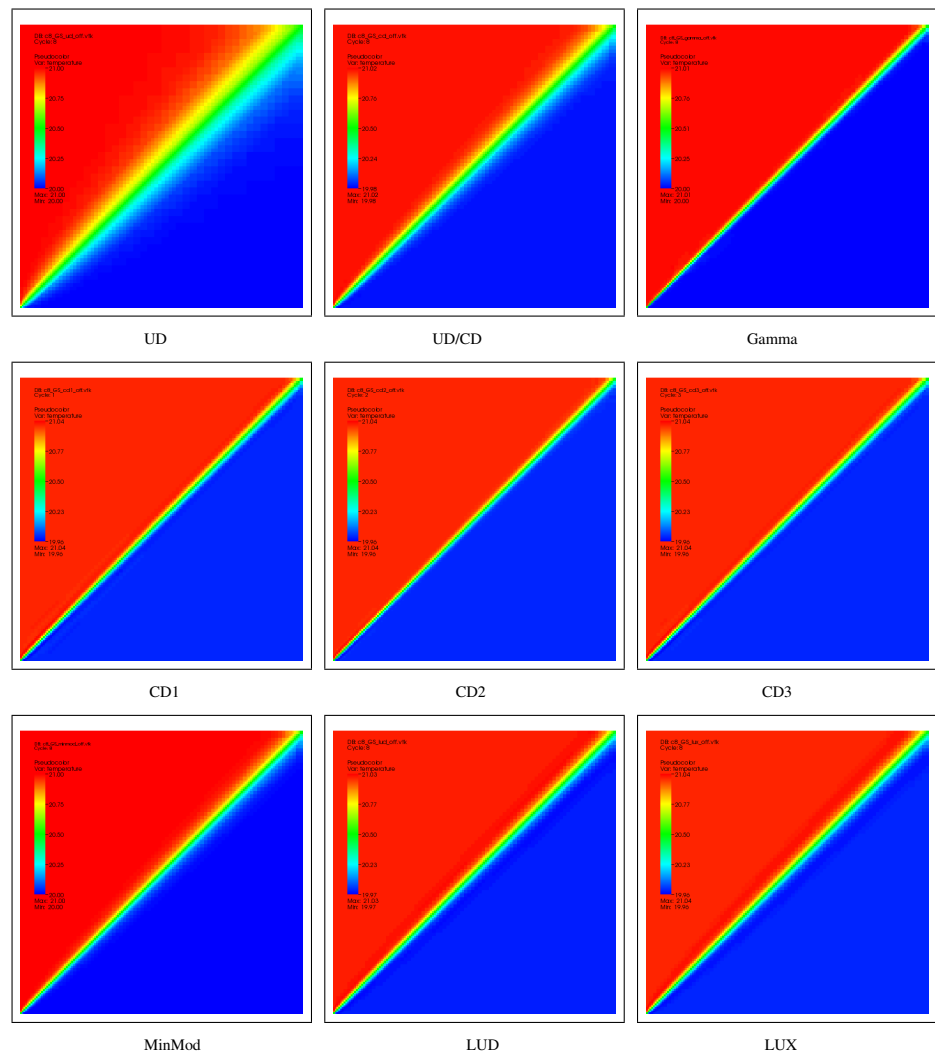


Figure 7.1: c8 refinement cases with Gauss, no limiter

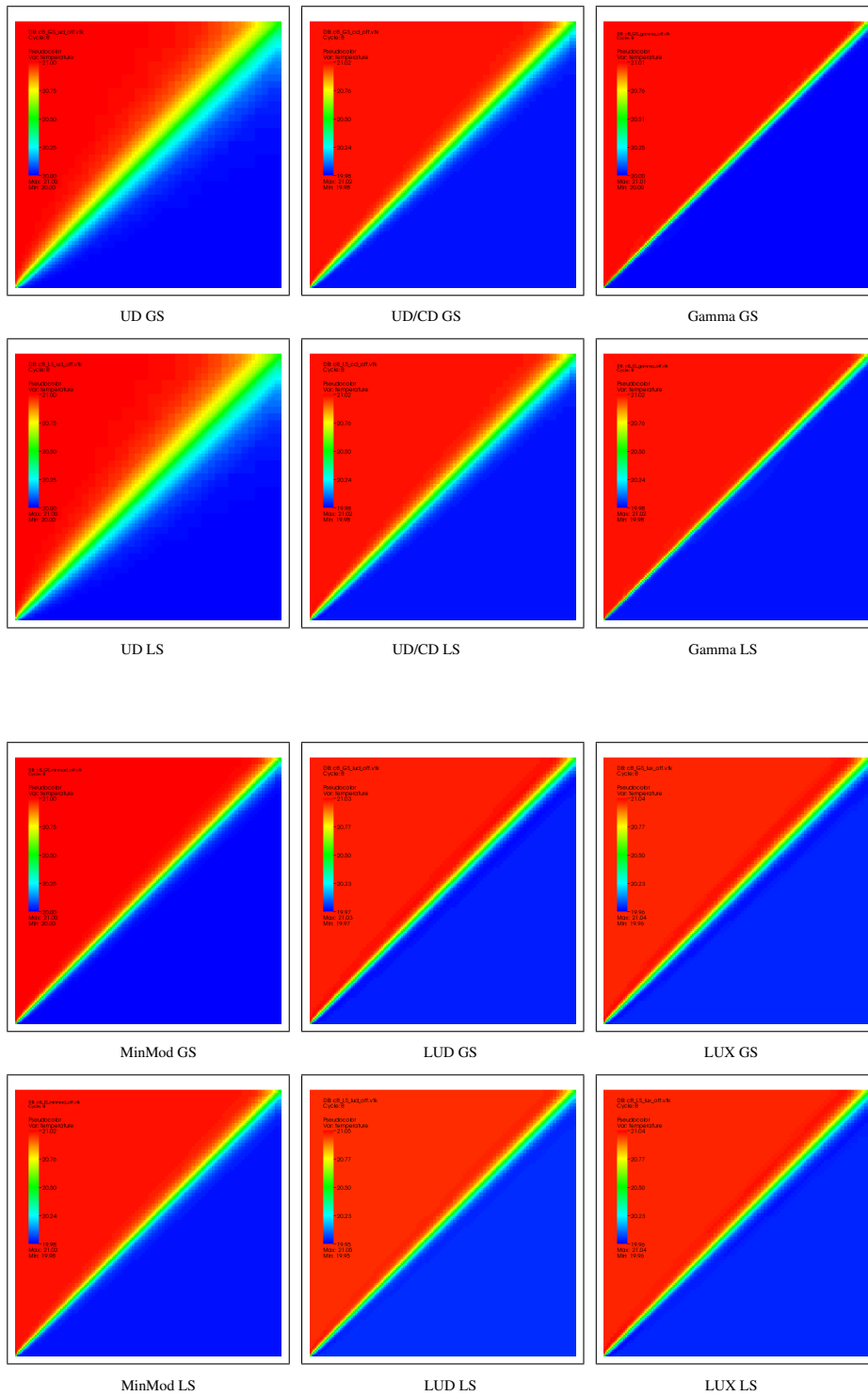


Figure 7.2: c8 refinement cases with Gauss (GS) and Least Squares (LS), no limiters used

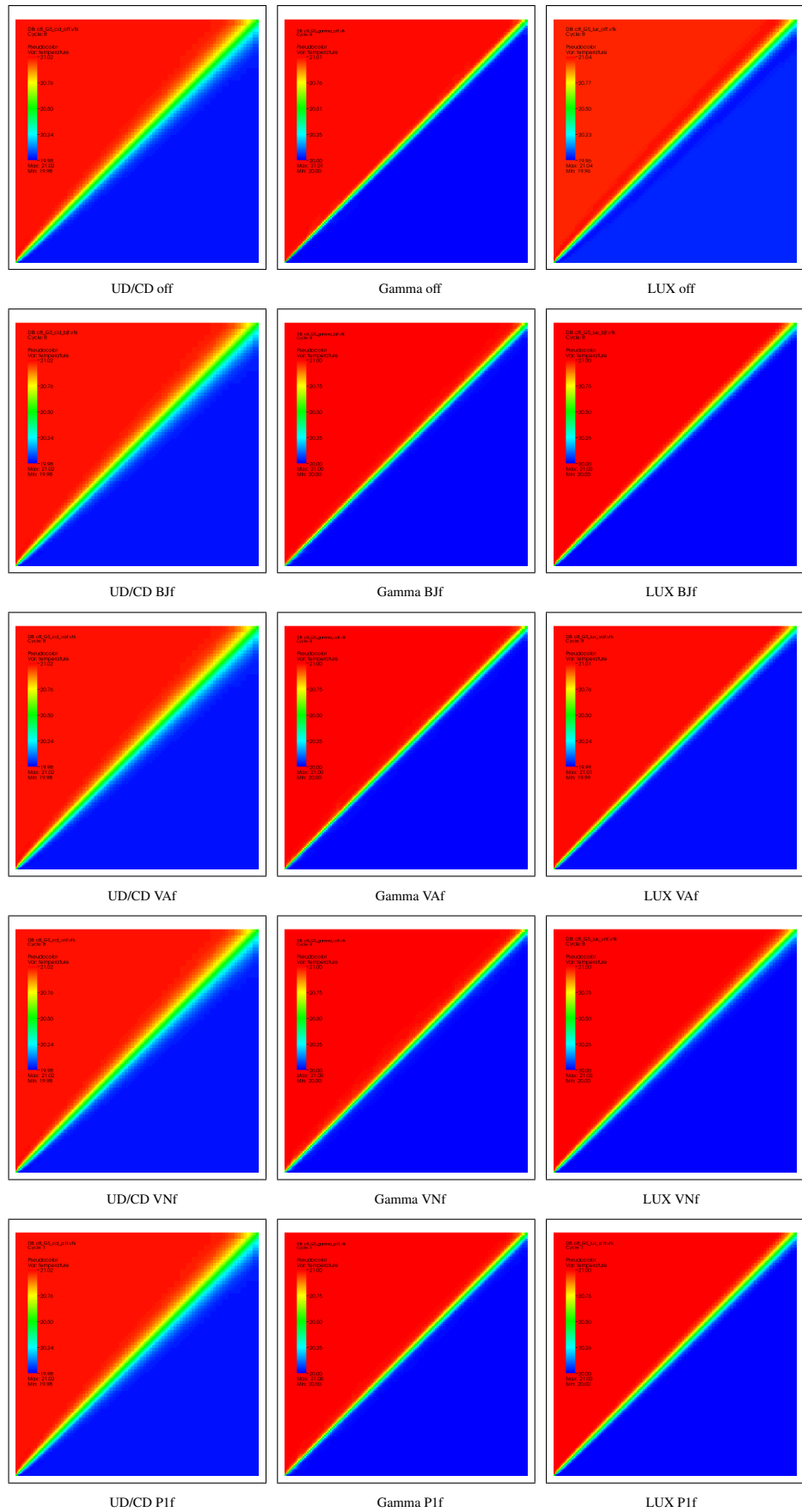


Figure 7.3: c8 refinement cases with Gauss and face based limiters

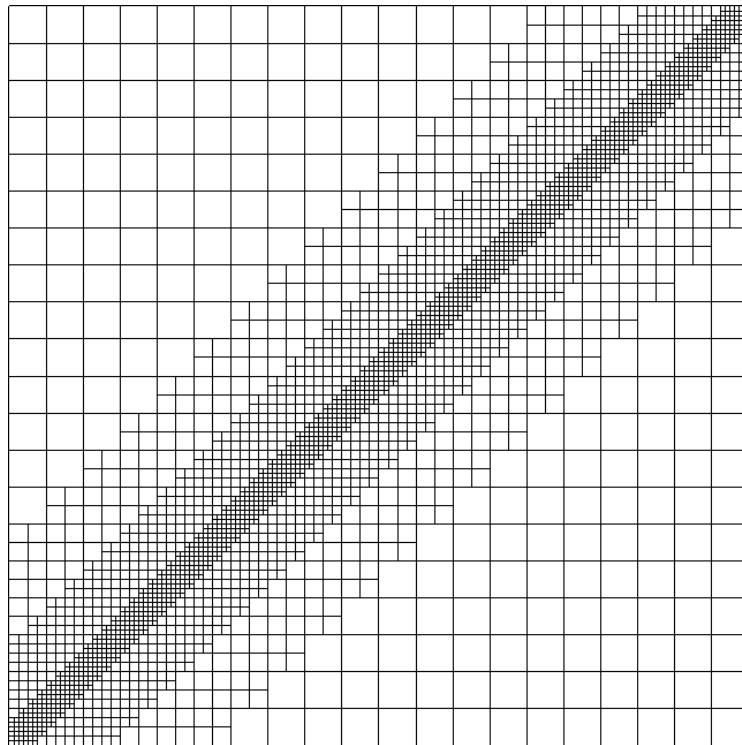


Figure 7.4: Mesh model c8

8 M6 Stagnation flow with embedded refinement

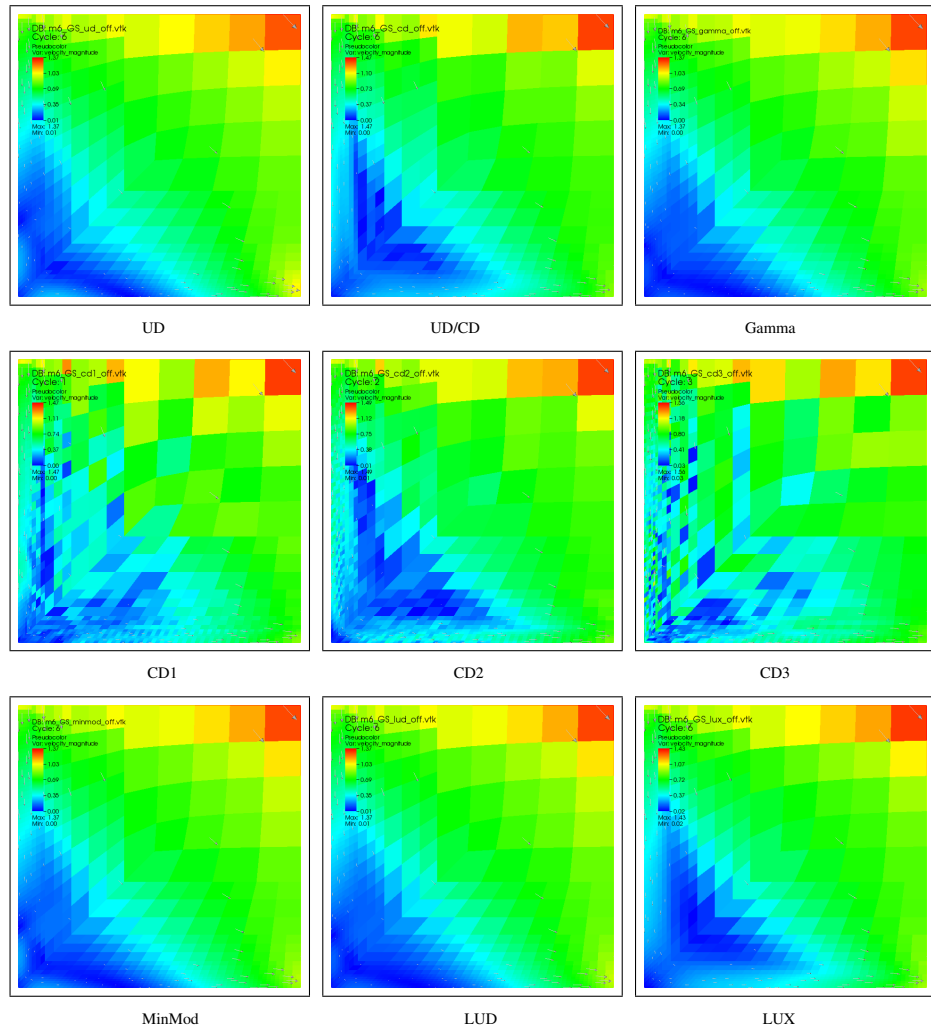


Figure 8.1: m6 refinement cases with Gauss, no limiter

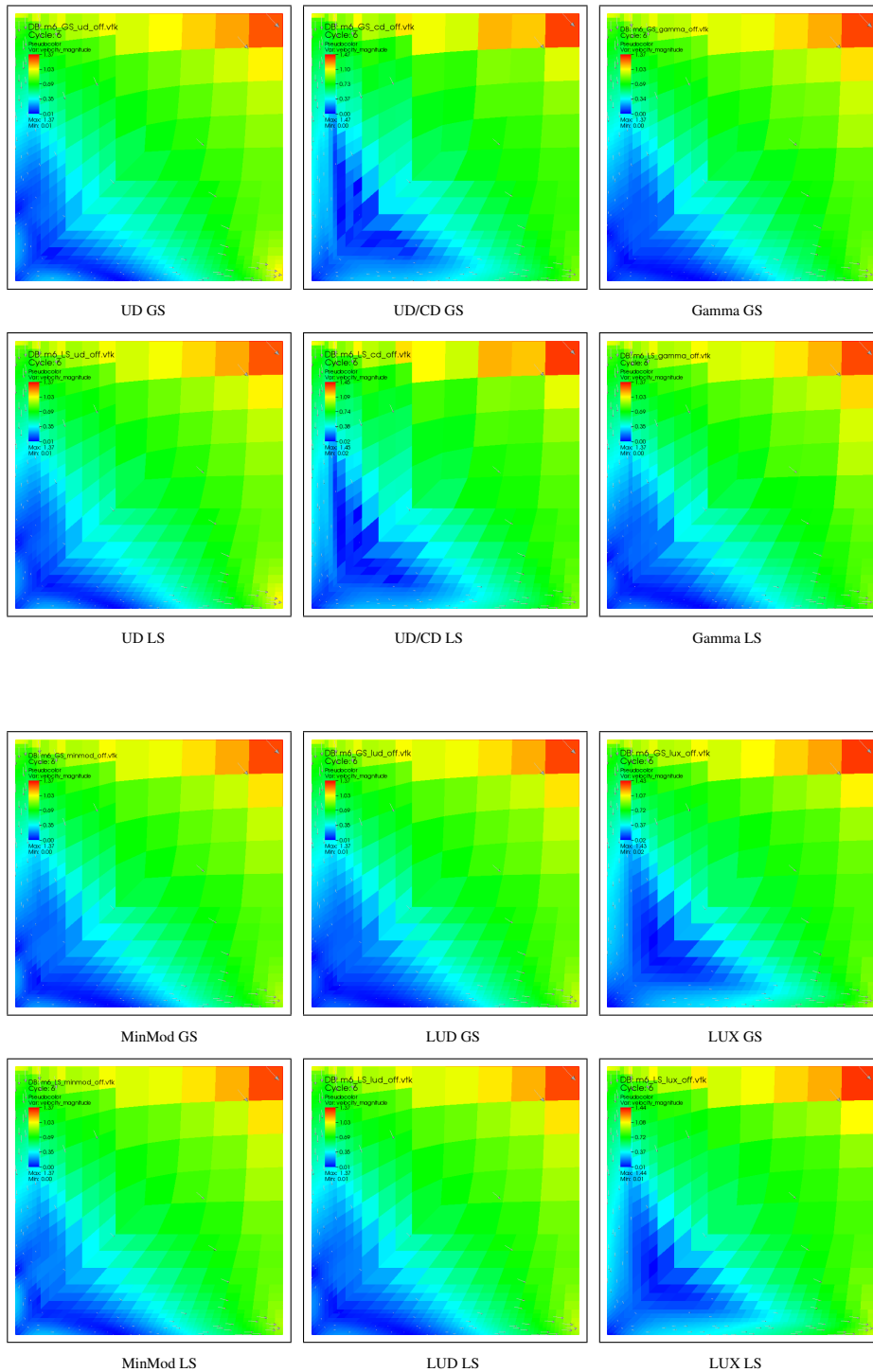


Figure 8.2: m6 refinement cases with Gauss (GS) and Least Squares (LS), no limiters used

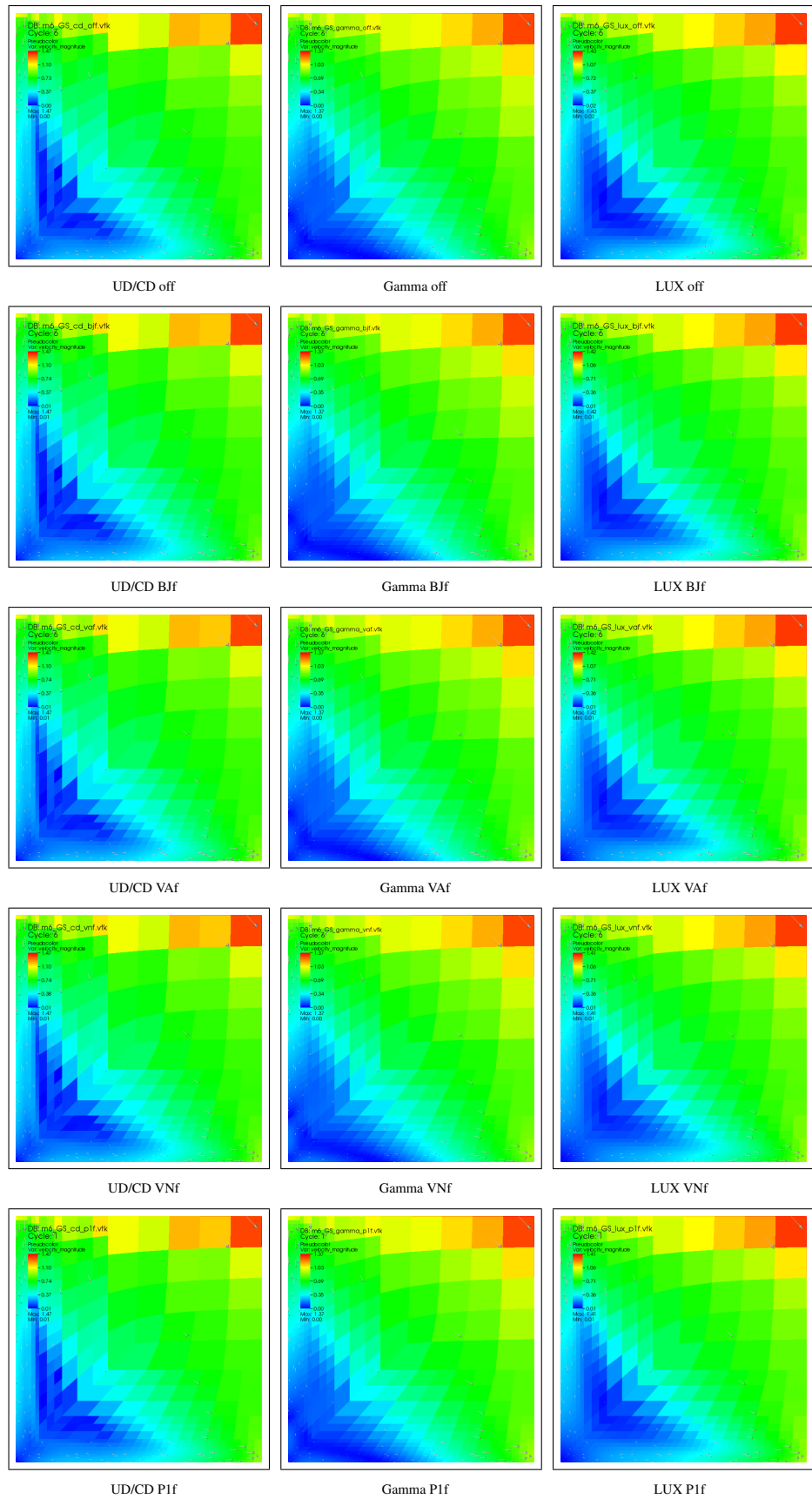


Figure 8.3: m6 refinement cases with Gauss and face based limiters

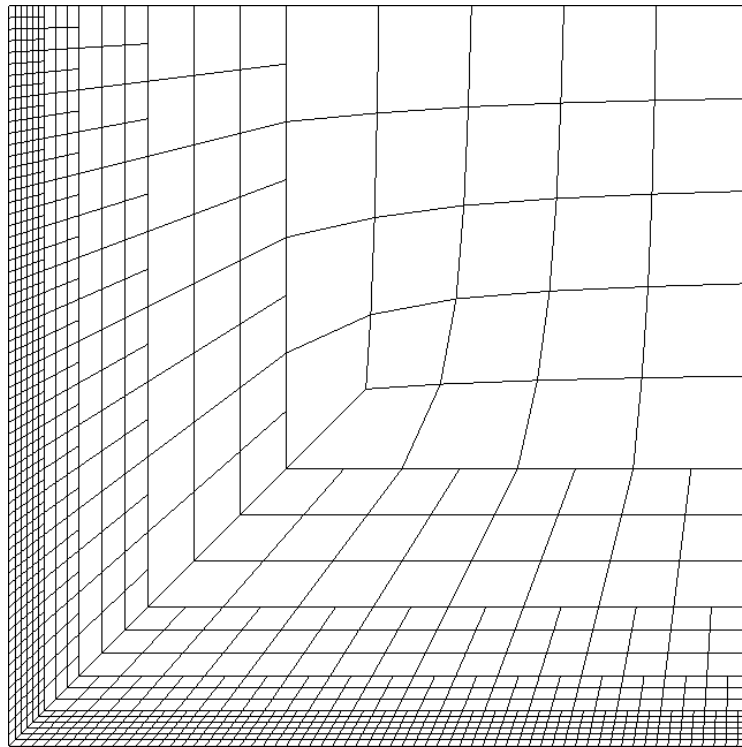


Figure 8.4: Mesh model m6

9

CAV Lid driven cavities

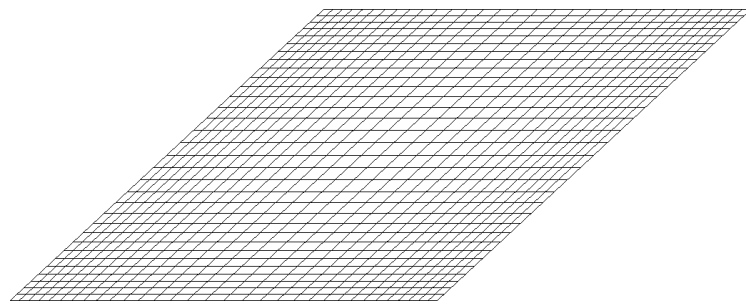


Figure 9.1: Mesh model cav45

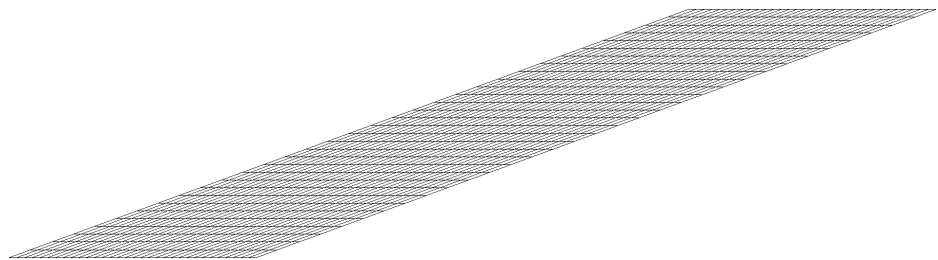


Figure 9.2: Mesh model cav20

9.1 Hexahedra at 45 degrees

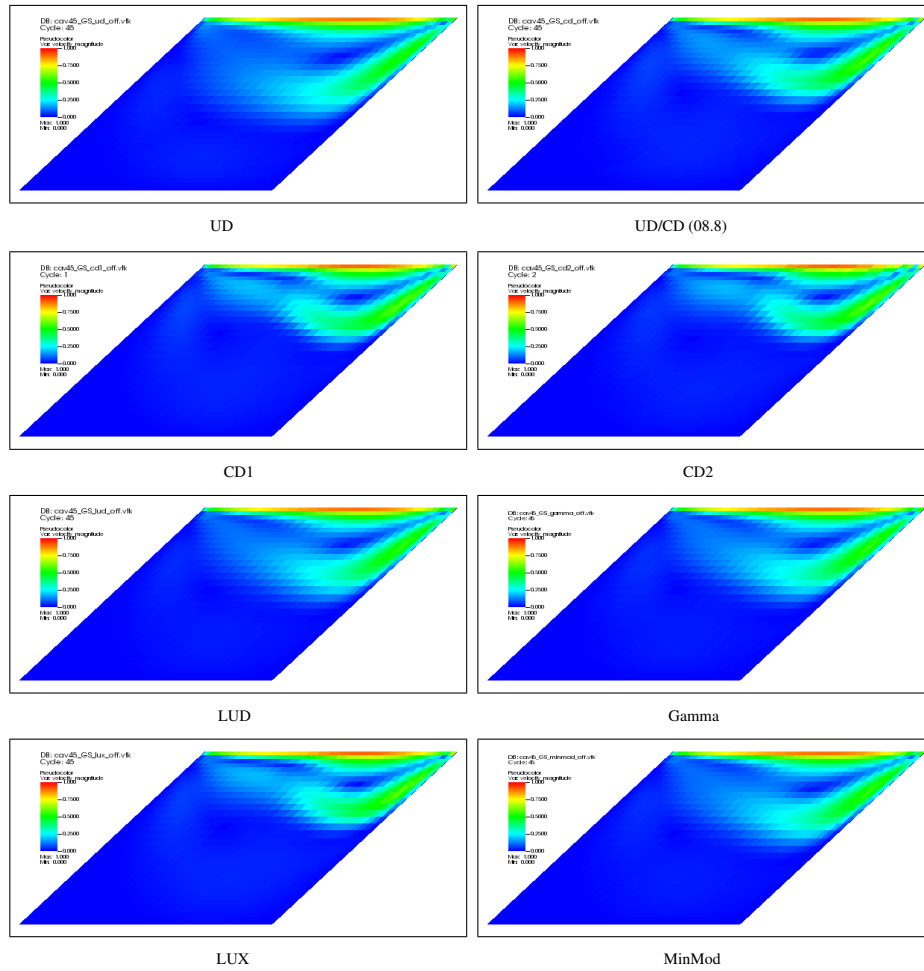


Figure 9.3: cav45 LDC at 45 degrees with Gauss, no limiter

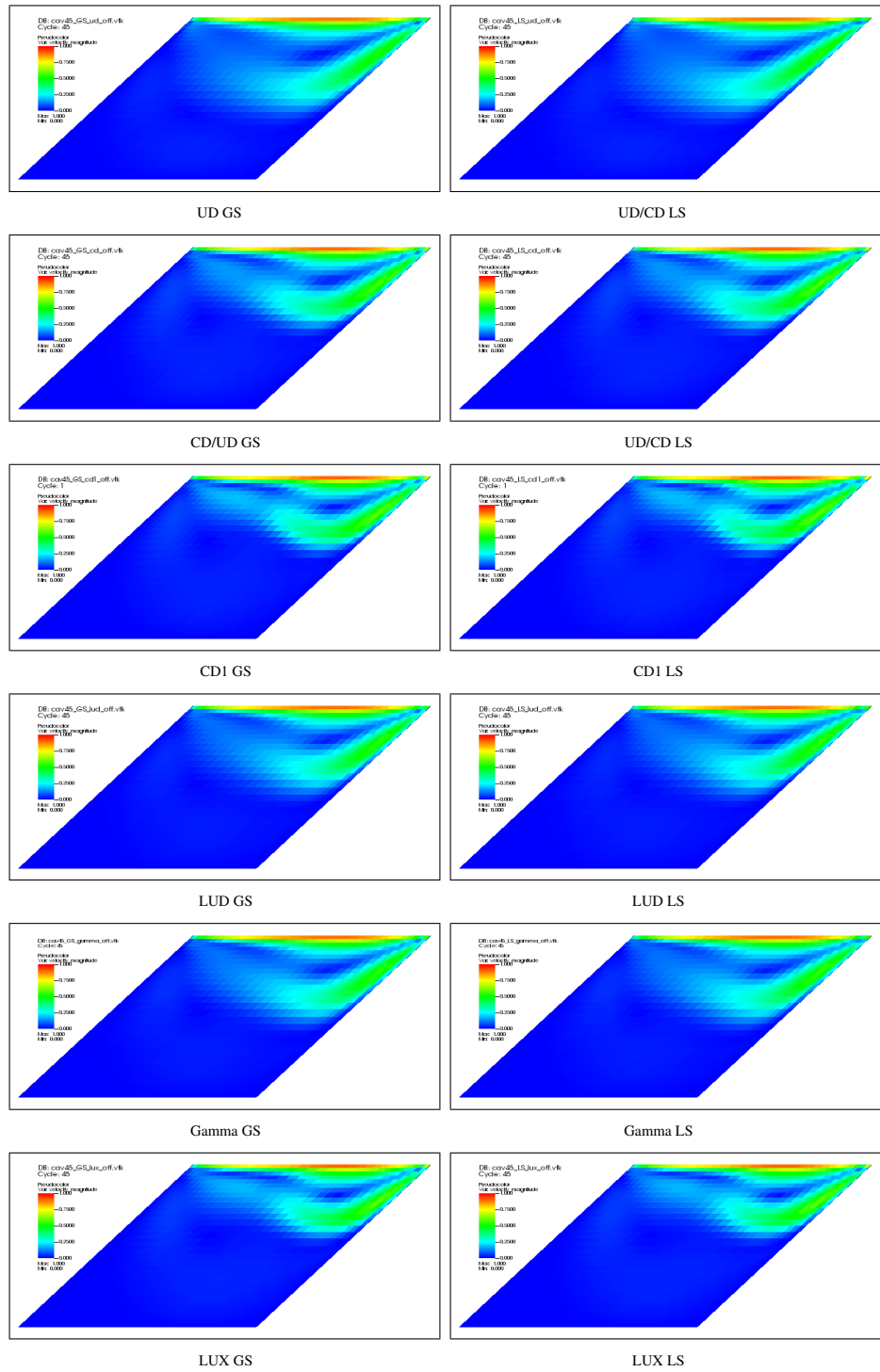


Figure 9.4: cav45 LDC 45 cases with Gauss and Least Squares, no limiters used

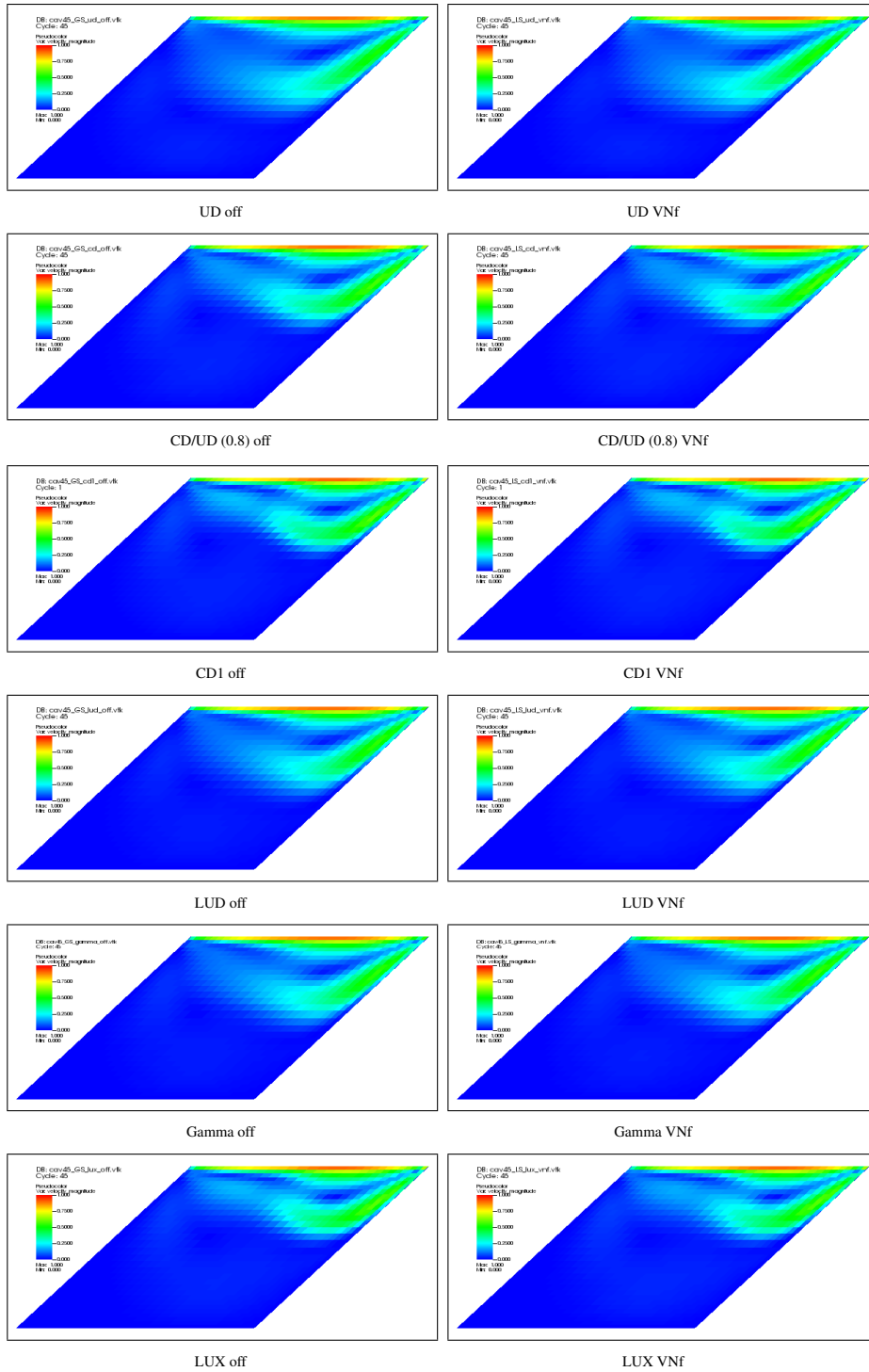


Figure 9.5: cav45 LDC 45 cases with Gauss and face based limiters

9.2 Hexahedra at 20 degrees

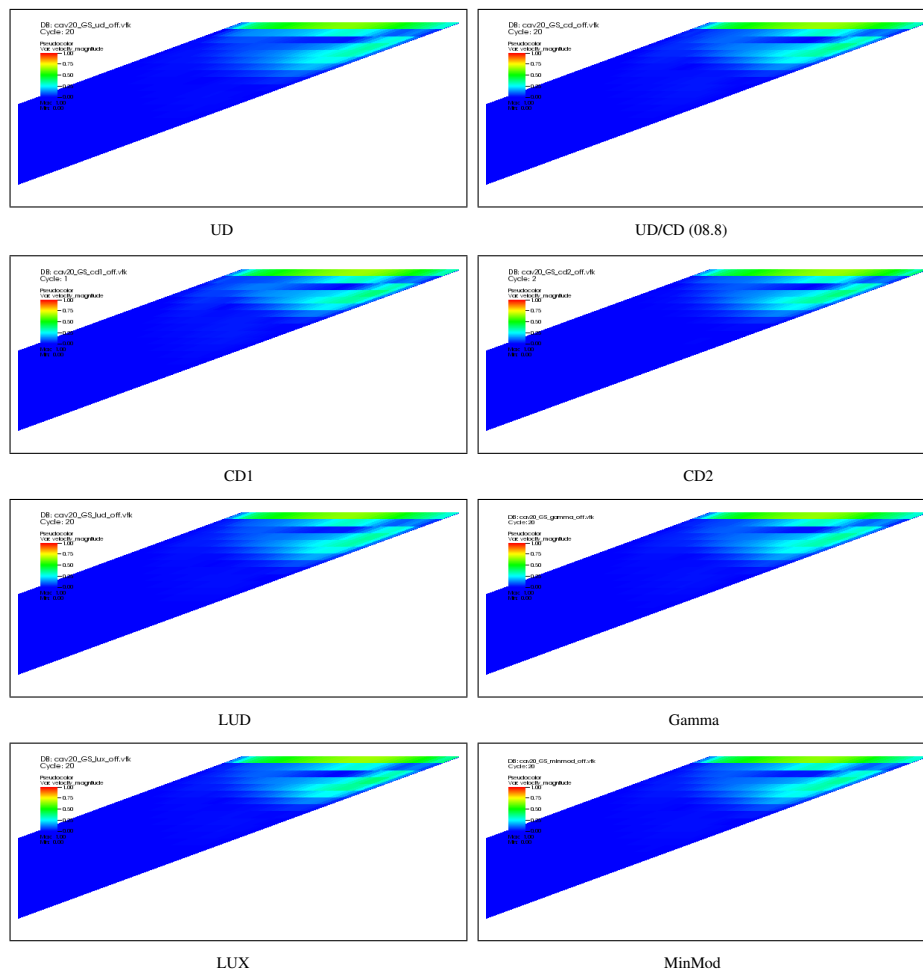


Figure 9.6: cav20 LDC at 20 degrees with Gauss, no limiter

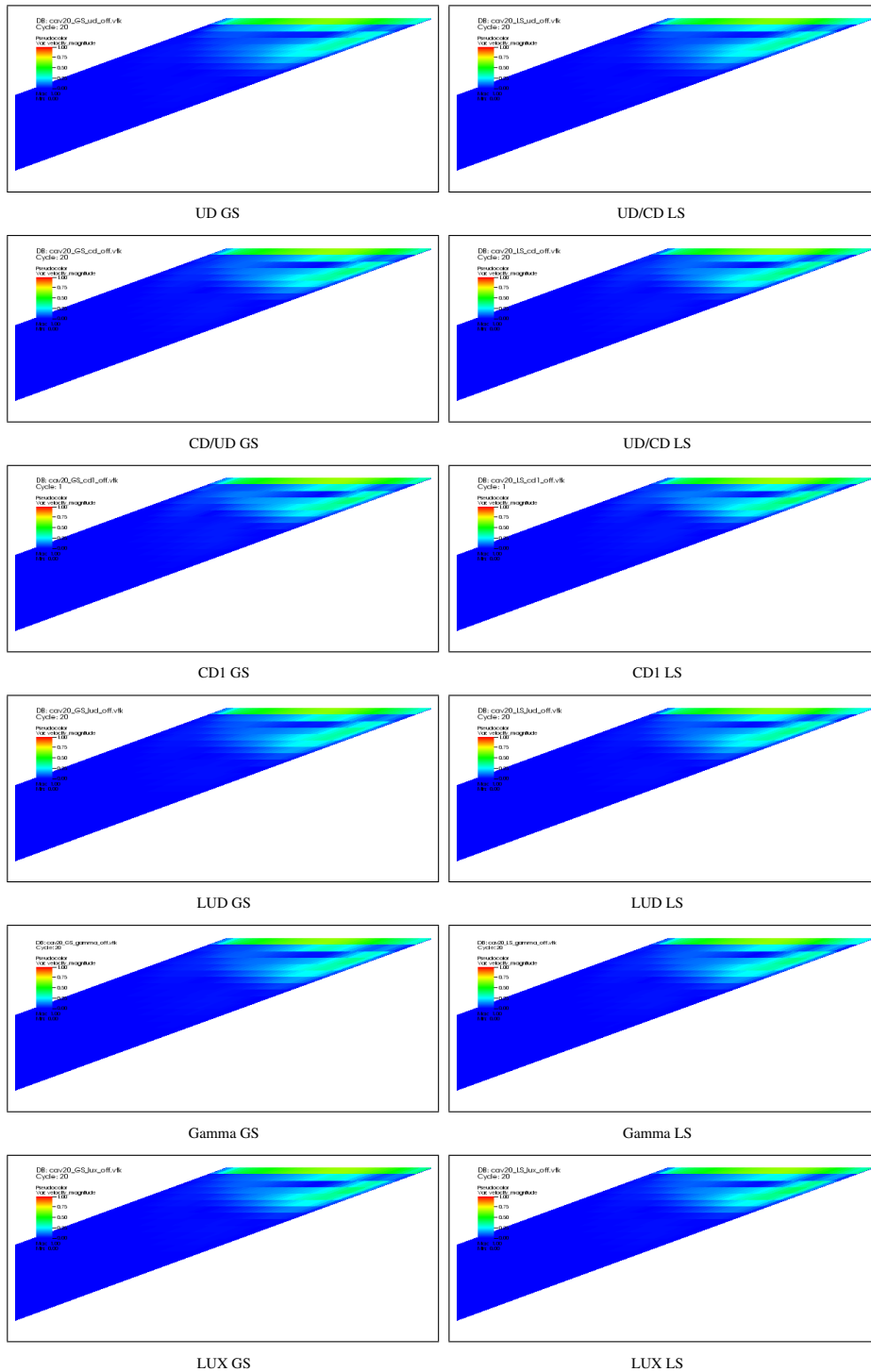


Figure 9.7: cav20 LDC 20 cases with Gauss and Least Squares, no limiters used

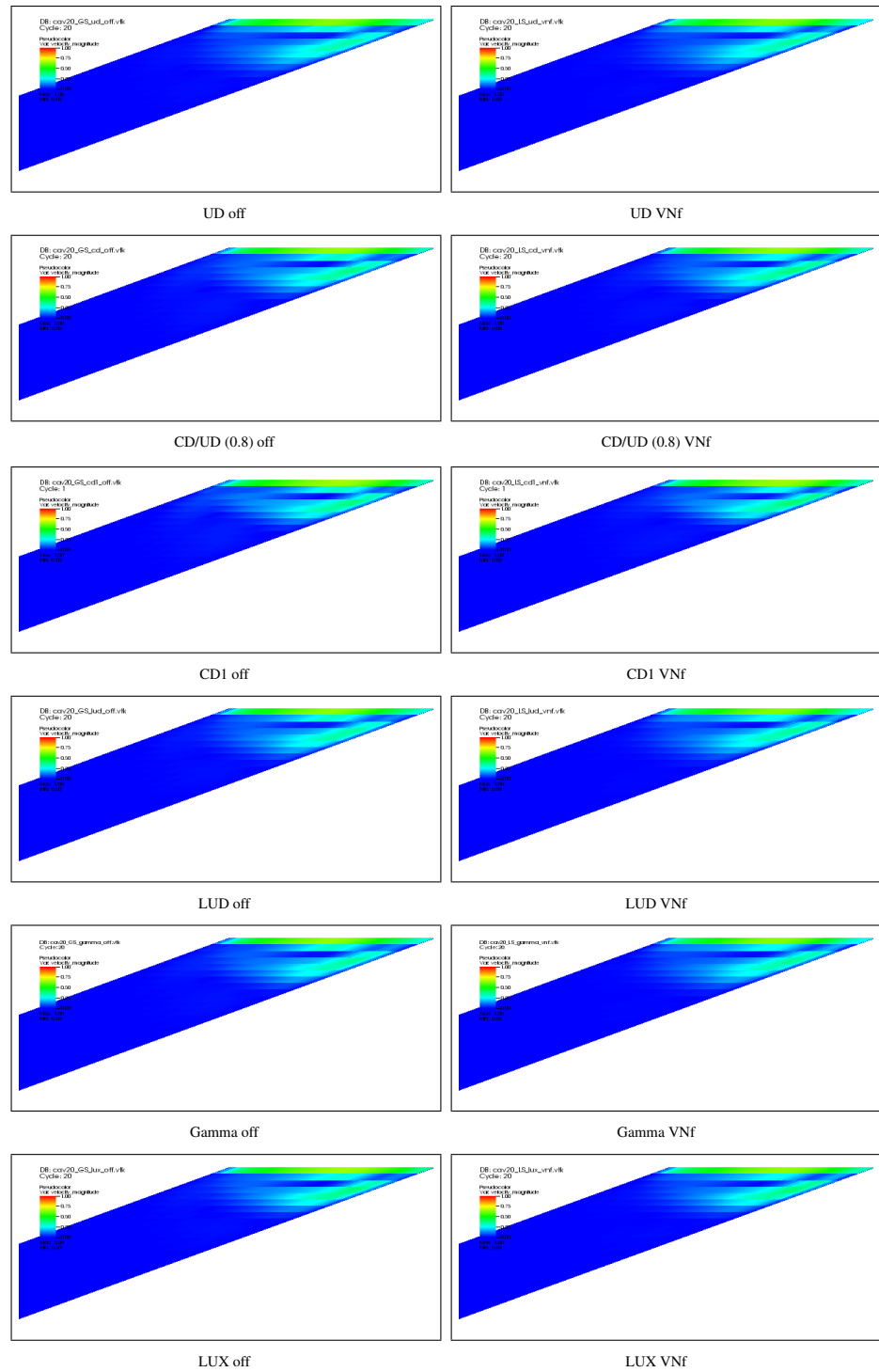


Figure 9.8: cav20 LDC 20 cases with Gauss and face based limiters

10

W1/W2 Wedge cell tests

10.1 Step cases

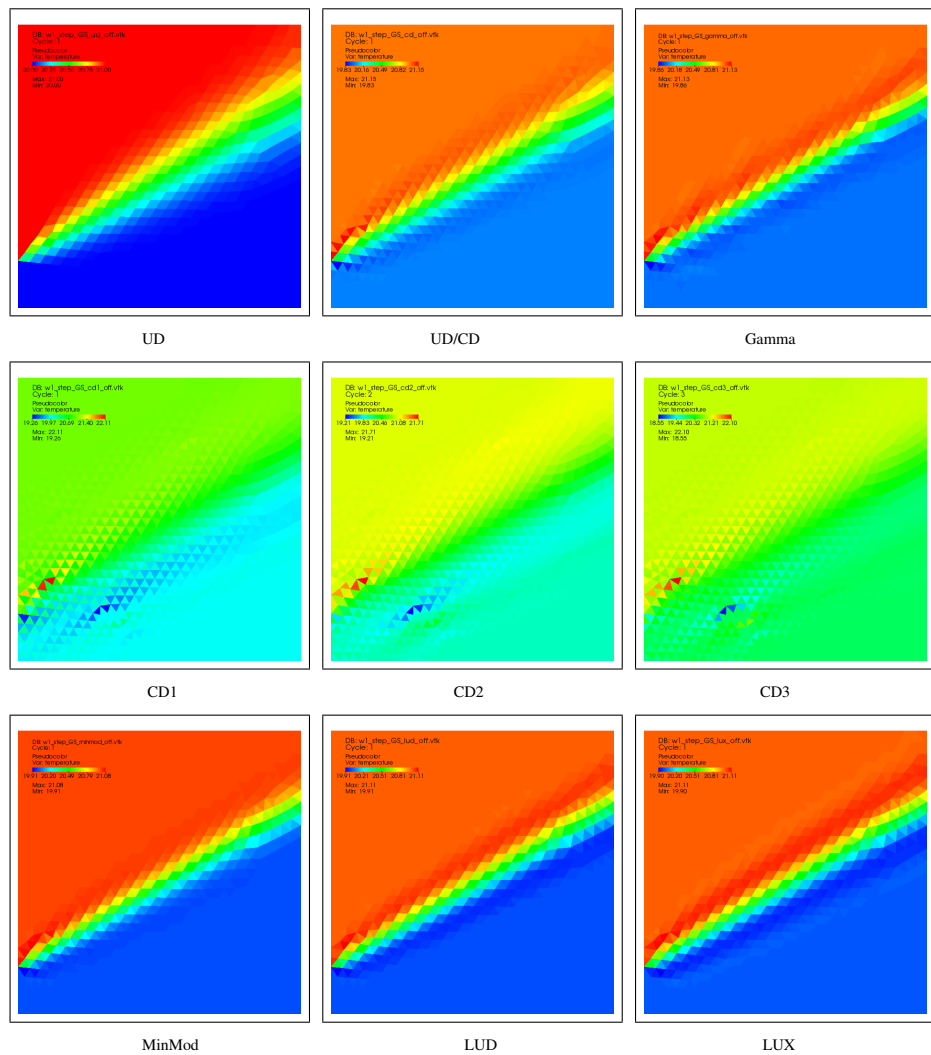


Figure 10.1: Standard Leonard step cases with Gauss, no limiter

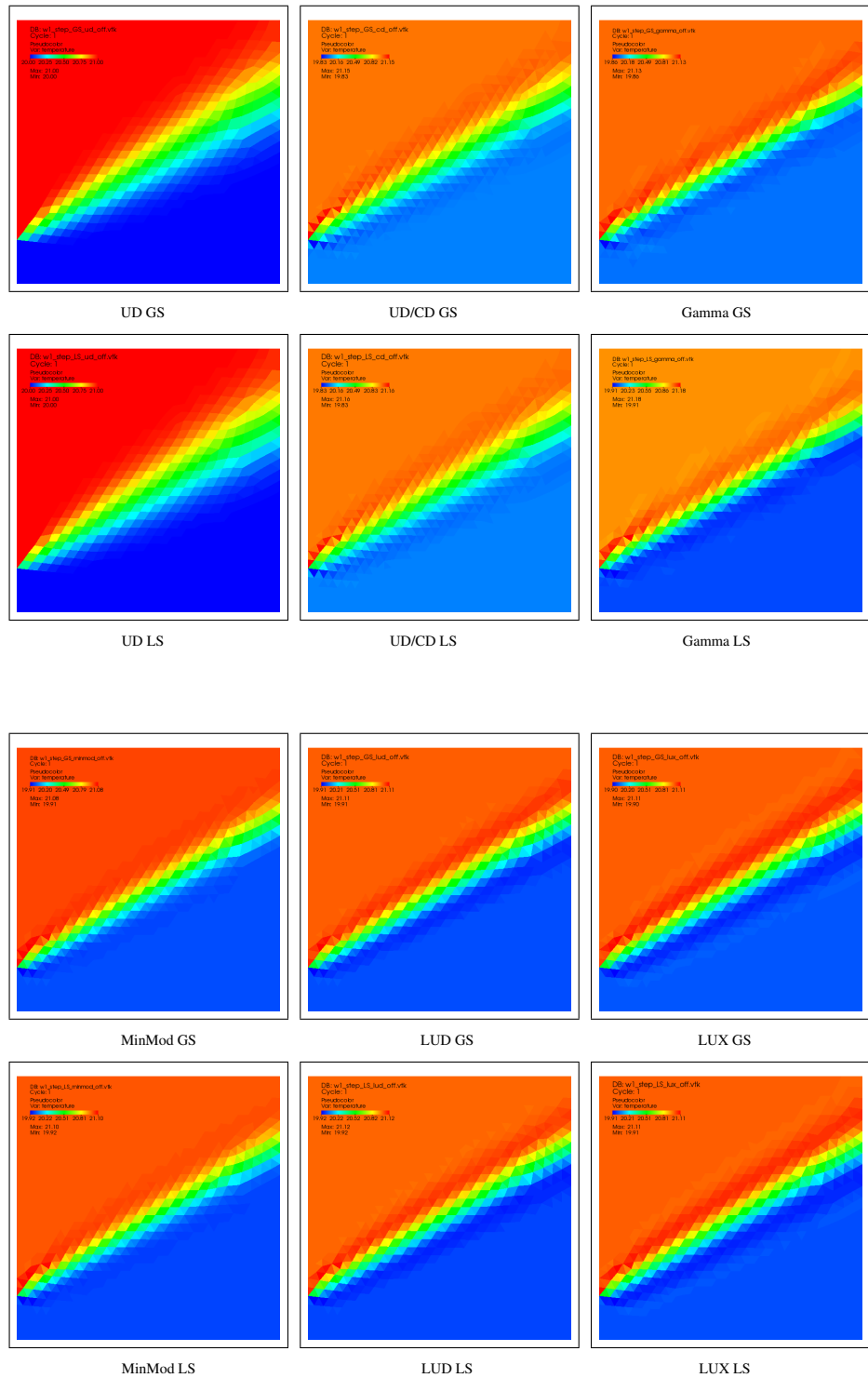


Figure 10.3: Standard Leonard step cases with Gauss (GS) and Least Squares (LS), no limiters used

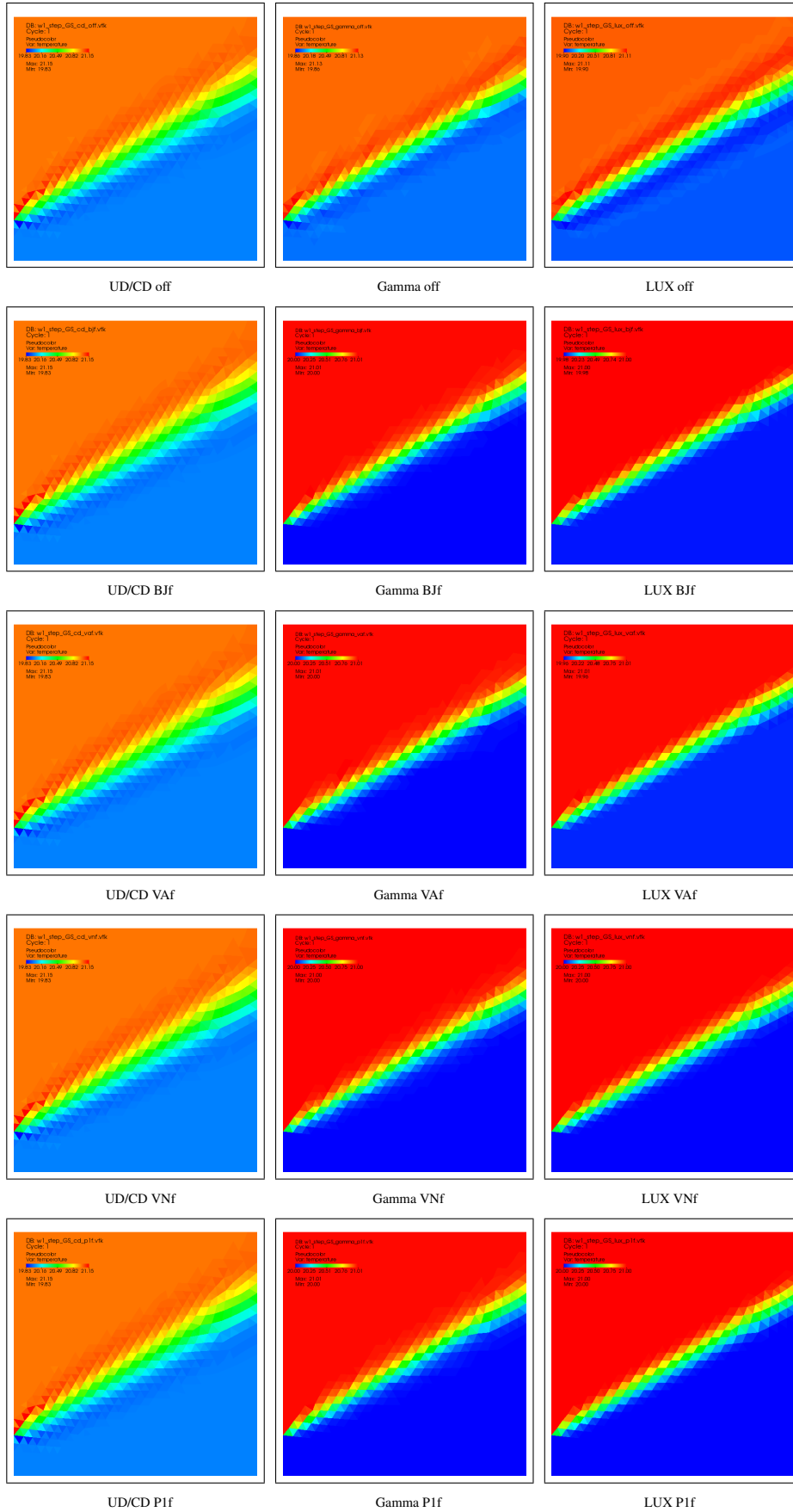


Figure 10.4: Leonard step cases with Gauss and face based limiters

10.2 Sin2 cases

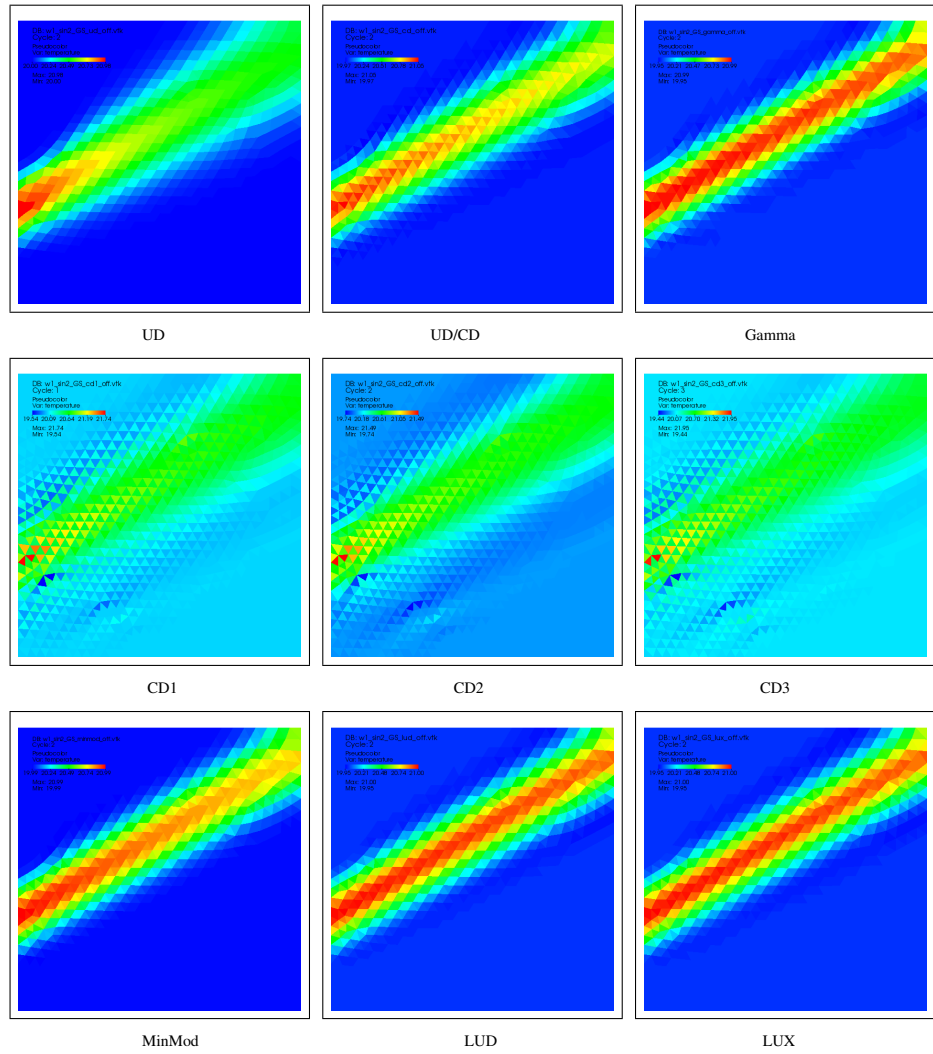


Figure 10.5: Standard Leonard sin2 cases with Gauss, no limiter

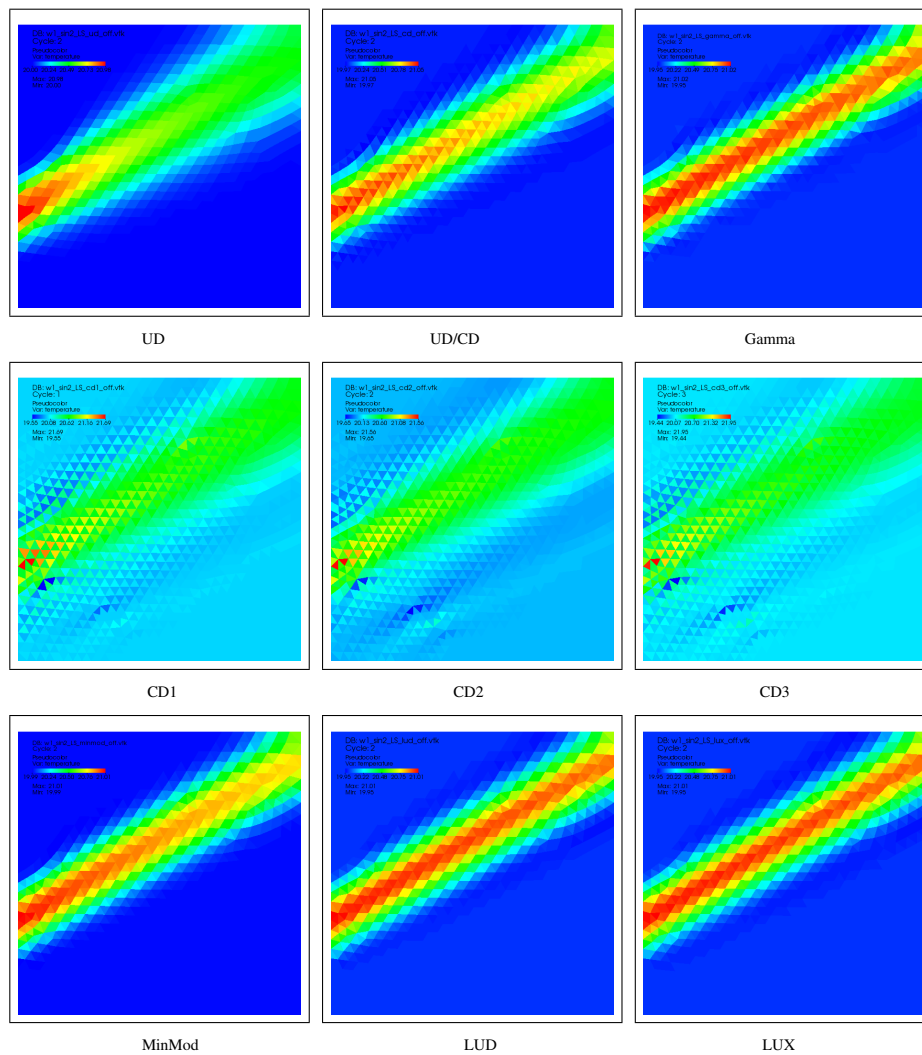


Figure 10.6: Standard Leonard sin2 cases with Least Squares, no limiter

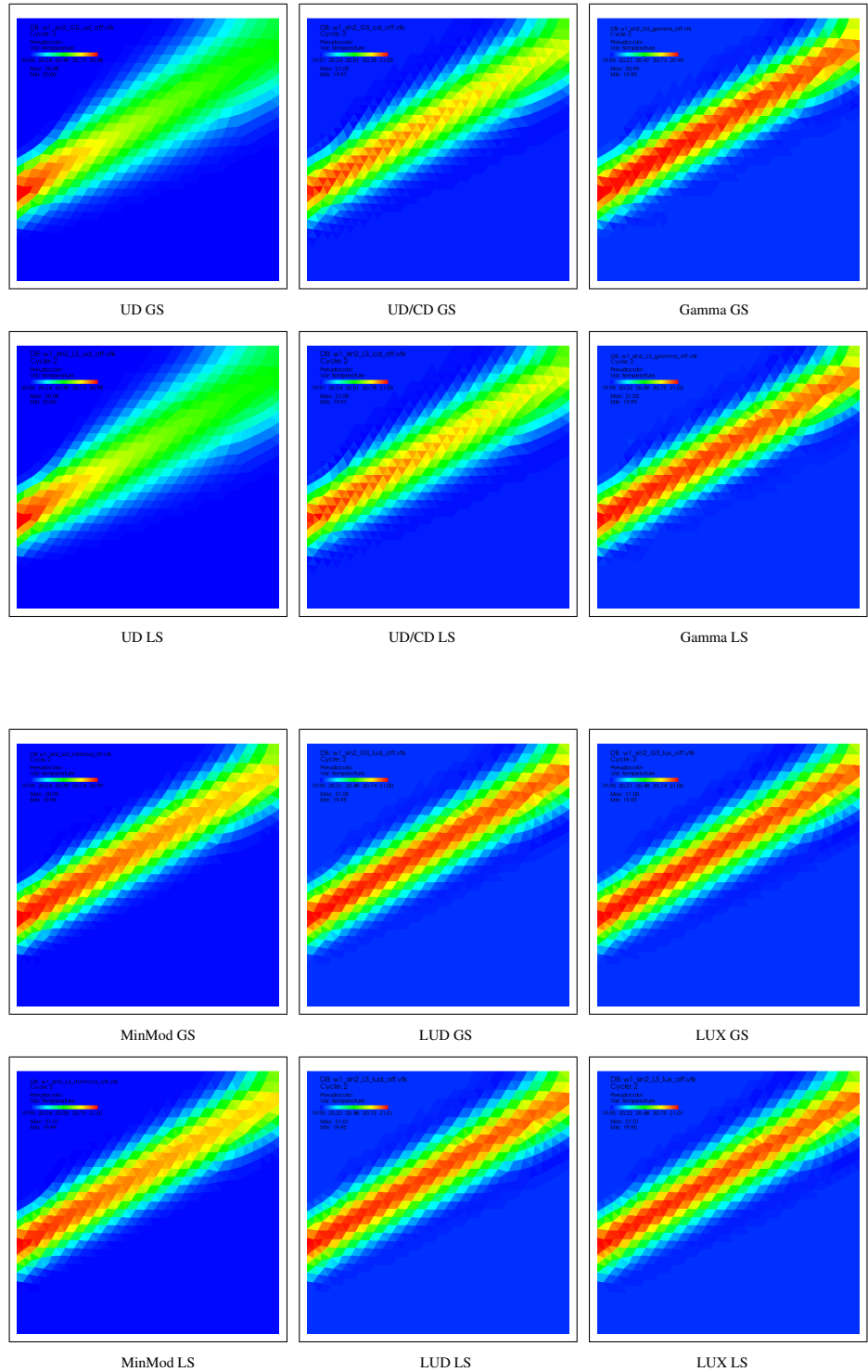


Figure 10.7: Standard Leonard sin2 cases with Gauss (GS) and Least Squares (LS), no limiters used

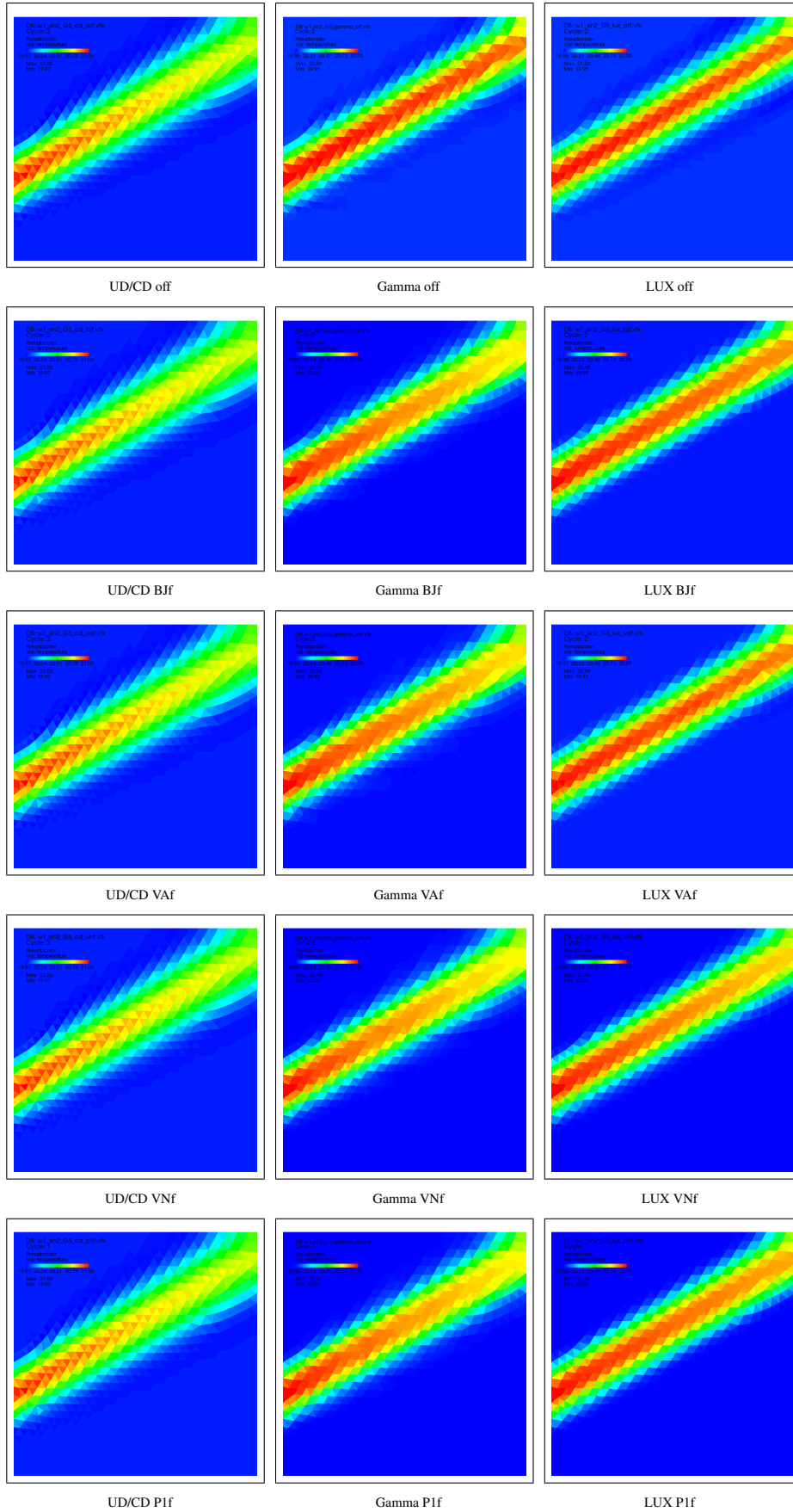


Figure 10.8: Leonard sin2 cases with Gauss and face based limiters

10.3 Semi ellipse cases

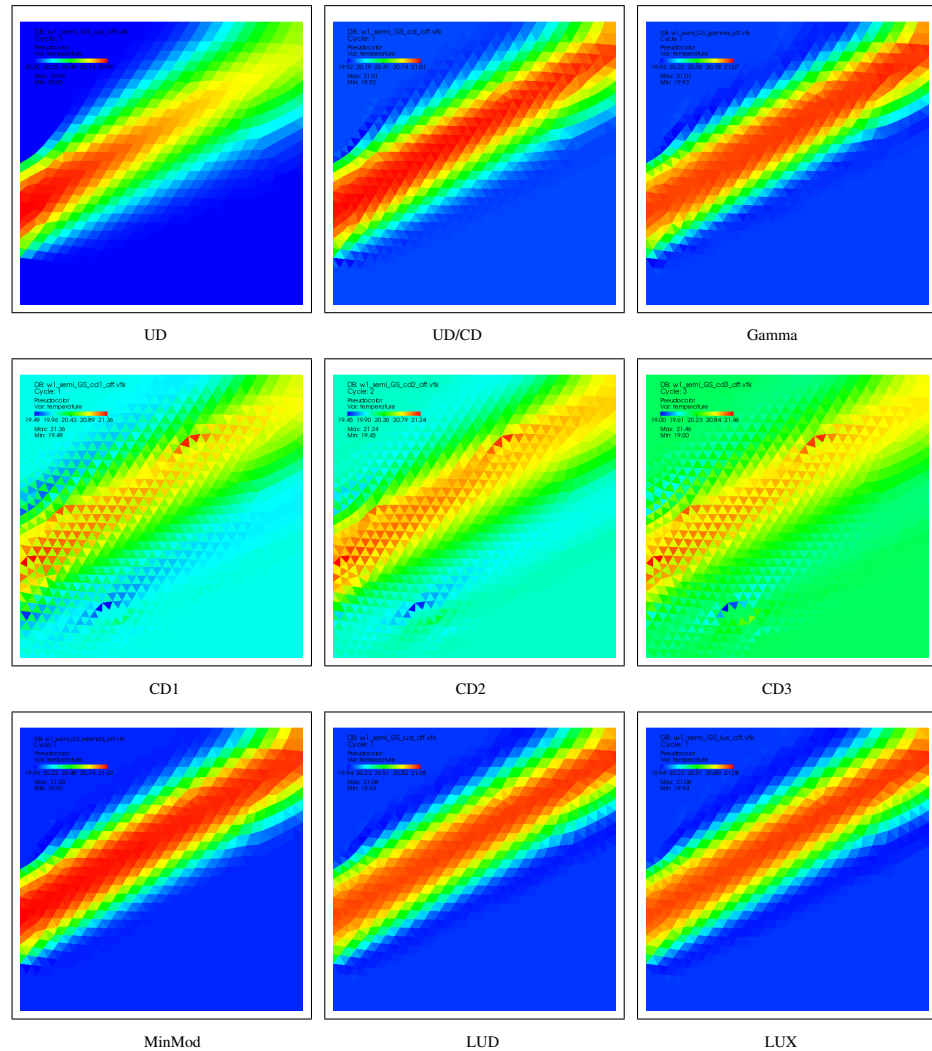


Figure 10.9: Standard Leonard semi cases with Gauss, no limiter

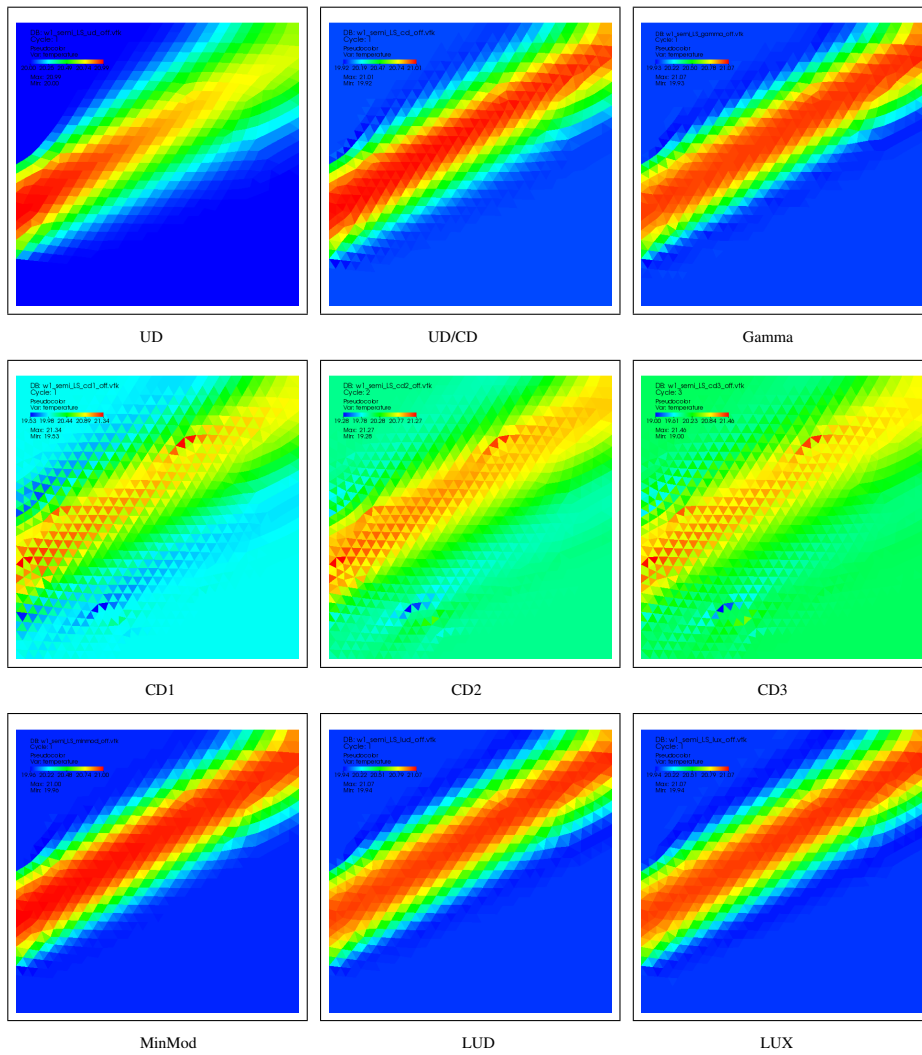


Figure 10.10: Standard Leonard semi cases with Least Squares, no limiter

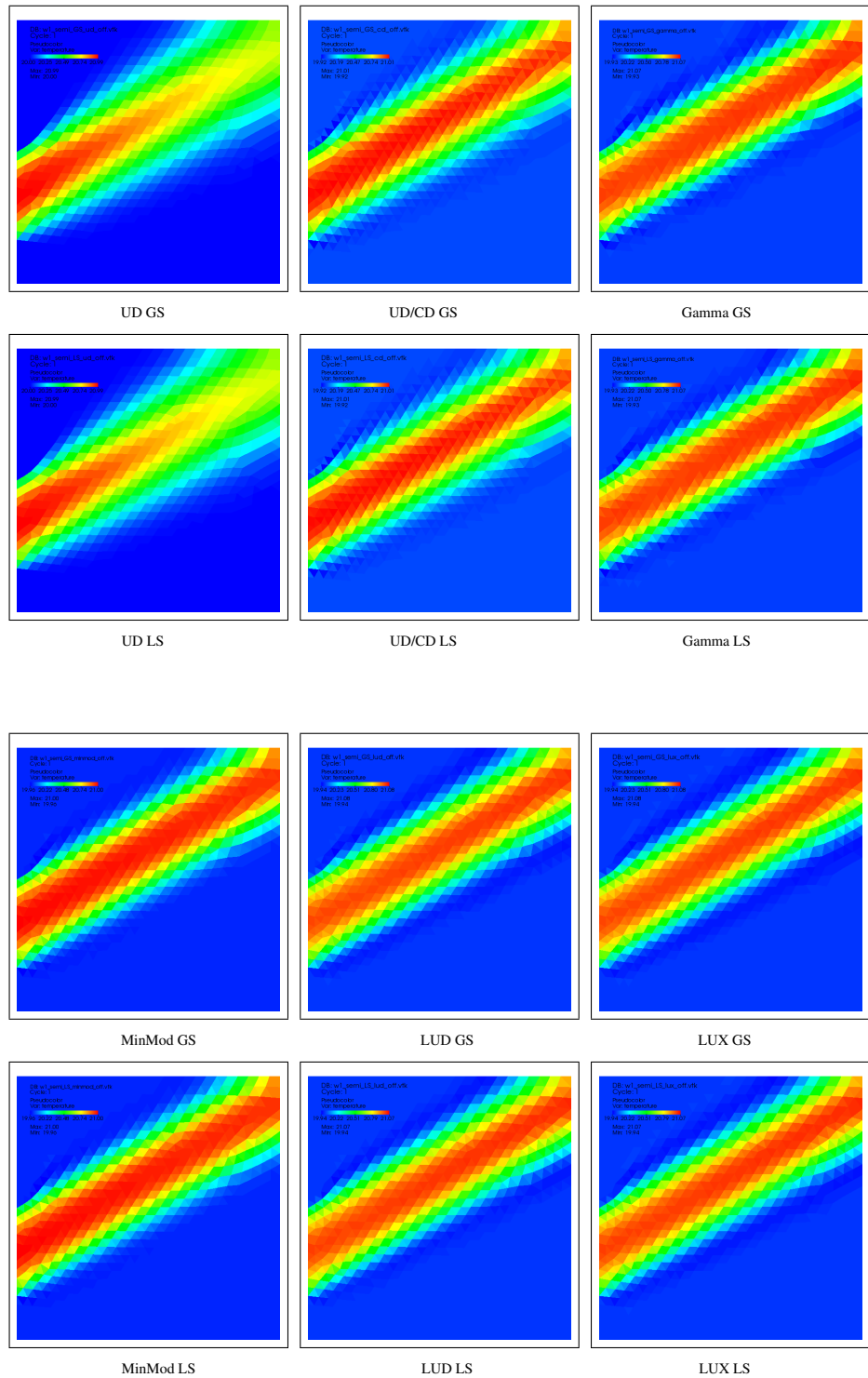


Figure 10.11: Standard Leonard semi cases with Gauss (GS) and Least Squares (LS), no limiters used

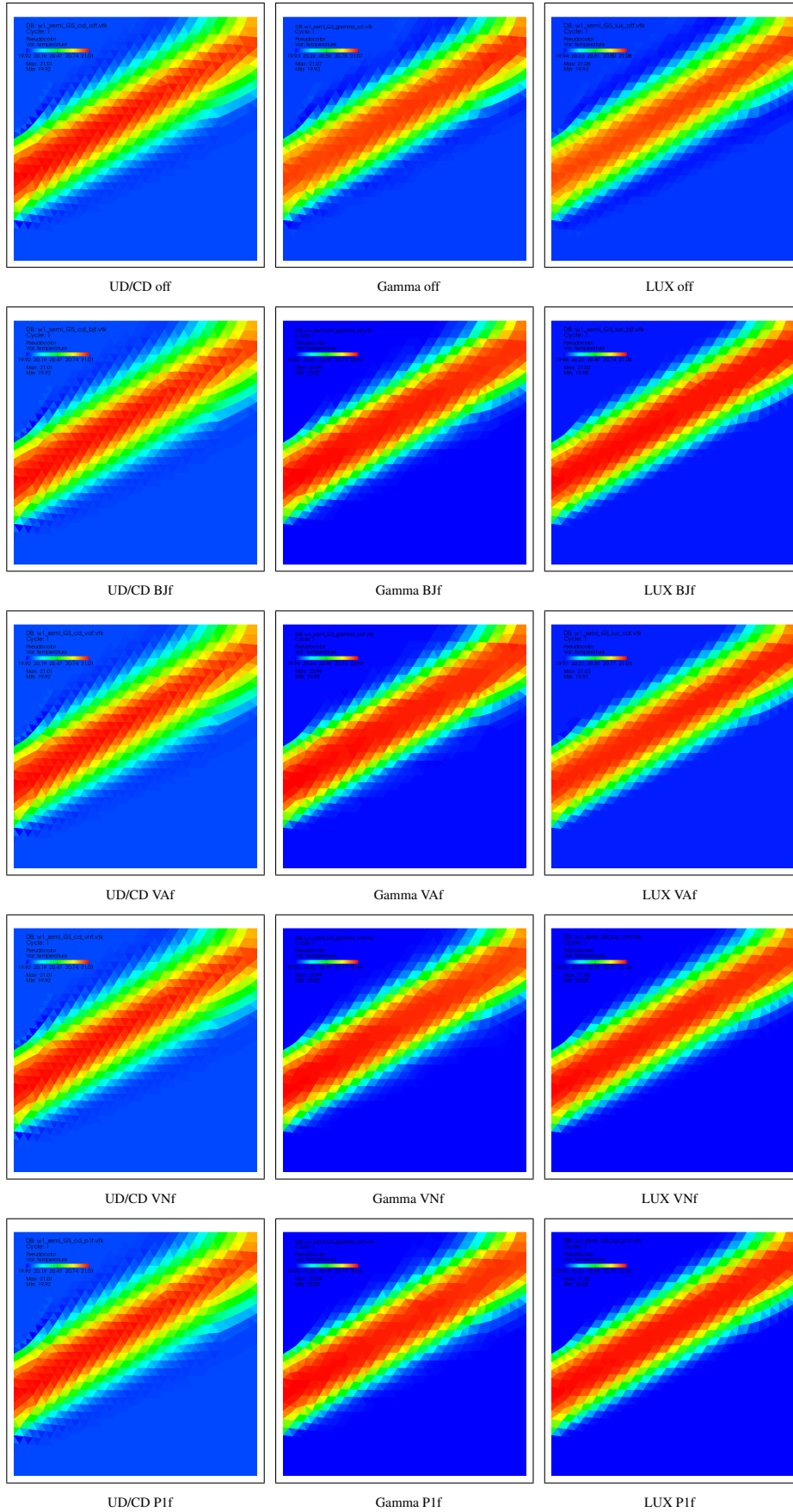


Figure 10.12: Leonard semi cases with Gauss and face based limiters

10.4 Lid driven cavity

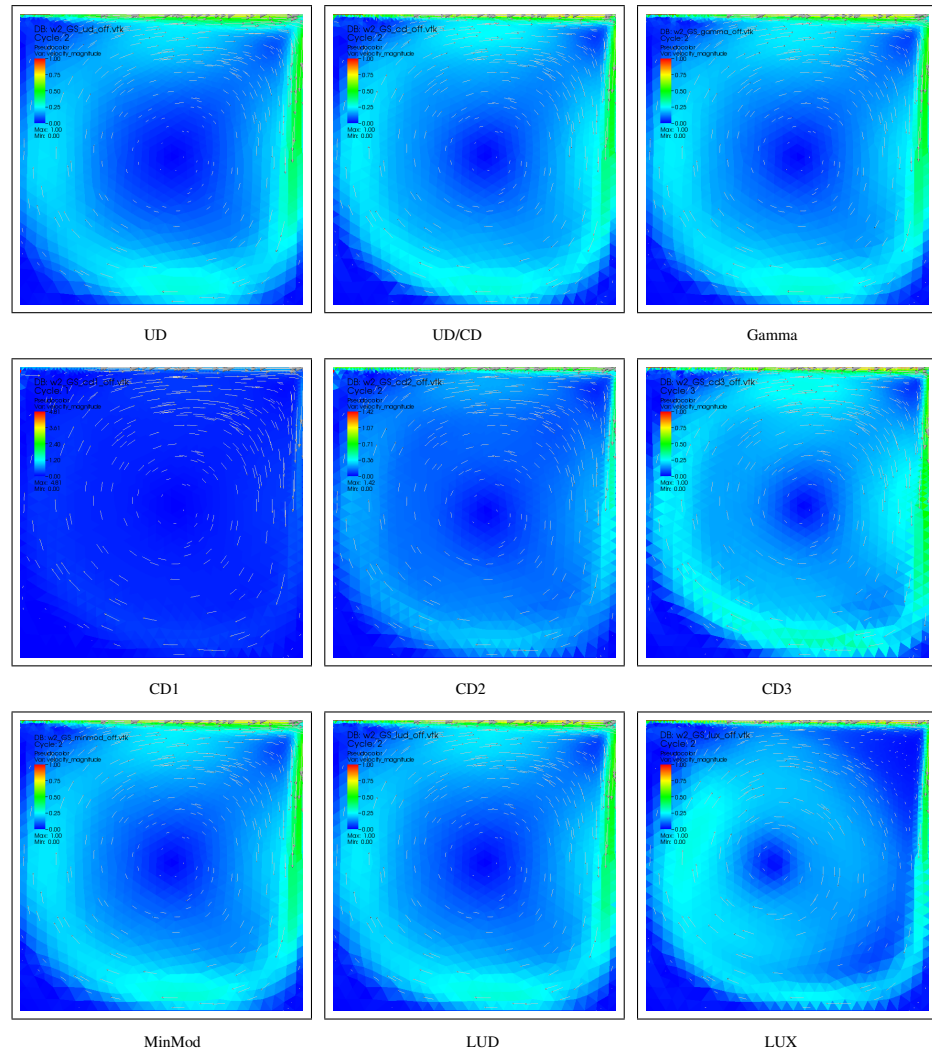


Figure 10.13: W2 LDC wedge cases with Gauss, no limiter

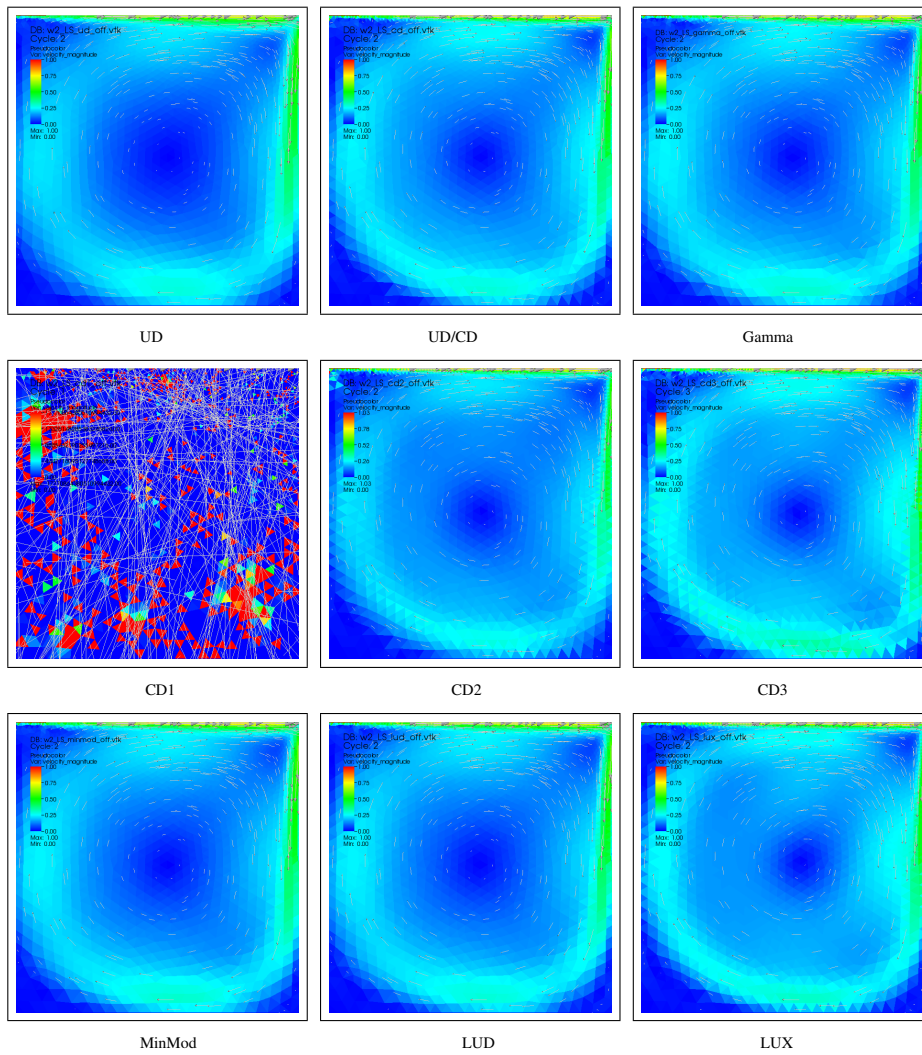


Figure 10.14: W2 LDC wedge cases with Least Squares, no limiter

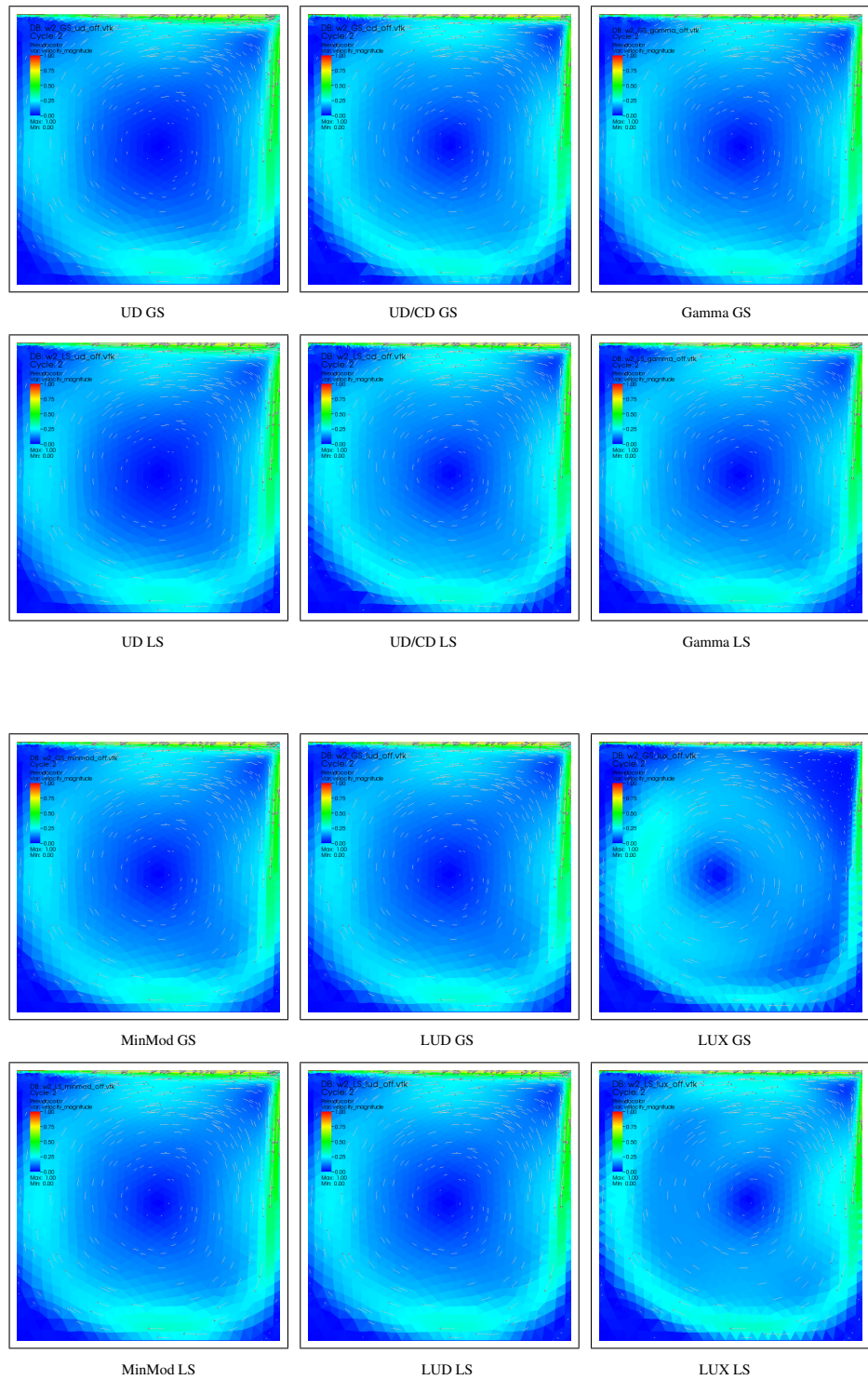


Figure 10.15: W2 LDC wedge cases with Gauss and Least Squares, no limiters used

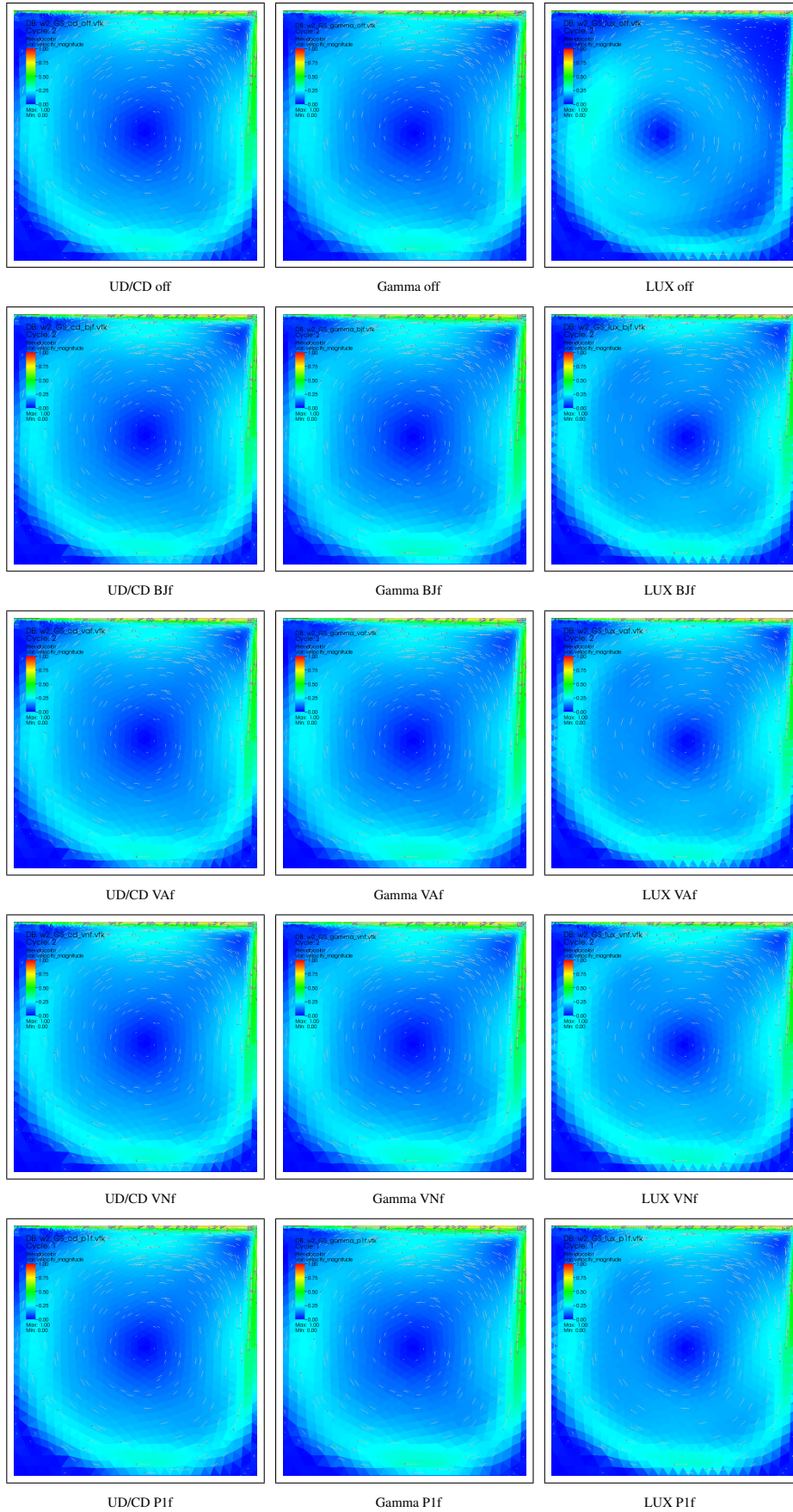


Figure 10.16: W2 LDC wedge cases with Gauss and face based limiters

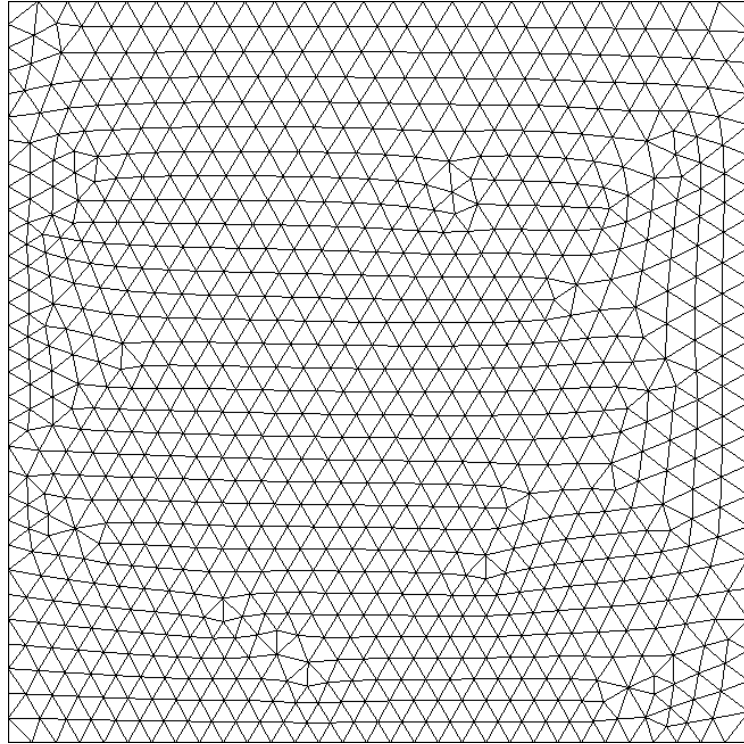


Figure 10.17: Mesh model w1

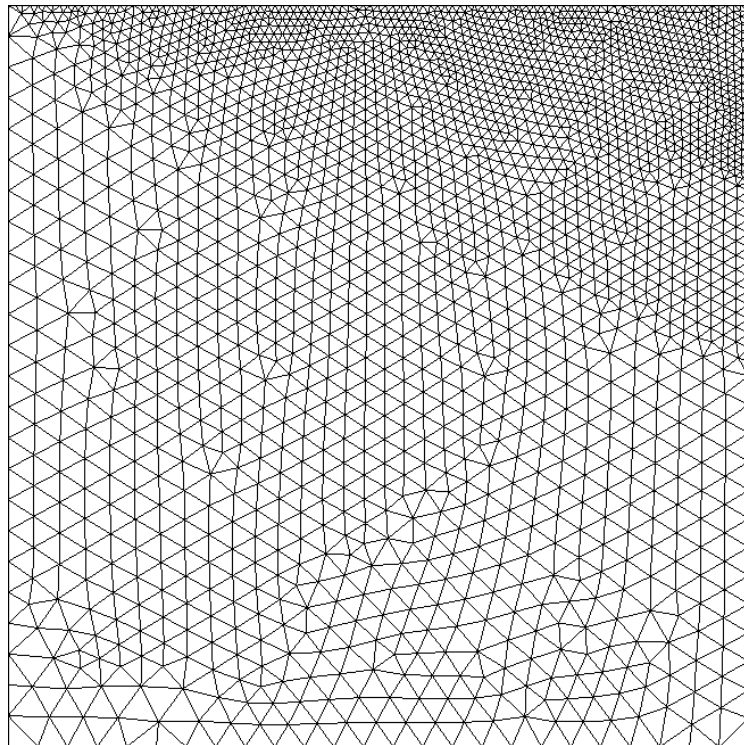


Figure 10.18: Mesh model w2

11

M3/M5 Tetrahedral cell tests

11.1 Lid driven cavity m3

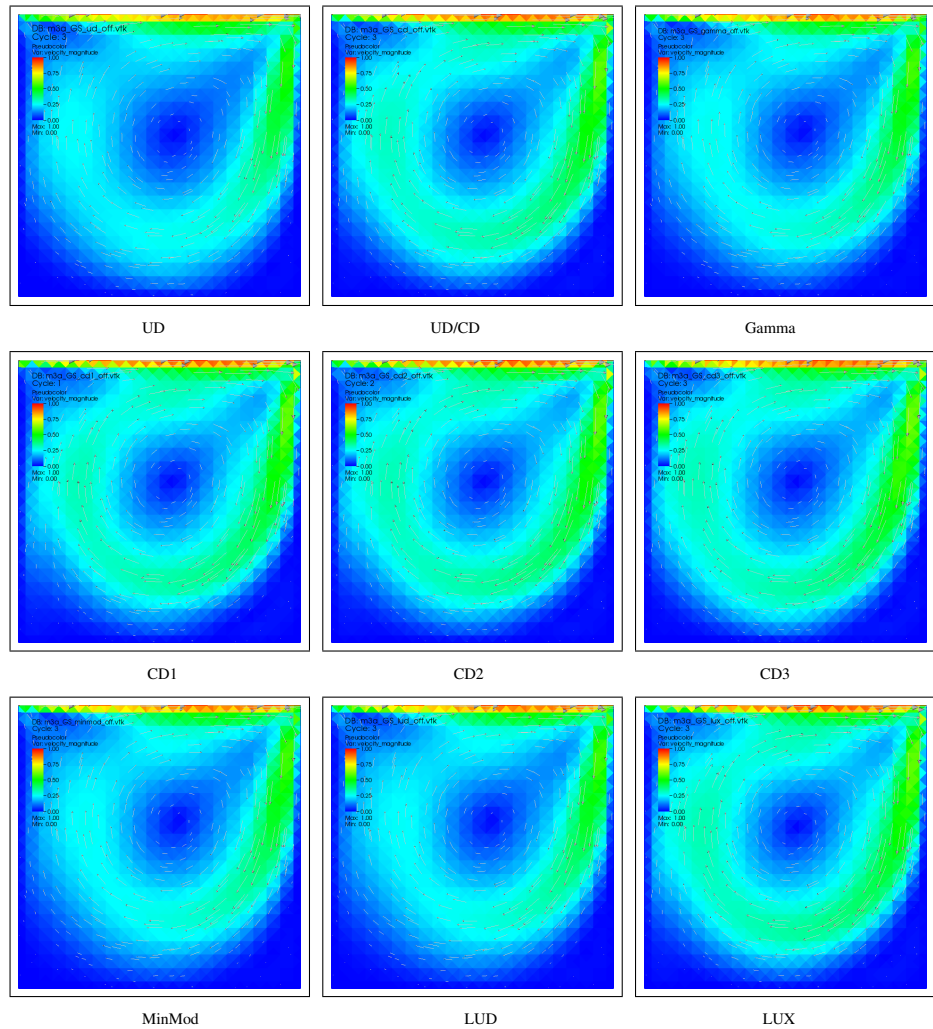


Figure 11.1: m3a LDC tet cases with Gauss, no limiter

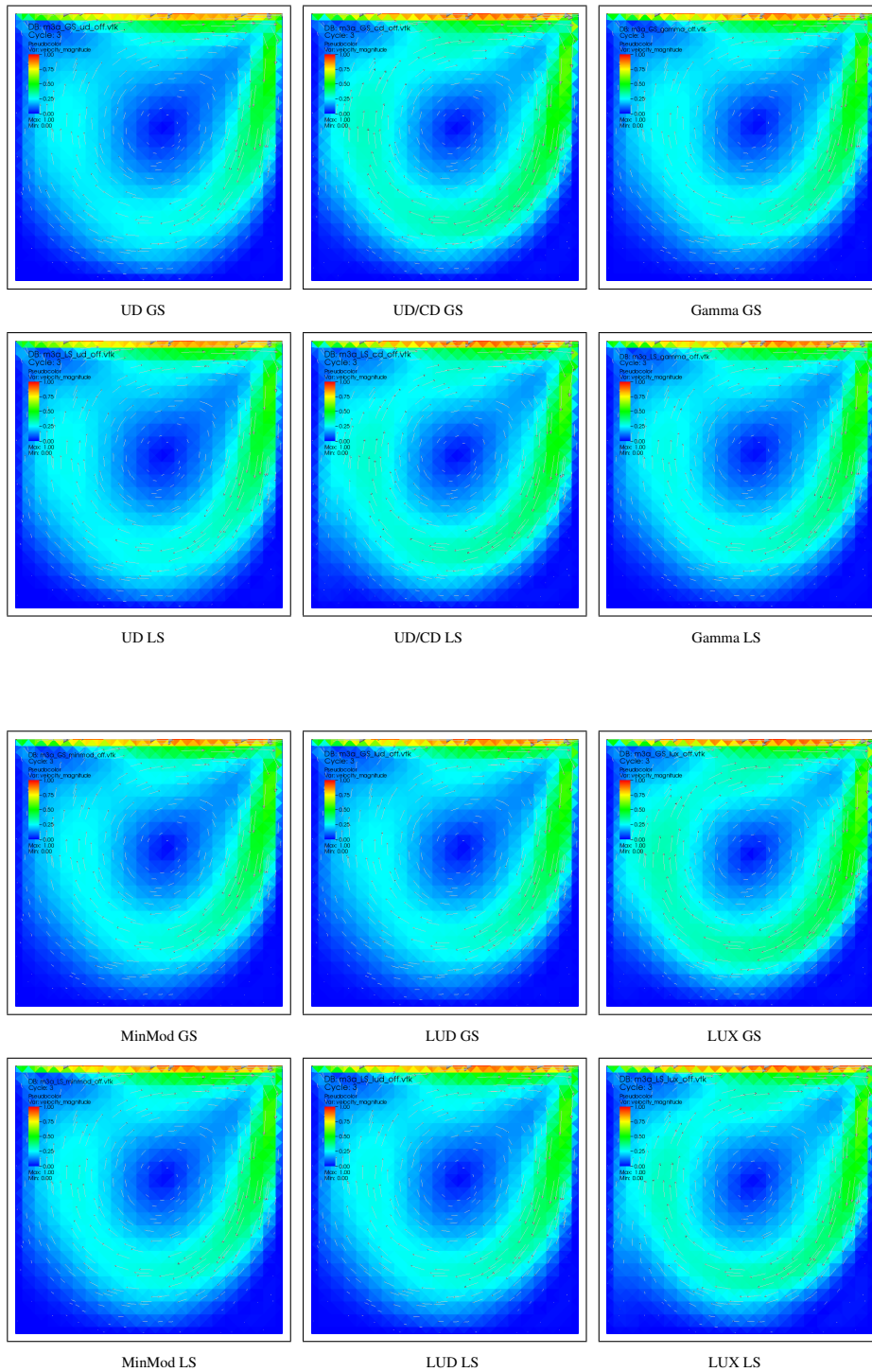


Figure 11.2: m3a LDC tet cases with Gauss and Least Squares, no limiters used

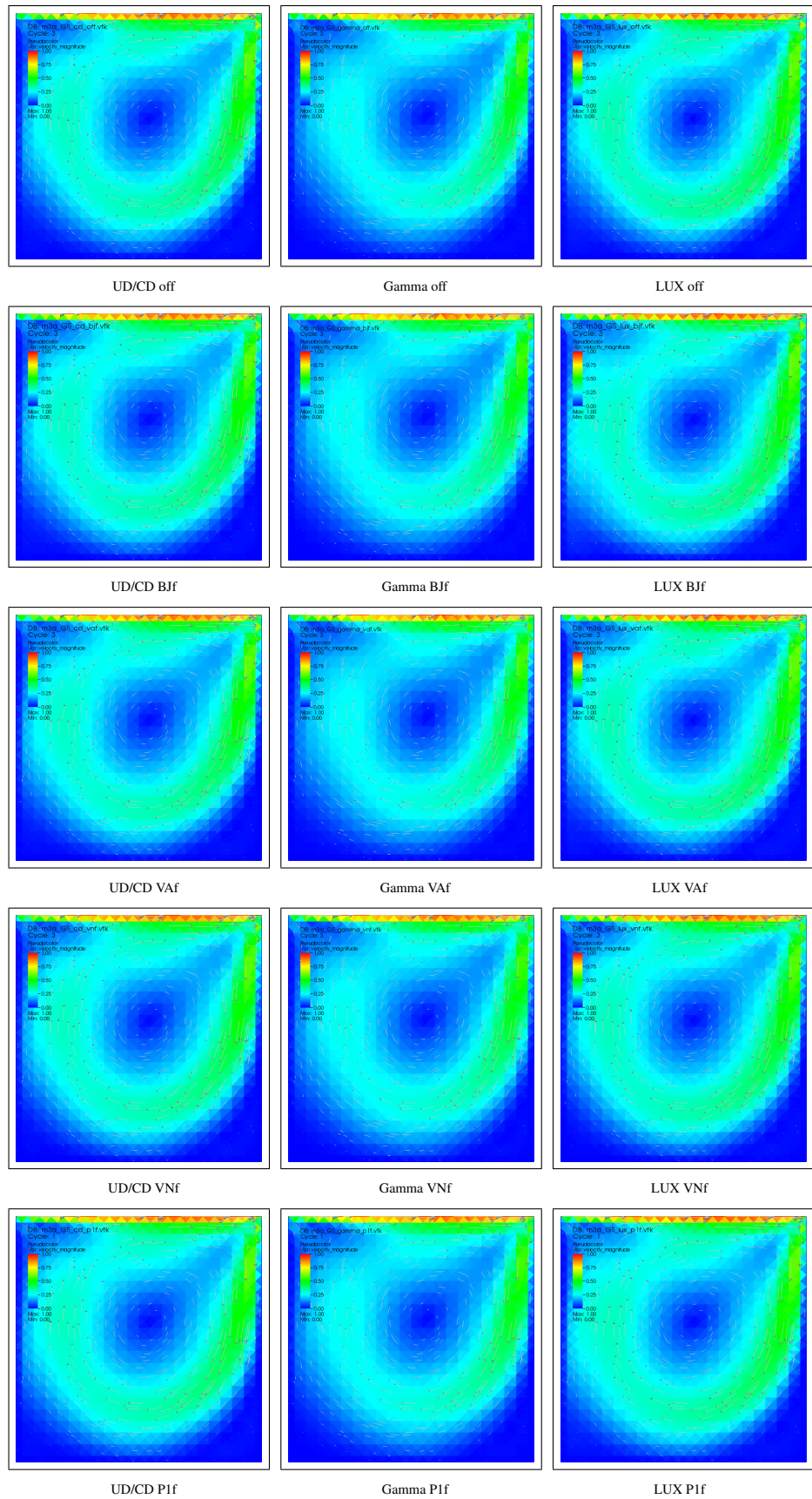


Figure 11.3: m3a LDC tet cases with Gauss and face based limiters

11.2 Plain flow from left to right

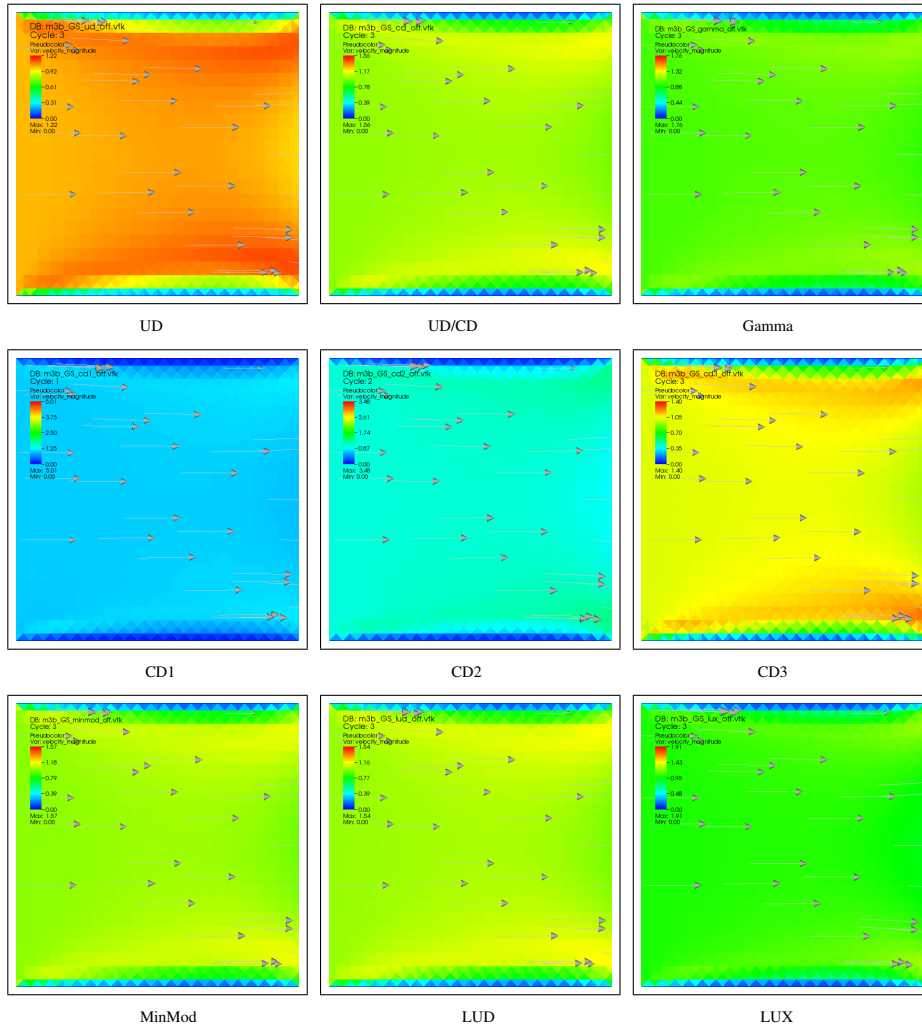


Figure 11.4: m3b plain flow tet cases with Gauss, no limiter

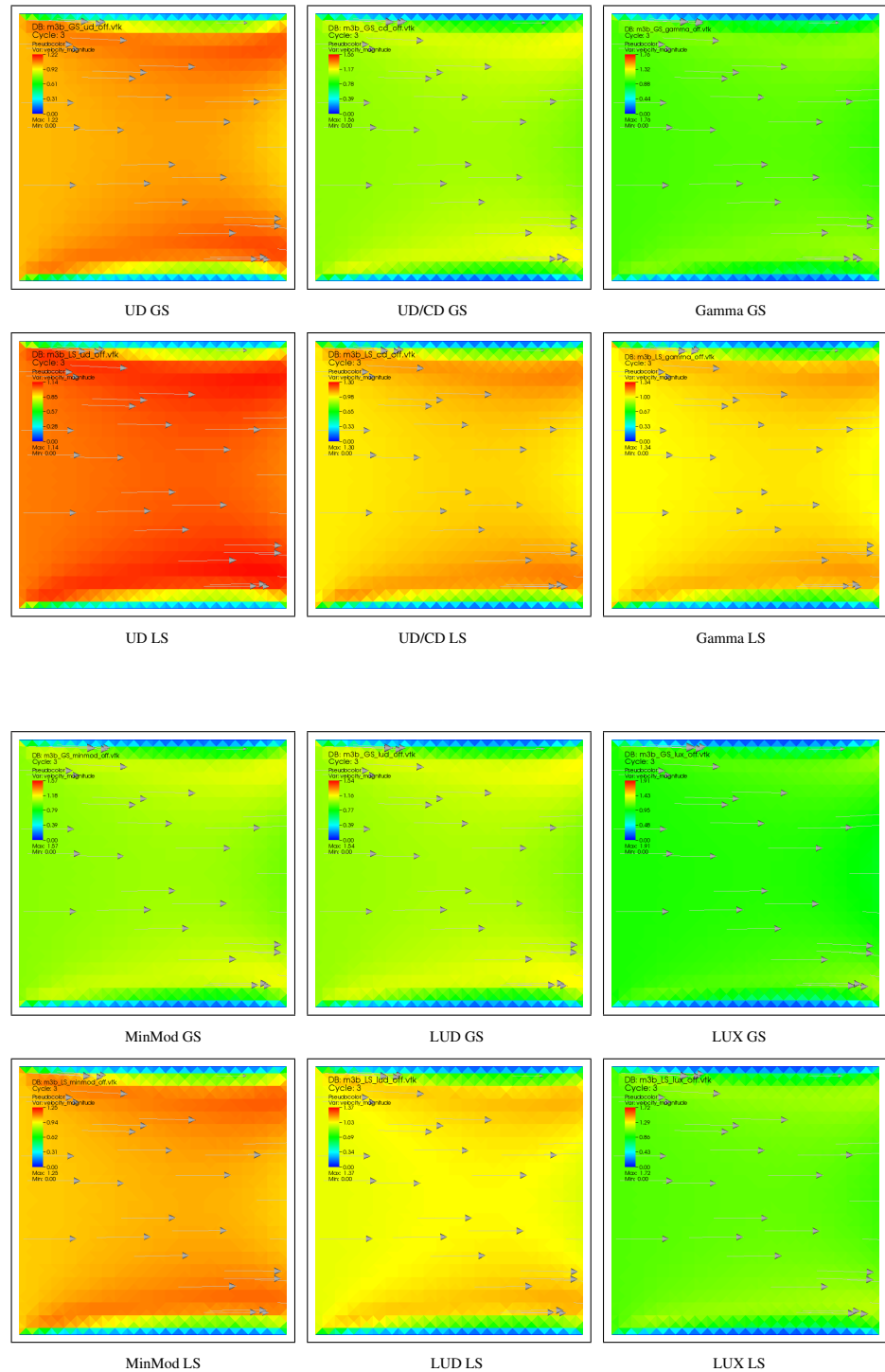


Figure 11.5: m3b plain flow tet cases with Gauss and Least Squares, no limiters used

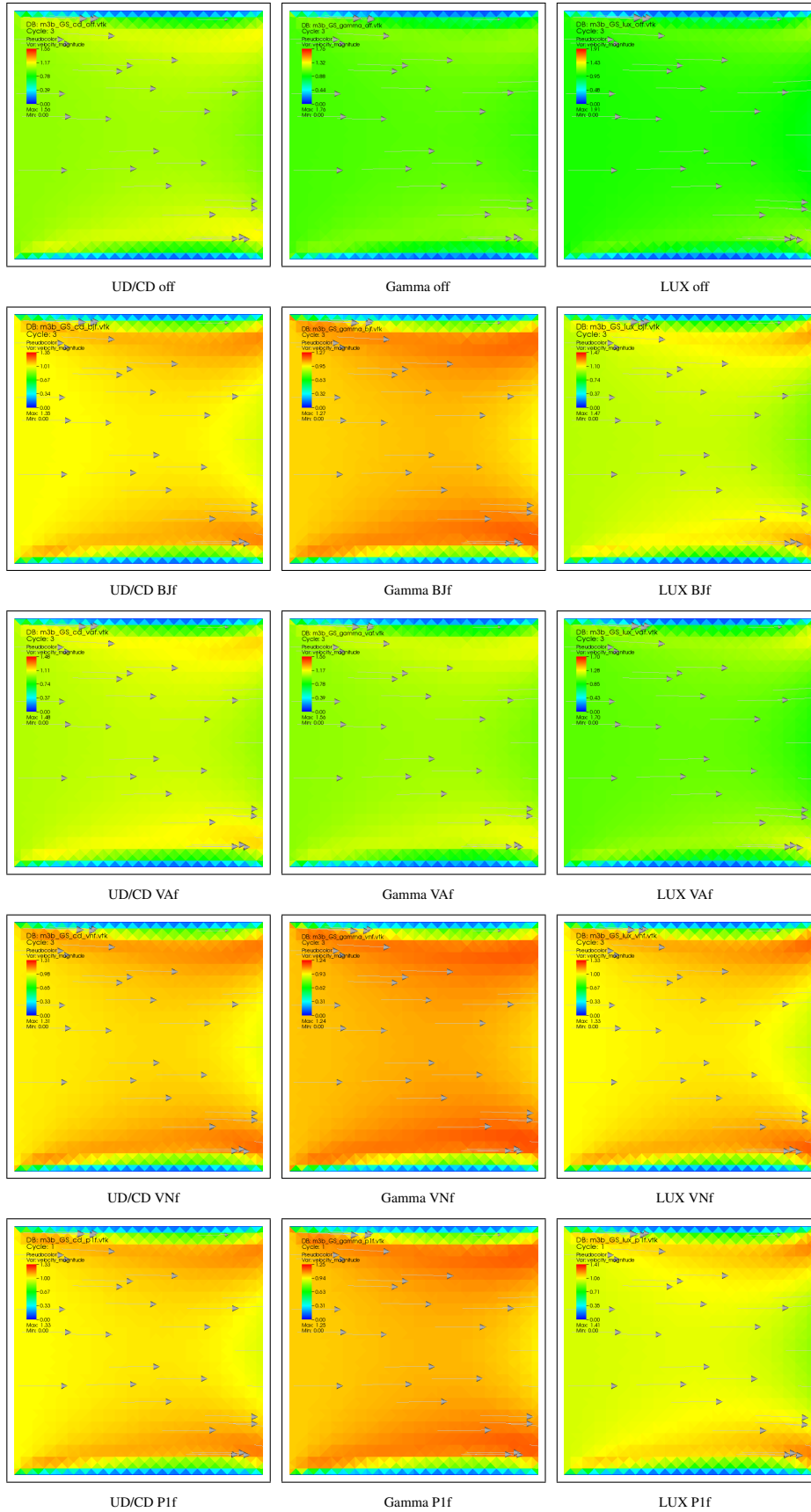


Figure 11.6: m3b plain flow cases with Gauss and face based limiters

11.3 Stagnation flow from top

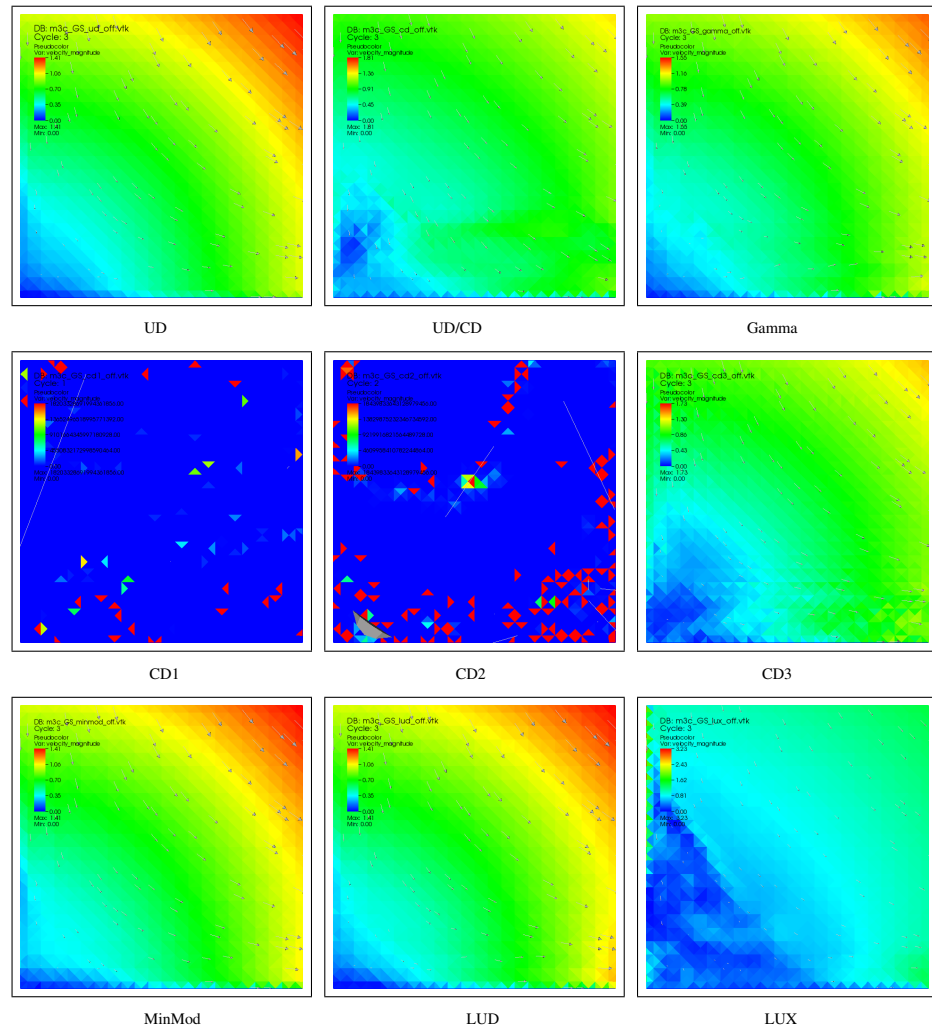


Figure 11.7: m3c stagnation flow tet cases with Gauss, no limiter

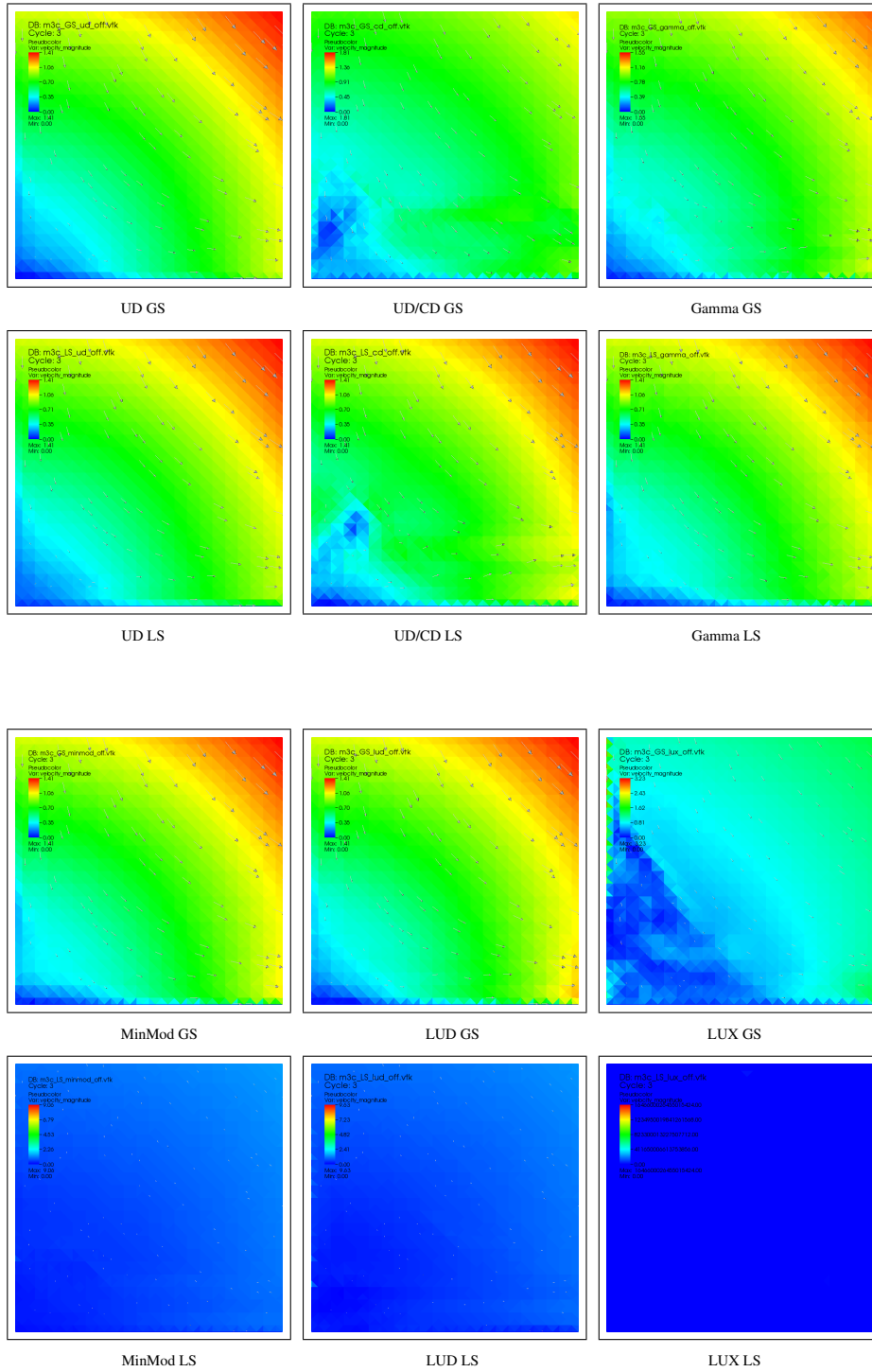


Figure 11.8: m3c stagnation flow tet cases with Gauss and Least Squares, no limiters used

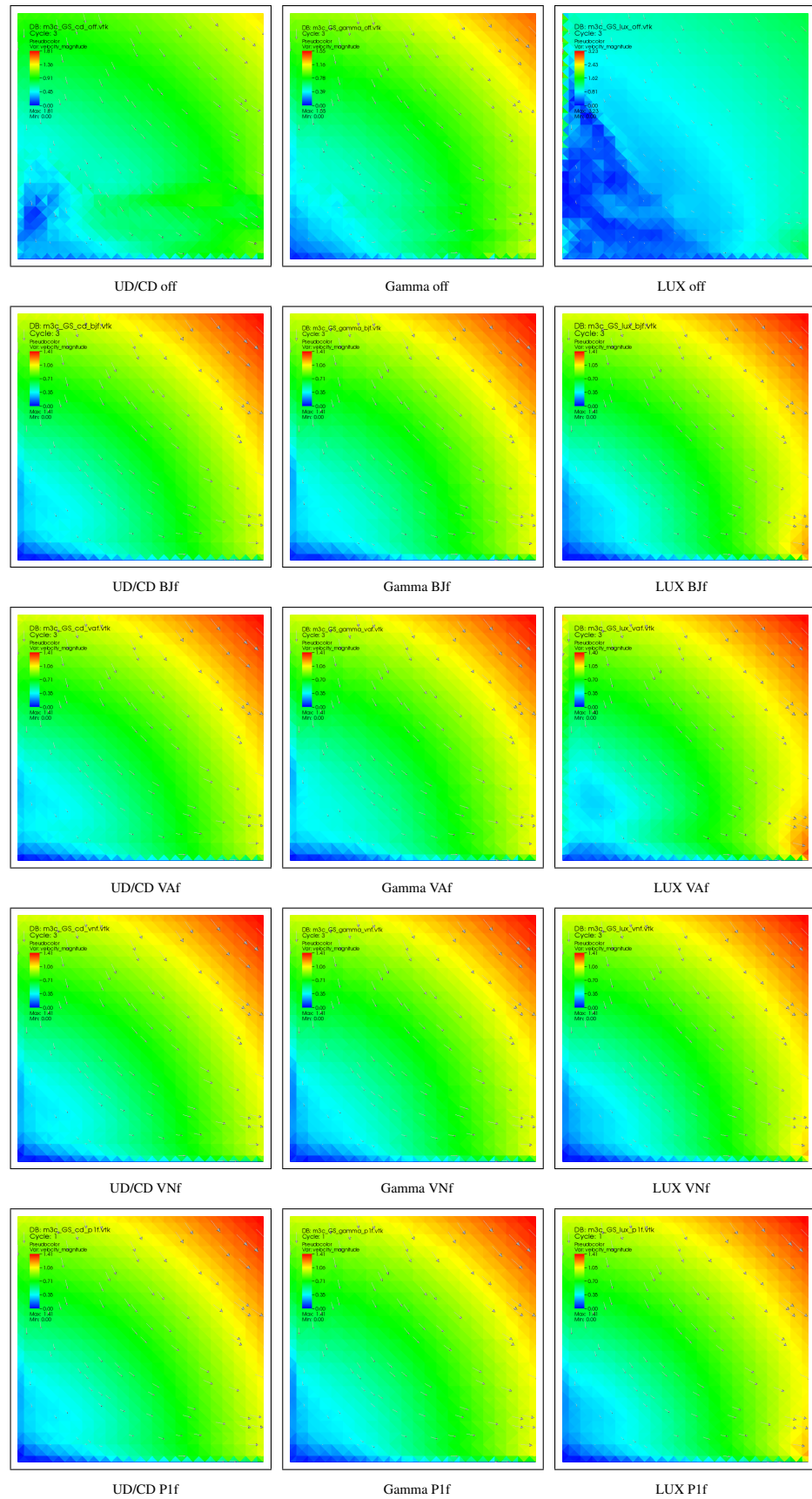


Figure 11.9: m3c stagnation flow cases with Gauss and face based limiters

11.4 Lid driven cavity m5

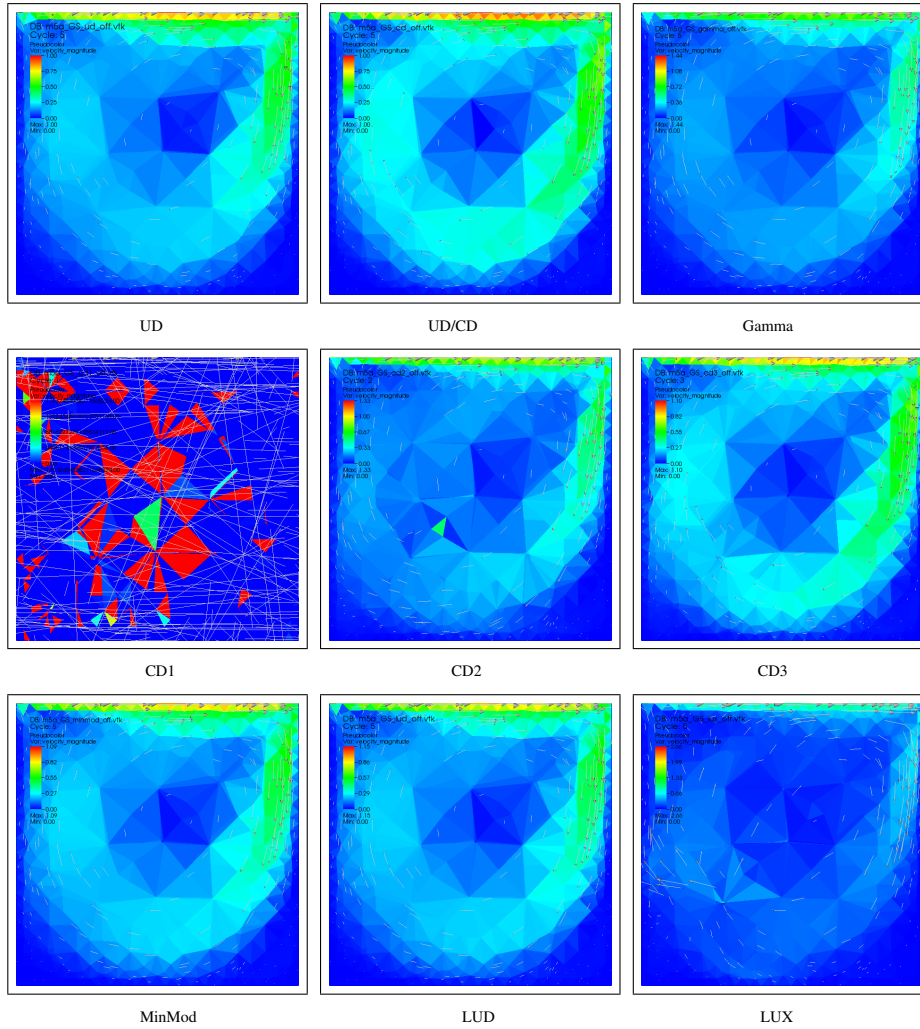


Figure 11.10: m5a LDC tet cases with Gauss, no limiter

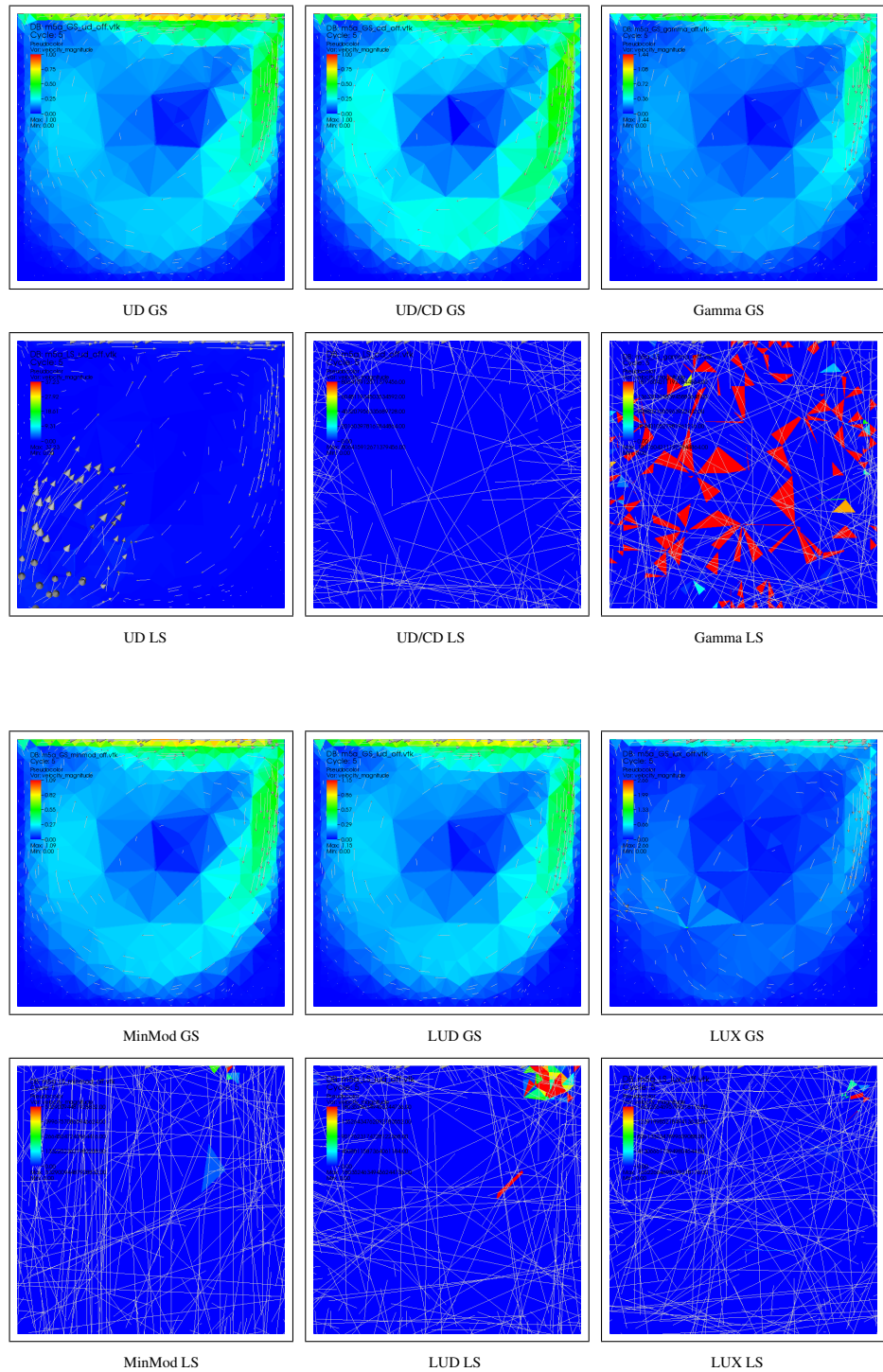


Figure 11.11: m5a LDC tet cases with Gauss and Least Squares, no limiters used

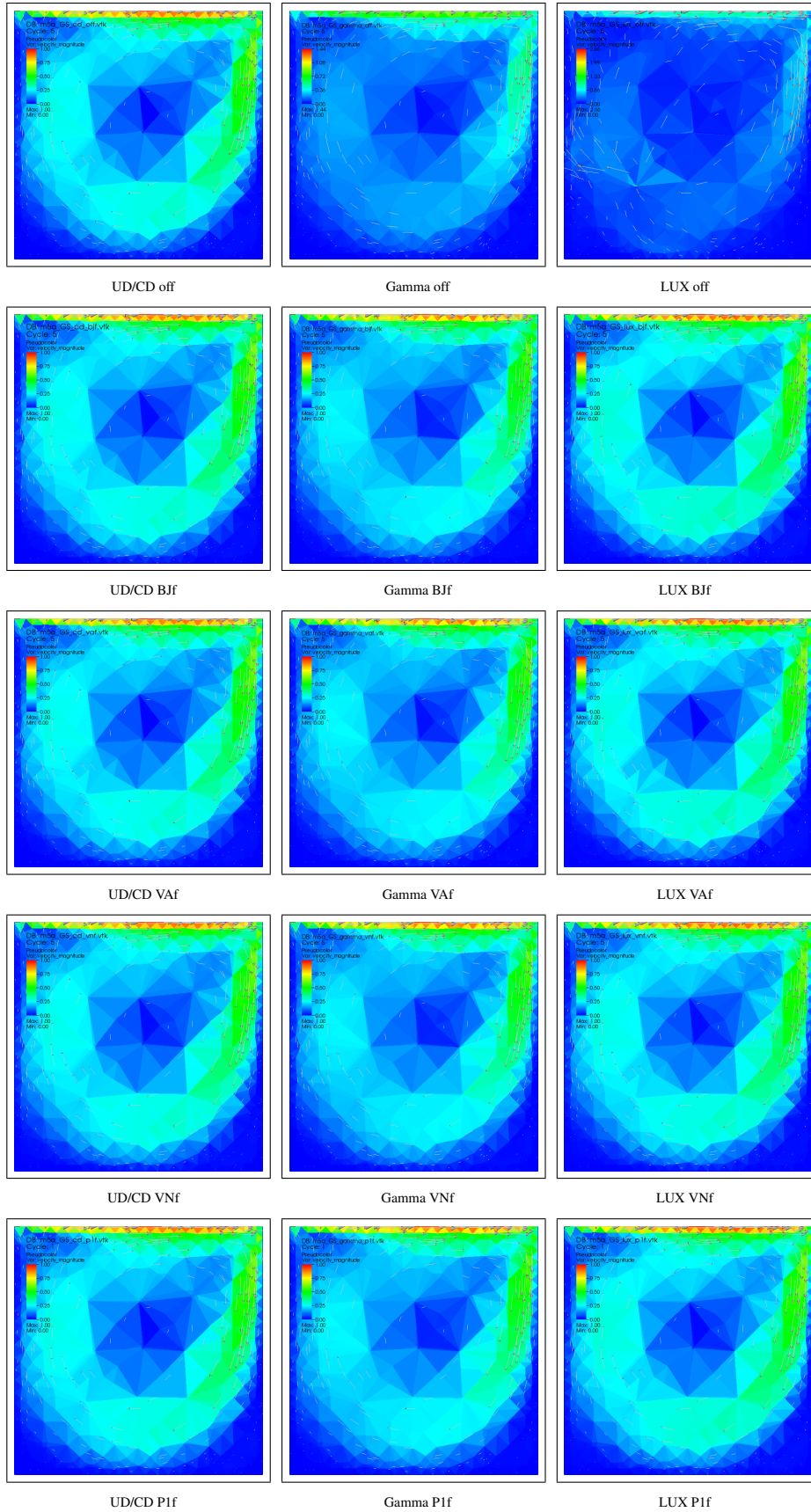


Figure 11.12: m5a LDC tet cases with Gauss and face based limiters

11.5 Plain flow from left to right

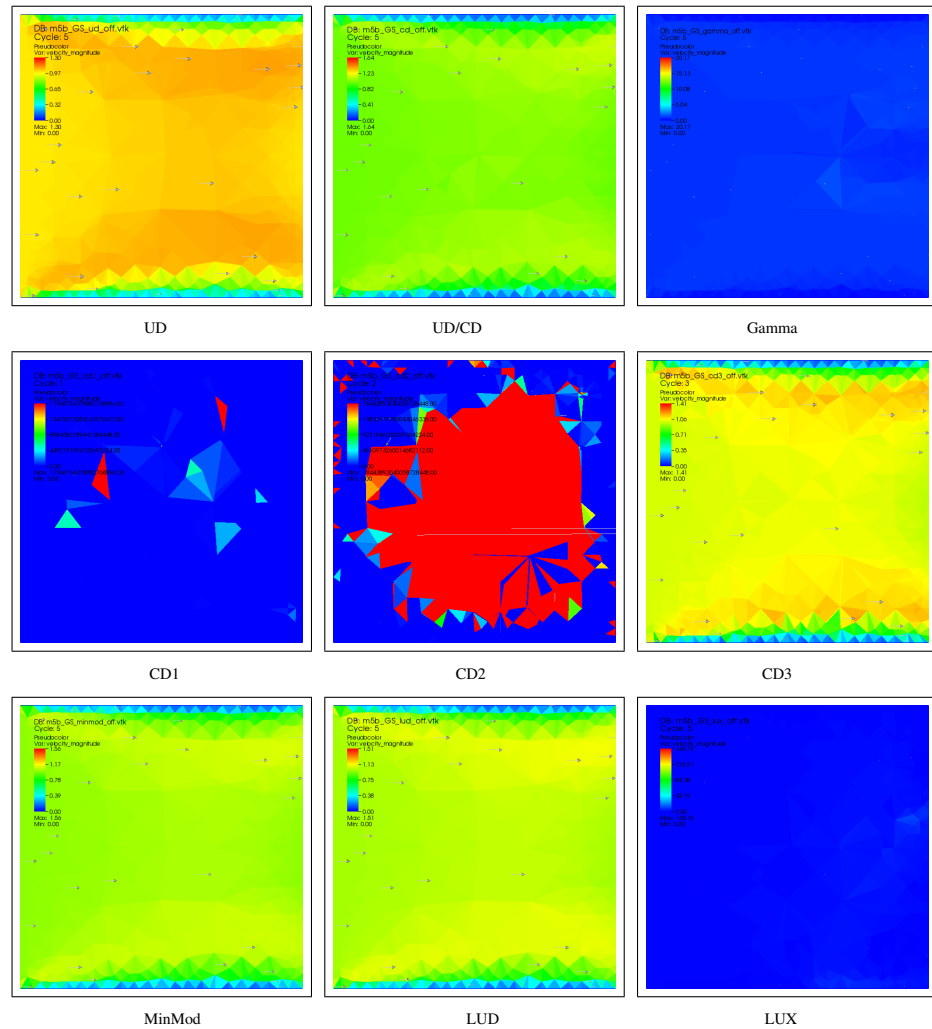


Figure 11.13: m5b plain flow tet cases with Gauss, no limiter

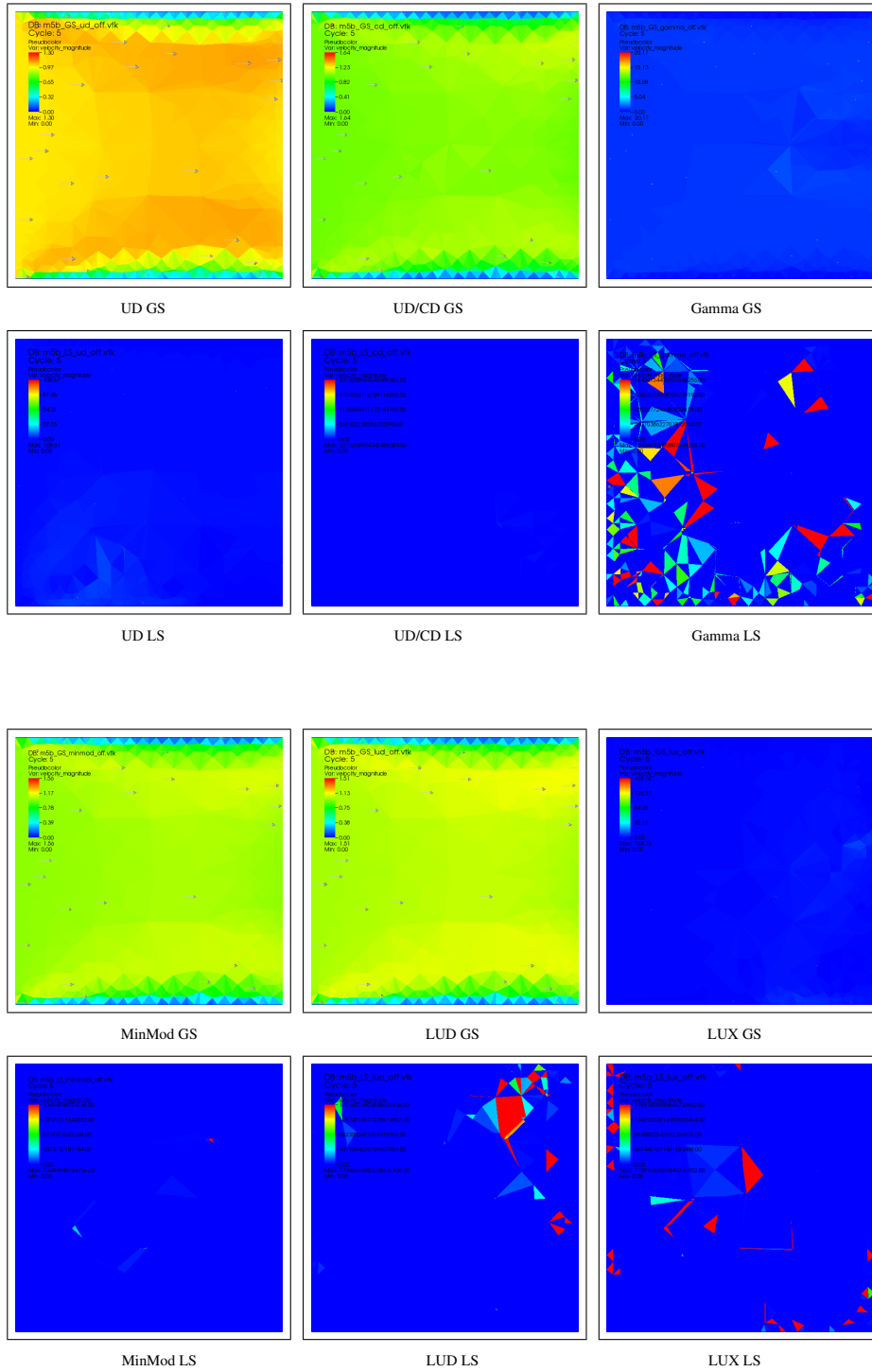


Figure 11.14: m5b plain flow tet cases with Gauss and Least Squares, no limiters used

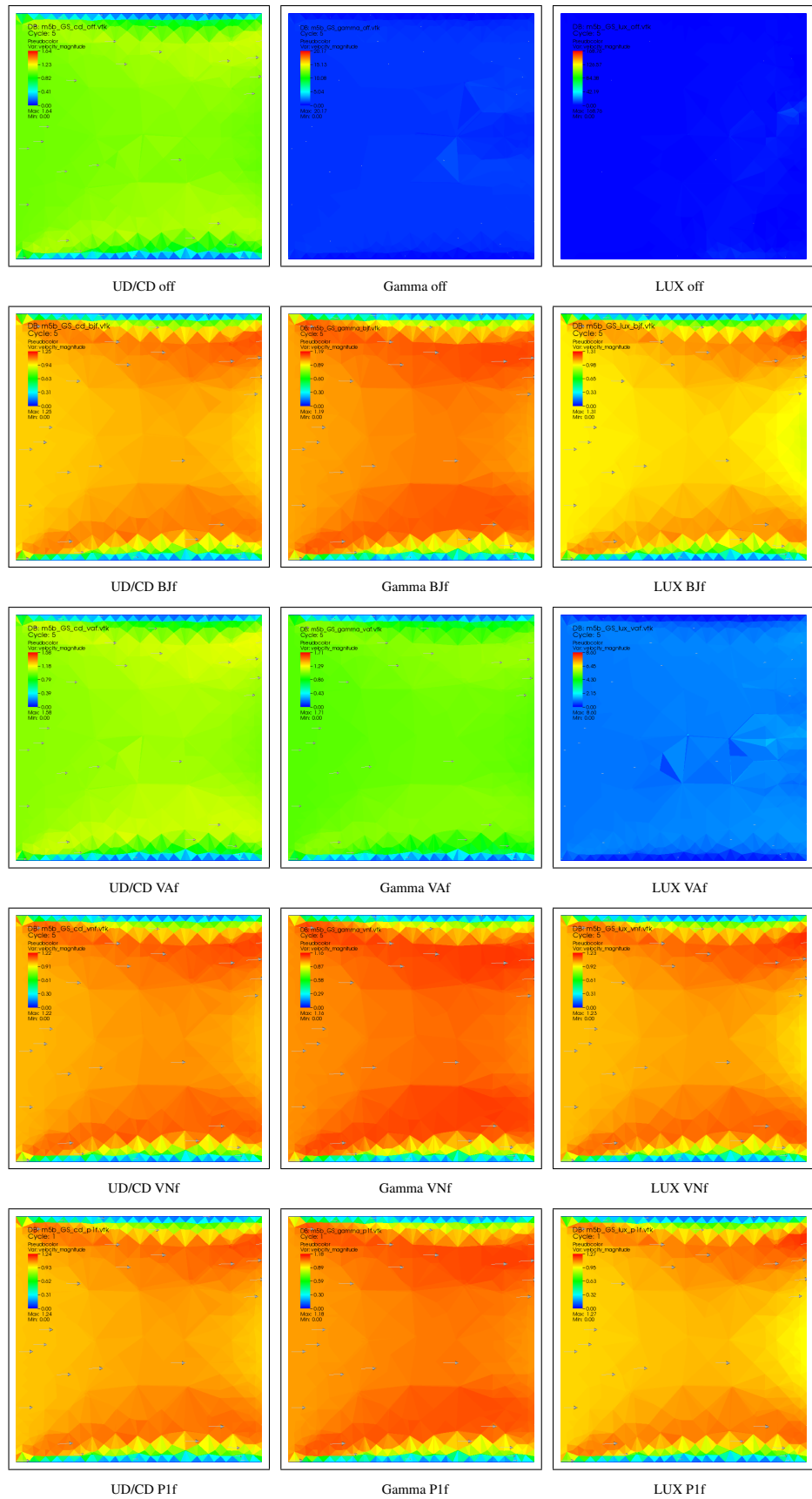


Figure 11.15: m5b plain flow cases with Gauss and face based limiters

11.6 Stagnation flow from top

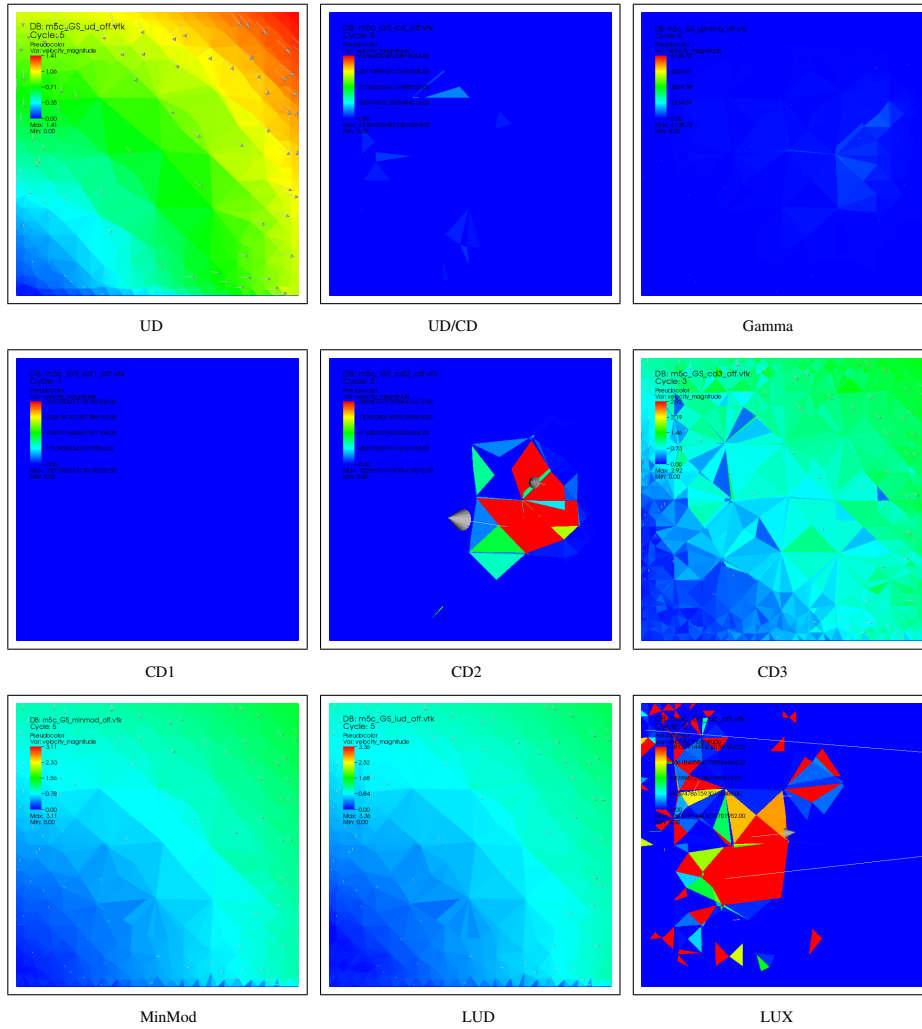


Figure 11.16: m5c stagnation flow tet cases with Gauss, no limiter

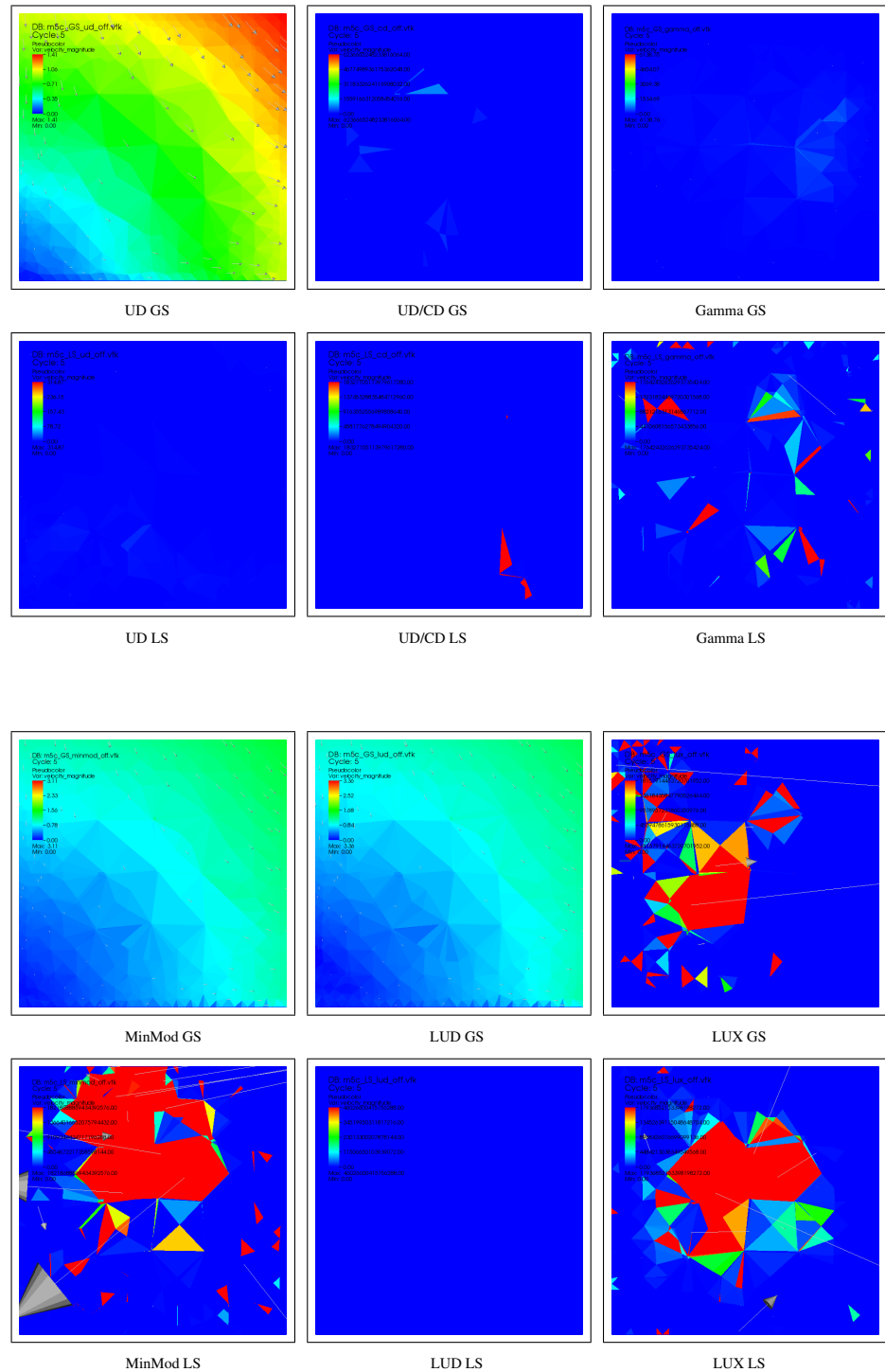


Figure 11.17: m5c stagnation flow tet cases with Gauss and Least Squares, no limiters used

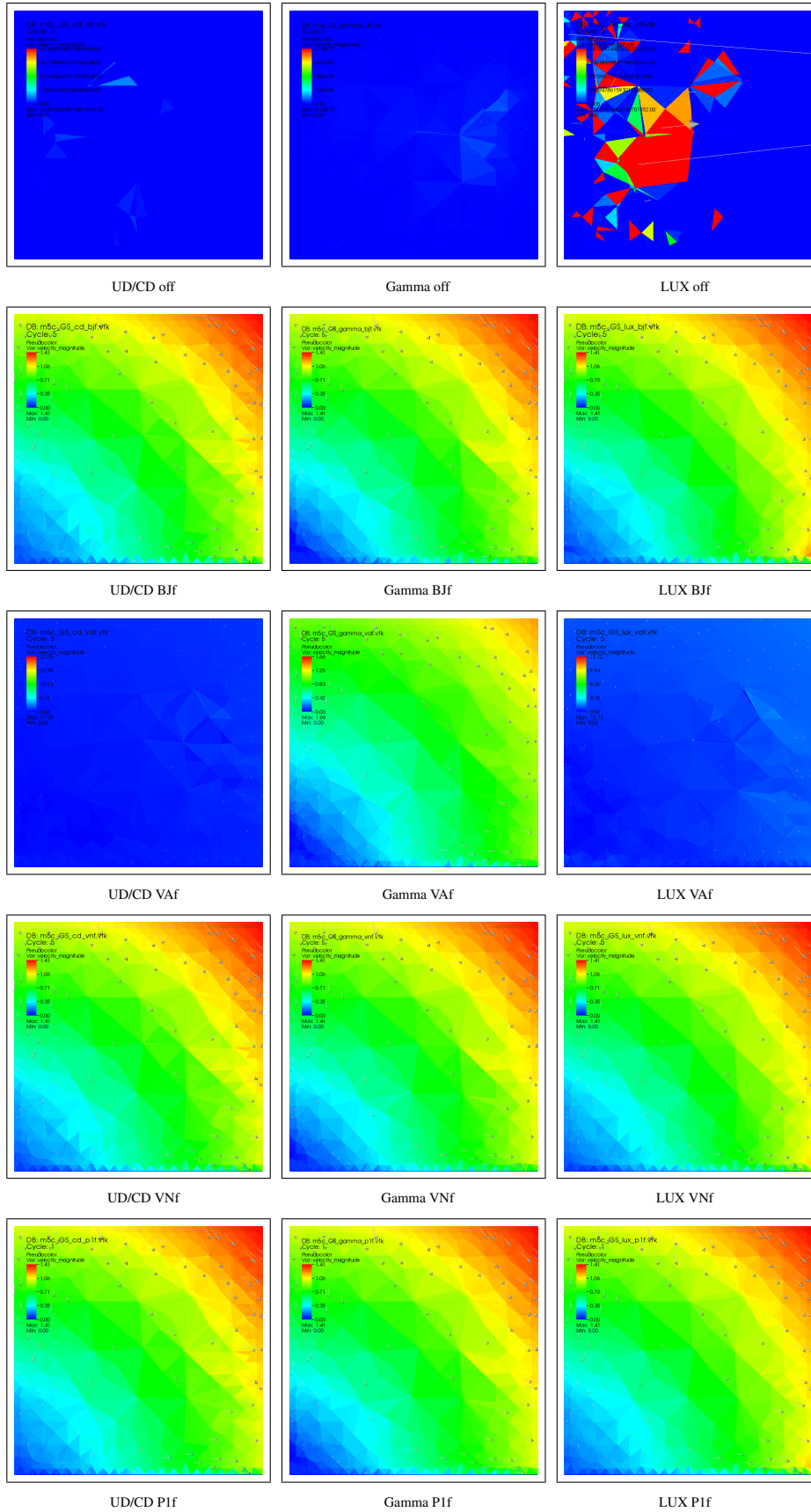


Figure 11.18: m5c stagnation flow cases with Gauss and face based limiters

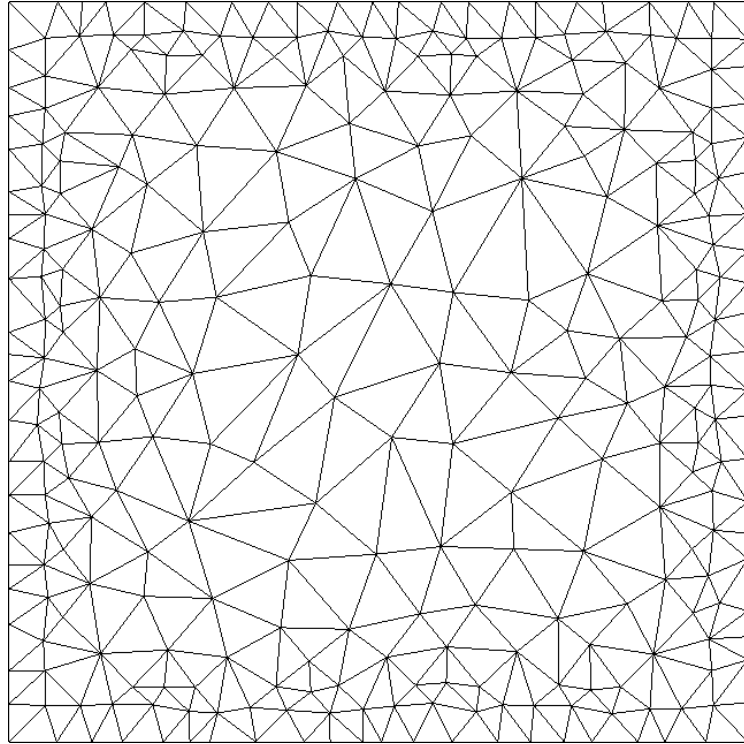


Figure 11.19: Mesh model m5

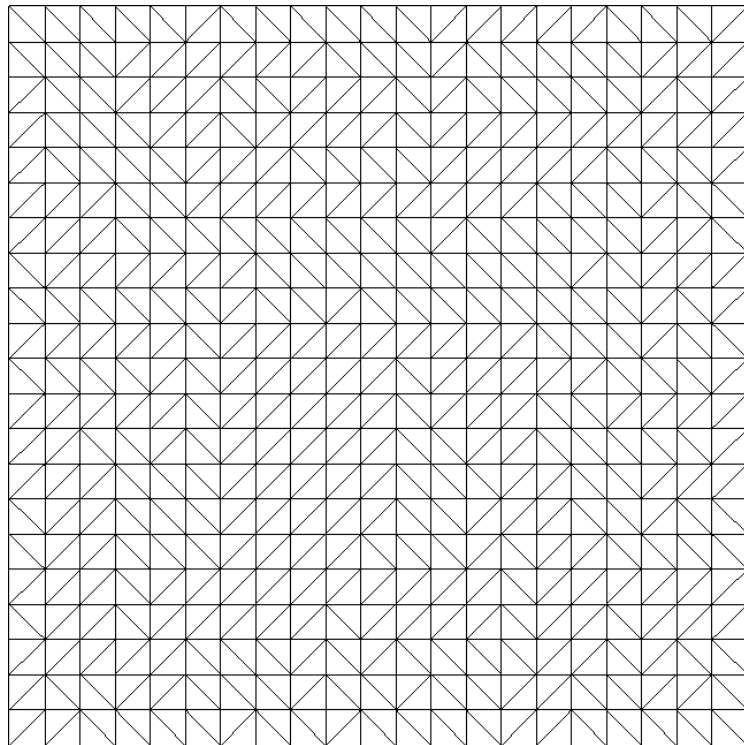


Figure 11.20: Mesh model m3